İSTANBUL TECHNICAL UNIVERSITY ★ INSTITUTE OF SCIENCE AND TECHNOLOGY

127190

TEXTURE CLASSIFICATION IN HYDROENTANGLED NONWOVENS

Ph.D. Thesis by

Ömer Berk BERKALP, M.Sc.

503972020

T.C. YÜKSEKÖĞRETİM KURULU
DOKÜMANTASYON MERKEZİ

Date of submission : 21 September 2002

Date of defence examination: 20 December 2002

Supervisor (Chairman): Assoc.Prof.Dr. Emel ÖNDER

Members of the Examining Committee Prof.Dr. Bülent ÖZİPEK (İTÜ)

Assoc.Prof.Dr. Fatma KALAOĞLU (İTÜ)

Prof.Dr. Güngör BAŞER (DEÜ)

Prof.Dr. Abdelfettah SEYAM (NC State)

DECEMBER 2002

127190

FOREWORD

In this long period, I had very hard times because of the work however by the help of my friends and my family, success had come and I also had great times in this period both in Turkey and in the United States during my stay. I first wish to express my sincere thanks and appreciation to my beloved family, especially to my Mom&Dad for their continuous support for 30 years without any expectation.

I would like to thank to my supervisor Assoc.Prof.Dr.Emel Önder for her support, guidance and encouragement in both masters and doctorate for 7 years during my thesis. I would also like to thank to my head of the department Prof.Dr.Bülent Özipek for always encouraging me to go to abroad for my study.

I wish to express my sincere thanks to Prof.Dr.Abdelfettah Seyam for inviting me to North Carolina State University. His valuable ideas had also directed this study. I wish to thank to Prof.Dr.Behnam Pourdeyhimi, director of Nonwovens Cooperative Research Center (NCRC) for his financial support and especially for his guidance and participation throughout the study. He was my mentor in image analysis.

My thanks also go to NCRC staff and students for their great help. Sincere thanks are also to all my friends in Turkey and USA for their friendship and support.

CONTENTS

ABBREVIATIONS v
LIST OF TABLES vi
LIST OF FIGURES vii
LIST OF SYMBOLS x
ÖZET xi
SUMMARY xiv

1. INTRODUCTION 1

2. HYDROENTANGLEMENT TECHNOLOGY 4
2.1. Fiber Selection 5
2.2. Fiber Preparation and Web Forming 6
2.3. Hydroentangling Process 9
2.3.1. Entangling unit 9
2.3.2. Water extraction 13
2.3.3. Water circulation and filtration 13
2.3.4. Drying 14
2.4. Hydroentanglement Lines 14
2.5. Parameters Affecting the Product Performance 18
2.6. Spunlace Fabric Characteristics 20
2.7. Advantages and Disadvantages of Hydroentanglement Technology 21
2.8 Applications and Future 22

3. PREVIOUS STUDIES 24
3.1. Hydroentanglement Research 24
3.2. Image Analysis in Textiles 26
3.2.1. Carpet texture studies 27
3.2.2. Evaluation of nonwovens using image analysis 31
3.2.3. Objective evaluation of woven and knitted fabrics 34

4. OBJECTIVES 39

5. EXPERIMENTAL 40
5.1. Methodology 40
5.2. Raw Materials 50
5.3. Sample Production 50
5.3.1. Formation of fiberweb 50
5.3.2. Hydroentangling 52
5.3.2.1. Calculation of specific energy 55

5.4. Samples Acquired from Industry 57
5.5. Image Processing System 57
5.6. Testing and Evaluation 58
5.7. Statistical Analysis 59

6. RESULTS AND DISCUSSION **60**
6.1. Texture Retention after Fabric-to-Fabric Abrasion 60
6.2. Texture Evolution in Hydroenatngled Nonwovens 66
6.3. Jet Streaks in Hydroentangled Nonwovens 75

7. CONCLUSION **81**

8. SUGGESTIONS AND FUTURE STUDIES **83**

REFERENCES **84**

ATTACHMENTS **91**

CURRICULUM VITAE **95**

ABBREVIATIONS

Edana	:	European Disposables and Nonwovens Association
ISO	:	International Organization for Standardization
UMCP	:	University of Maryland at College Park
PTT	:	Polytrimethylene Terephthalate
PET	:	Polyethylene Terephthalate
WRONZ	:	Wool Research Organization of New Zealand
GLRLM	:	Gray level run length matrix (GLRLM),
SGLRDM	:	Spatial gray level dependence method
NGLRDM	:	Neighboring gray level dependence matrix
GLDM	:	Gray level difference matrix
LIV	:	Local intensity variation
HT	:	Hough Transform
CCD	:	Charged Coupled Device
ASTM	:	American Society for Testing and Methods
AATCC	:	American Association of Textile Chemists and Colorists
DFT	:	Discrete Fourier Transform
FFT	:	Fast Fourier Transform
PGI	:	Polymer Group Incooperation
LED	:	Light Emitting Diode

LIST OF TABLES

	Page no
Table 1.1. World production of nonwovens.....	2
Table 2.1. Comparison of metal and plastic wires.....	10
Table 2.2. Examples of machine parameters for web bonding by hydroentanglement.....	11
Table 2.3. Energy requirements for partial or complete entanglement.....	19
Table 3.1. Studies on textile structures using image analysis.....	27
Table 3.2. Carpet characteristics and applied image analysis techniques.....	28
Table 5.1. Processing Parameters of Experimental Fabrics.....	56
Table 5.2. Fabrics and wear levels.....	58
Table 6.1. Periods of fabrics from their spectral density graphs.....	80

LIST OF FIGURES

Page no

Figure 1.1. : End uses of nonwovens in Western Europe in 1999 (tons)..... 3
Figure 2.1. : Schematic of hydroentanglement bonding..... 9
Figure 2.2. : A typical weave pattern (two shed (1x1) plain weave) of a forming wire..... 11
Figure 2.3. : Cross-section of a hydroentanglement unit..... 12
Figure 2.4. : Typical configurations of hydroentanglement unit..... 16
Figure 2.5. : Various spunlace lines for different purposes..... 17
Figure 2.6. : Shear modulus - strength of fabrics..... 21
Figure 3.1. : Principle of laser triangulation technique..... 37
Figure 3.2. : Diagram of the optical roughness meter..... 38
Figure 5.1. : An example for strongly ordered and disoriented texture..... 41
Figure 5.2. : Construction of co-occurrence matrix..... 43
Figure 5.3. : Co-occurrence matrix of images in three dimensional space..... 44
Figure 5.4. : Typical co-occurrence functions..... 45
Figure 5.5. : The change of co-occurrence functions with the addition of random noise..... 45
Figure 5.6. : The change of co-occurrence functions with different texture coarseness..... 46
Figure 5.7. : The change of co-occurrence function with fixed increment deviation in x-direction..... 46
Figure 5.8. : Analysis of a function with the same period but different amplitude. 49
Figure 5.9. : Analysis of a function with a different period but same amplitude.... 49
Figure 5.10. : Decomposing textural elements in a function with two periods and amplitudes..... 50
Figure 5.11. : High speed flat card used in the nonwoven industry (Trutzchler DK903)..... 51
Figure 5.12. : Crosslapping process..... 51
Figure 5.13. : Pilot scale of the Honeycomb hydroentanglement machine..... 52
Figure 5.14. : Jet manifolds of the Honeycomb hydroentanglement machine..... 53
Figure 5.15. : Sketch of the Honeycomb hydroentanglement machine..... 53
Figure 5.16. : Herringbone designed forming belt..... 54
Figure 5.17. : Trials using a 50-g/m2 web at a pressure of 96.5 bars by herringbone designed belt (1 pass and 2 passes respectively)..... 54
Figure 5.18. : Twill designed forming belt..... 55
Figure 5.19. : Illumination and capture set-up..... 58
Figure 6.1. : Images of woven twill fabric after abrasion..... 61
Figure 6.2. : Images of Miratec hydroentangled fabric with twill texture after abrasion..... 61

Figure 6.3. : Images of hydroentangled fabric with herringbone texture after abrasion..... 61
Figure 6.4. : Co-occurrence results of woven twill fabric: horizontal (left), vertical (right)..... 62
Figure 6.5. : Co-occurrence results of Miratec twill fabric: horizontal (left), vertical (right)..... 63
Figure 6.6. : Co-occurrence results of hydroentangled herringbone fabric: horizontal (left), vertical (right)..... 63
Figure 6.7. : Intensity profiles for Miratec twill fabric..... 64
Figure 6.8. : Frequency analysis of contrast data for woven twill: horizontal (left), vertical (right)..... 64
Figure 6.9. : Frequency analysis of contrast data for Miratec twill: horizontal (left), vertical (right)..... 65
Figure 6.10. : Frequency analysis of contrast data for hydroentangled herringbone: horizontal (left), vertical (right)..... 66
Figure 6.11. : Images of Fabrics using a PET 100 g/m2 web - 1 pass (left) and 2 passes (right) under different pressures..... 67
Figure 6.12. : Images of Fabrics using a PET 150 g/m2 web - 1 pass (left) and 2 passes (right) under different pressures..... 68
Figure 6.13. : Co-occurrence analysis using a PET 150 g/m2 web - 1 pass..... 68
Figure 6.14. : Power of PET 100 g/m2 web - 1 pass: horizontal (left) and vertical (right) contrast..... 69
Figure 6.15. : Power of PET 100 g/m2 web - 2 passes: horizontal (left) and vertical (right) contrast..... 69
Figure 6.16. : Power of PET 150 g/m2 web - 1 pass: horizontal (left) and vertical (right) contrast..... 70
Figure 6.17. : Power of PET 150 g/m2 web - 2 passes: horizontal (left) and vertical (right) contrast..... 70
Figure 6.18. : Power of PET 100 g/m2 web: horizontal (left) and vertical (right) contrast..... 71
Figure 6.19. : Power of PET 150 g/m2 web: horizontal (left) and vertical (right) contrast..... 71
Figure 6.20. : Transmitted illumination set-up..... 72
Figure 6.21. : Image of the forming wire and its respective co-occurrence analysis 72
Figure 6.22. : Examples from apertured fabrics (PET 100 g/m^2, 2 pass), images by directed light and transmitted light respectively..... 73
Figure 6.23. : Co-occurrence analysis of images respectively from figure 6.22..... 74
Figure 6.24. : Images of jet streaks from fabric A (left) and B (right)..... 76
Figure 6.25. : Images of jet streaks from fabric C (left) and D (right) 76
Figure 6.26. : Co-occurrence results of jet streaks on fabric A (horizontal and vertical)..... 77
Figure 6.27. : Power spectrum from fabric A (horizontal and vertical)..... 77
Figure 6.28. : Co-occurrence results of jet streaks on fabric B (horizontal and vertical)..... 78
Figure 6.29. : Co-occurrence results of jet streaks on fabric C (horizontal and vertical)..... 79

T.C. YÜKSEKÖĞRETİM KURULU DOKÜMANTASYON MERKEZİ

Figure 6.30. : Co-occurrence results of jet streaks on fabric D (horizontal and vertical)..... 79
Figure A.1. : Co-occurrence analysis using a PET 100 g/m2 web - 1 pass..... 91
Figure A.2. : Co-occurrence analysis using a PET 100 g/m2 web - 2 passes..... 91
Figure A.3. : Co-occurrence analysis using a PET 150 g/m2 web - 2 passes..... 92
Figure A.4. : Examples from apertured fabrics (PET 100 g/m^2, 1 pass), images by directed light and transmitted light respectively..... 92
Figure A.5. : Examples from apertured fabrics (PET 150 g/m^2, 1 pass), images by directed light and transmitted light respectively..... 92
Figure A.6. : Examples from apertured fabrics (PET 150 g/m^2, 2 pass), images by directed light and transmitted light respectively..... 93
Figure A.7. : Power Spectrum from Fabric B (Horizontal and Vertical)..... 93
Figure A.8. : Power Spectrum from Fabric C (Horizontal and Vertical)..... 93
Figure A.9. : Power Spectrum from Fabric D (Horizontal and Vertical)..... 94

LIST OF SYMBOLS

C_d = Orifice coefficient (assumed 0.7)
d = Diameter of jet orifice (m)
d_p = Distance between pixel
e = Base of the natural logarithm (~2.718)
E = Specific energy (kj/kg) applied to the fiber web by water jets in a manifold
E_t = The total specific energy applied to the fabric (Kj/kg)
f(x) = Time (spatial) domain
F = Estimated frequency
F(u)= Fourier transform
$F_i(u)$ = Imaginary part of F(u)
$F_r(u)$ = Real part of F(u)
i ,m = Intensity values
$j = \sqrt{-1}$
k = Pixels/mm
M = Matrix
M(u)= Magnitude of F(u)
N = Number of jets/m per manifold
NxN = Dimensions of matrix
P = Water pressure (N/m^2) in the manifold
P(u) = Power spectrum of F(u)
S = The line speed in m/min
u = Variable frequency
ρ = Water density (g/m^3)
W = Basis weight of the web (g/m^2)
θ = Direction of the pixel
$\phi(u)$ = Phase of F(u)

SUYLA İĞNELENMİŞ DOKUNMAMIŞ KUMAŞLARIN GÖRÜNÜM SINIFLANDIRMASI

ÖZET

Suyla iğneleme teknolojisi dokunmamış kumaş sektörü içinde lider teknolojilerden biridir. Üreticilerin amaçları bu sistemle geleneksel tekstiller üretmek olmasına rağmen, ilk önce bu teknolojideki bazı zorlukların üstesinden gelmelidirler. Bu araştırmanın başlığı tekstil alanında yeni bir çalışma olan: "Suyla İğnelenmiş Kumaşların Sınıflandırılması" dır. Kumaş ve halıların objektif olarak değerlendirilmesinde görüntü analiz tekniklerini birçok araştırmacı kullanmasına rağmen, suyla iğnelenmiş kumaşlar üzerinde bir araştırma yapılmamıştır. Bunun yanında, aynı yöntem ile bu kumaşlarda görülen jet çizgileri de incelenmiştir.

Bu noktadan çıkıldığında, bu araştırmanın amacı suyla iğnelenmiş dokunmamış kumaşların görünüm sınıflandırması için optik bir yöntemin ve özel bir görüntü sisteminin geliştirilmesidir. Bu sayede suyla iğnelenmiş kumaşların ve yerlerini alacakları planlanan normal kumaşların görünüm benzerlikleri, güvenilir ve etkili bir objektif değerlendirme metodunun geliştirilmesiyle yüzey yapılarının objektif olarak ölçülebilmesi düşünülmüştür.

Amaca ulaşabilmek için önce bir görüntü analiz sistemi kurulmuş ve buradan alınan görüntülerin görünüm analizleri adım adım yapılmıştır. Yöntem ve kullanılan malzemeler önce "Deneysel" kısım da açıklanmıştır. Daha sonra tüm sonuçlar "Sonuçlar ve Tartışma" kısmında verilmiş ve çalışmadan çıkan sonuçlar tartışılmıştır. Bu bölüm üçe bölünerek verilmiştir. Araştırmanın ilk bölümünde, yöntemin geçerliliğini göstermek için aşınmanın görünüm değişikliğinin üzerine etkisi incelenmiştir. İkinci bölümde ise farklı işlem şartları altında üretilmiş değişik yüzey görünümünde üretilen kumaşlar incelenmiştir. Özel bir tip (delikli kumaşlar) için ise iki farklı ışık sisteminin kullanımı karşılaştırılmıştır. Son

bölümde ise, bu tip kumaşlarda bir problem olan jet çizgileri analiz edilmiştir. Üreticiler ve ürün kalitesi için çok önemli olan bu çizgilerin peryodikliği saptanmıştır. Son olarak çalışma sonuçlandırılmış ve gelecek çalışmalar için fikirler verilmiştir.

Bu çalışmadan çıkan bazı sonuçlar şu şekildedir:

- Eş-oluşum metodlarının incelenen kumaşlardaki yapısal ve görünüm değişikliklerine hassas olduğu gösterilmiştir. Bunun yanında Fourier analizinden bulunan "güç" ün de kumaş belirginliği için iyi bir gösterge olduğu ortaya konmuştur.

- Kumaşlardaki aşınma sonrası contrast eğrilerinin büyüklüklükleri küçülmüş ve spektral analiz sonuçları da bu gerçeği güç değerlerinin azalmasıyla desteklemiştir.

- İşlem esnasında dokunun oluşmasında suyla iğneleme basıncının belirgin bir rolü vardır. Genel olarak, basıncın ve kumaşın geçiş sayısının artmasıyla (enerjinin arttırılması demektir) yeterince kuvvetlendirilmiş tüllerde yüzey dokusunun oluşumu belli bir noktaya göre artmakta daha sonra ise düşmektedir. Tülün kuvvetlendirilmemesi durumunda ise yüksek basınçlar doku yüzeyinin bozulmasıyla beraber düşük bir görünüm belirginliği vermektedir.

- Belli bir enerji seviyesinden sonra, kumaşlarda deliklerin boyutları aynı kalmaktadır. Temiz delik oluşumu için belli bir değerde bir eşik enerjisi mevcuttur.

- Jet çizgileri, bu çalışmada kurulan görüntü analizi sistemiyle tespit edilebilmektedir ancak kumaş yüzey yapısının karmaşık bir yapısı olmasından dolayı kumaşlarda birden fazla periyodisite görülmüştür. Buna rağmen birçok kumaşda baskın frekansın yaklaşık olarak 0,57 mm olduğu saptanmıştır. Peryodların da 0,508-0,635 mm aralarında bulunması, bu sonuçların büyük olasılıkla jet çizgilerine ait olduğunu göstermektedir.

T.C. YÜKSEKÖĞRETİM KURULU
DOKÜMANTASYON MERKEZİ

- Tüm sonuçlar, örnekleme aralığına göre oluşturulan eş-oluşum istatistiklerinin peryodik değişimlere hassas oldukları ve spektral analizin peryodiklik gücünü ölçmek için iyi bir ölçü olduğunu göstermiştir.

Eş-oluşum analizi yüzey görünümü belirlemek için uygun bir gösterge oluşturmaktadır. Yüzey görünümünün belirlenmesinde kullanılan yatay ve dikey contrast fonksiyonları ve bunların muadili güç spektral analizlerinin kullanışlı yöntem oldukları gösterilmişt ir. Tüm sonuçlar kumaş görüntülerinin subjektif analizleri ile tutarlıdır. Bu method hem yüzey görünümü ve hem de peryodikliği ile ilgili güvenilir sonuçlar vermiştir.

TEXTURE CLASSIFICATION IN HYDROENTANGLED NONWOVENS

SUMMARY

Hydroentanglement technology is one of the leading technologies in the nonwovens sector. Manufacturers aim to produce textiles alike conventional textiles whereas they have to overcome some difficulties in the technology. The topic of this research: "Texture Classification in Hydroentangled Nonwovens", is a new study in the textiles field. Many researchers have used image analysis techniques for objective evaluation of fabrics and carpets, however hydroentangled nonwovens' texture analyses are not studied so far. Assessment of jet streaks (a defect that appear on the surface of hydroentangled fabric in the machine direction due to jet force) of these fabrics to identify their source were also investigated using image analysis.

From this point, the intention of this research is to develop an optical method and a turnkey imaging system for classifying texture in hydroentangled fabrics so as to compare the texture similarity of hydroentangled fabrics and those of fabrics they are to replace by measuring surface properties for the purposes of developing a reliable and efficient method objectively evaluate hydroentangled fabrics.

To achieve our aim, an imaging system is developed and texture analysis are applied to the images step by step. Methodology and materials are first explained in details in the "Experimental" chapter. In "Results and Discussion" chapter, the results and the outcomes of the study are reported and discussed. The "Results and Discussion" chapter is divided into three parts. In the first part, the effect of abrasion on texture change has been investigated in order to demonstrate the viability of our methodology. In the second part, fabrics which are manufactured with different textures under various processing conditions, are analyzed. Two lighting systems are also compared for a specific type (apertured fabrics). In the

last part, jet streaks have been analyzed. The periodicity of the jet streaks, which is very vital for the quality of the fabric, are determined. Finally, the study is concluded, and new research topics are suggested for the future study.

The following findings were concluded from the study:

- It was demonstrated that the co-occurrence methods are sensitive enough to structural and textural changes in the fabrics examined. Additionally, the power from Fourier analysis is a good indicator for fabric texture definition.

- The magnitude of the contrast curves has become smaller as a result of abrasion, and spectral analysis results have supported this fact as the power values have decreased.

- Jet pressure has a marked effect on the manner in which texture develops during the process. In general, increasing pressure and the number of passes (which means energy) will result in a better texture definition up to a certain point provided that the web is sufficiently consolidated. If the web is not consolidated, higher pressures will result in perturbing the web with a concomitantly lower texture definition.

- After a certain energy level, the formation of apertures is kept in a certain dimension. There is a threshold energy level corresponding to clear aperture formation.

- Jet streaks can be determined by the image analysis systems employed in this research, however, the surface structure of the fabric is complex since there are more than one periodicity on the fabrics. Yet the dominant frequencies for most of the fabrics are found to be approximately 0.57 mm (distance between the successive jets). Since the periods are found between 0.508-0.635 mm, it is a strong indication that these results are very probably belongs to the jet streaks.

- The results has indicated that co-occurrence statistics used as a function of sampling distance are sensitive to periodic changes of texture and that of the spectral analysis are good measure of the strength of the periodicity.

- Co-occurrence analysis is a good indicator for determining the surface texture properties. It is demonstrated that horizontal and vertical contrast functions and their respective power spectral analysis data provide a useful tool for quantifying texture. All results of the objective assessment are consistent with subjective evaluation from the fabric images. This method has given reliable results for both texture and periodically.

1. INTRODUCTION

A nonwoven fabric is a fibrous assembly, which is generally defined as a sheet or web structure made by bonding and interlocking fibers by mechanical, thermal, chemical or solvent means. Nonwovens are used in a wide range of fields, including sports, construction and civil engineering, medicine, electronics, aeronautics and the automobile industry.

The definition of nonwovens from Edana (European Disposables and Nonwovens Association) is similar to that of ISO (International Organization for Standardization) which defines a nonwoven as a manufactured sheet, web or batt of directionally or randomly orientated fibers, bonded by friction, and/or cohesion and/or adhesion, excluding paper (see note below) and products which are woven, knitted, tufted, stitch-bonded incorporating binding yarns or filaments, or felted by wet-milling, whether or not additionally needled. The fibers may be of natural or man-made origin, they may be staple or continuous filaments or be formed in situ [1].

- Note: to distinguish wet-laid nonwovens from wet-laid papers, a material shall be regarded as a nonwoven if
  a) more than 50% by mass of its fibrous content is made up of fibers (excluding chemically digested vegetable fibers) with a length to diameter ratio greater than 300; or, if the conditions in a) do not apply, then or,
  b) more than 30% by mass of its fibrous content is made up of fibers (excluding chemically digested vegetable fibers) with a length to diameter ratio greater than 300 and its density is less than 0.40 g/cm^3.

There are primarily two stages to nonwoven production: web formation and consolidation, which can be followed by finishing. A web can be made of randomly or directionally orientated fibers and is produced by one of the following methods: dry-laying, wet-laying, spun-laying and meltblowing. Once a web is formed it can be consolidated using one or more of the following methods: chemical bonding, thermal bonding and mechanical bonding.

The earlier success in the development of bonded nonwovens, as a part of the textile industry, occurred in the 1950's and by the 1960's and by then, the success of nonwovens in such end-uses as linings, filtration, disposable diapers, wipes, sanitary and medical applications etc. was well established. However the developments could not penetrate into traditional textile applications such as apparel, and it was understood that the wovens and knits were hard to replace with this nonwovens. Consequently the early growth of the nonwovens was limited due to the characteristics of the products, and the availability was limited to the number of the bonding technologies. Soon after new end-uses are found and newer technologies are developed (such as stitch bonded, spun bonded and hydroentanglement), new markets are created and nonwovens are used in a large variety of applications beginning to substitute traditional textiles. Nonwovens are currently a global industry with estimated worldwide consumption approaching 2.7 million tons. Volume growth exceeds 6% per year and is expected to reach about 3.5 million tons by 2003. The three major developed markets are North America, Western Europe and Japan, which account for about 75% of the worldwide roll goods market (Table 1.1). The growth rate in nonwoven consumption has emerged in several developing markets in the Pacific Rim countries and more recently, in Latin America. These new geographic markets are expected to account for a third marketplace in the global market at the beginning of 21st century [2].

Table 1.1. World production of nonwovens

	1999 (tons)	%
West Europe *	909 800	33.8
North America	985 000	36.5
Japan	309 300	11.5
Others	490 000	18.2
Total	2 694 100	100.0

Source : Edana

*Western European figures do not include most needlepunched, stitch-bonded and glass fiber webs [1].

The end-use applications of nonwovens have been the driving factors in the development of materials and new technologies. The requirements of the desired properties for an end use application determine the type of fiber, the method of production, and the bonding employed. Nonwovens can be classified into two groups according to their end-uses: disposables and durables. The examples of the

T.C. YÜKSEKÖĞRETİM KURULU
DOKÜMANTASYON MERKEZİ

disposable type nonwovens include disposable diapers, sanitary napkins, filters, packaging, medical and surgical supplies. The primary considerations in their use are absorbency and liquid repellency. The semi durable nonwovens include wiping cloth, pillow covers, and other nonwovens that have to be laundered a few times. In most end-use applications the disposable nonwovens have replaced knits, paper or lightweight durable nonwovens.

Durable nonwovens on the other hand include such materials as interlining and interfacing, automobile interiors, trunk liners, and hood insulators, substrates for vinyl coated upholstery, luggage, furniture, furnishings (mattress covers, under spring covers, draperies, etc.), carpet backing (primary and secondary), blankets, floppy disk covers, wall coverings, garment insulation, fiber fill (pillows, sleeping bags etc.), roofing tiles, architectural fabrics, suede-like composite structures, and geotextiles. The main end-uses of nonwovens in Western Europe [1] are given in Figure 1.1.

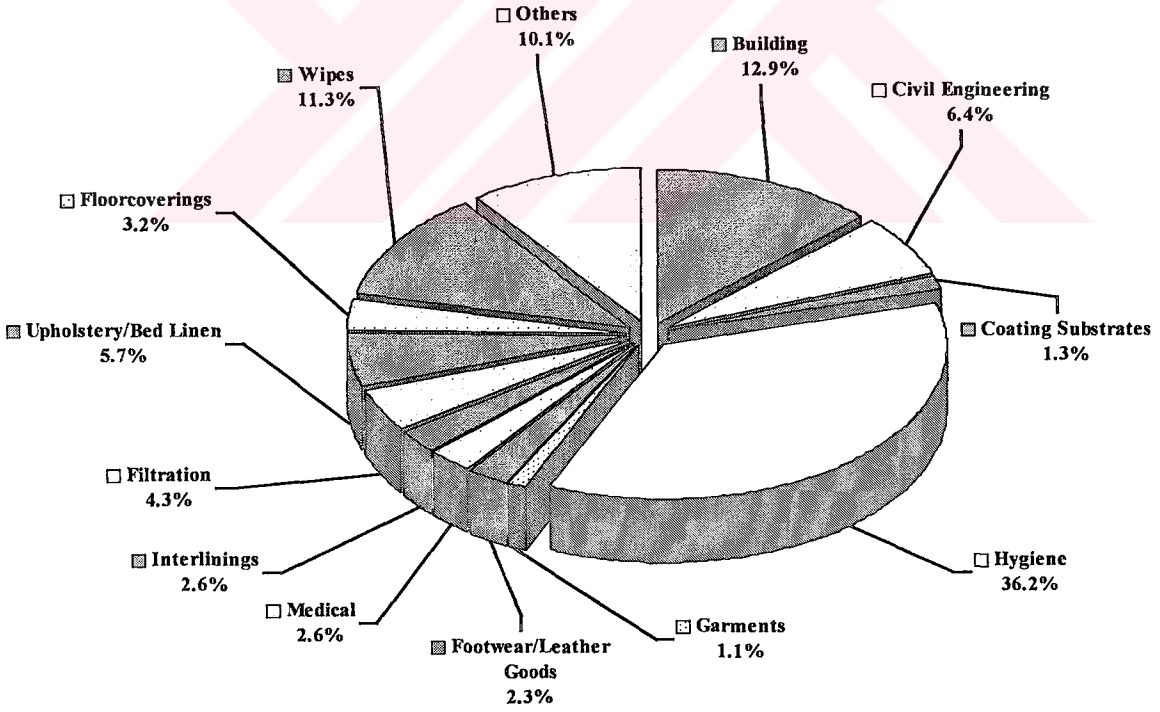

Figure 1.1. End uses of nonwovens in Western Europe in 1999 (tons) [1].

2. HYDROENTANGLEMENT TECHNOLOGY: A REVIEW

Hydroentanglement, spunlacing, hydraulic needling and water jet needling are all the terms that describe a versatile process for manufacturing nonwoven fabrics, is a method of mechanical bonding using fine, closely spaced, high-velocity jets of water to rearrange and entangle loose arrays of fibers.

This technology in its various forms has existed for over forty years. Chicopee developed the basic concepts in the early 1950's using a low-energy patterning process. Du Pont started up the first high-energy spunlaced plant in 1974 using proprietary high-speed web forming and hydraulic needling technology [3]. The development of high-energy spunlace technology allowed production at high-speed while producing aesthetically sound hydroentangled fabrics. With such development, the market for hydroentanglement was expanding. For example, the European spunlaced market has expanded to an unprecedented degree in the past two years, with a conservative estimate adding 60,000 tones of new capacity. Even excluding Du Pont's major plant at Austria's in Spain - which has a capacity itself of 20,000 tones and started shipping limited quantities of material prior to full production increase - European output is well over 100,000 tones (year 2000). In 1996, Edana estimated overall output at just 29,000 tones [4]. While the growth rate for the nonwovens industry is an estimated 7-8% that for hydroentanglement is believed to be as much as 20% [5].

Hydroentangled fabrics rely primarily on fiber-to-fiber friction to achieve physical integrity and are characterized by relatively high strength, conformability and aesthetics closely approaching woven and knitted fabrics [6].

The production of hydroentangled fabrics requires several steps. These are:

- Fiber selection
- Fiber preparation and web forming
- Hydroentangling process
  - The entangling unit (water jets, forming wire)
  - Water extraction
  - Water circulation and filtration
  - Drying
- Winding
- Finishing (optional)

2.1. Fiber Selection

The spunlacing process can entangle many different fibers. The fiber or fiber blends selected will be determined by the forming wire characteristics and the fabric attributes desired such as absorbency, abrasion resistance, tensile strength, tear resistance, thermal stability, and permeability. This selection will have a significant effect on the amount of entanglement achieved, cost and productivity. Most of the commercial spunlaced fabrics are made from these or combinations of these fibers: polyester, rayon, woodpulp, cotton, polypropylene, lyocell, tencel and additionally specialty fabrics have also been made containing these fibers: acrylic, nylon, aramid (like Kevlar and Nomex), fluoropolymer, binder fibers, splittable fibers, and silk.

Spunlacing is basically an energy transfer process. High velocity water jets insert fibers from the surface into the body of the fibrous web and entangle the inserted fibers around other fibers and themselves due to local energy released by deflection and interruption of the jets. This requires that fibers bend easily around small radii and have some degree of mobility. The most important properties affecting the ease of fiber entanglement include those related to polymer composition and fiber geometry [3]:

- Modulus: Fibers with low bending modulus require less entangling energy than those with high bending modulus. Therefore low wet-modulus fibers such as rayon and cotton would entangle more easily than polyester or an aramid.

- Fineness: For a given polymer type, larger diameter fibers are more difficult to entangle than smaller diameter fibers because of their greater bending rigidity. For example, a 6-denier fiber is 16 times stiffer than a 1.5-denier fiber. For polyester the optimum fiber denier ranges from 1.25 to 1.5 denier per fiber. When higher denier fibers are required for some attribute such as bulk, low denier fibers can be blended to improve fabric integrity.
- Cross-section: For a given polymer type and fiber denier, a triangular shaped fiber will have 1.4 times the bending stiffness of a round fiber. An extremely flat, oval or elliptical shaped fiber could have only 0.15 times the bending stiffness of a round fiber.
- Length: Shorter fibers are more mobile and will produce more entanglement points per unit fiber length than longer fibers. Fabric strength, however, is proportional to fiber length; therefore, fiber length must be selected to give the best balance between the number of entanglement points and fabric strength. Typical fiber length for polyester is 1.9-3.8 cm. Blends or composites of short and long fibers can produce strong and well-entangled fabrics; for example, woodpulp fibers blended with polyester staple web.
- Crimp: Crimp is required in staple fiber processing systems (opening, blending, carding and web formation) and contributes to fiber bulk. Too high crimp levels, however, can result in lower fabric strength and entanglement because of reduced fiber mobility and difficulty during entanglement stage.
- Fiber wettability: Hydrophilic fibers entangle more easily than hydrophobic fibers because of the higher drag forces. Finishes can be applied in fiber production process that will increase the wettability of fibers and improve entanglement.

2.2. Fiber Preparation and Web Forming

Like all sheet processes, hydroentangled fabric properties depend to a larger extent on web formation and in turn web forming mechanism. A high-speed web former capable of producing a randomly oriented and uniform structure is the ideal system. In practice it is the web former that limits the line speed since, in principle, the entanglement is not a speed limited process; jet manifolds may be added, as line speed is increased [7].

Practically, any dry-laid, wet-laid, spunbond or combinations of these web forming processes can be used to produce precursor webs for spunlacing with varying degrees of success. Poor original web formation makes it almost impossible to entangle or requires the expenditure of too much energy to achieve good physical and mechanical properties. Chicopee and Dupont, the first United States' producers of spunlace nonwovens who have developed their own proprietary forming systems, have recognized the need for good initial web formation for many years. Newer entrants to the spunlace market have only recently realized the importance of good initial web formation [8].

There are two methods of dry-laying: carding and air-laying. Carding is a mechanical process which starts with the opening of bales of fibers which are blended and transferred to the next stage by air transport. They are then combed into a web by a rotating drum or series of drums covered in fine wires or teeth. The precise configuration of cards will depend on the fabric weight and fiber orientation required. The web can be parallel-laid, where most of the fibers are laid in the machine direction, or they can be random-laid. Typical parallel-laid carded webs result in good tensile strength, low elongation and low tear strength in the machine direction and the reverse in the cross direction. Relative speeds and web composition can be varied to produce a wide range of properties. In air-laying, the fibers, which can be very short, are fed into an air stream and from there to a moving belt or perforated drum, where they form a randomly oriented web. Compared with carded webs, air-laid webs have a lower density (or higher bulk), a greater softness and an absence of laminar structure. Air-laid webs offer great versatility in terms of the fibers and fiber blends that can be used [1]. The qualities necessary to the precursor web are good evenness, low machine direction/ cross direction ratio (isotropic webs), and three-dimensional formation. Air-laid random webs are particularly suitable to the spunlacing process, and they generally provide better results than conventional carded webs. The energy required to obtain similar physical properties using these two processes also might vary from two to three times [8].

The formation of the precursor web for entanglement is best achieved by using wet-formed nonwoven systems. In a wet-laid system, a dilute slurry of water and fibers are deposited on a moving wire screen and drained to form a web. The web is further dewatered, consolidated, by pressing between rollers, and dried. Impregnation with

binders is often included in a later stage of the process. Wet-laid web-forming allows a wide range of fiber orientations ranging from near random to near parallel. The strength of the random oriented web is rather similar in all directions in the plane of the fabric. A wide range of natural, mineral, synthetic and man-made fibers of varying lengths can be used [1]. Wet-forming systems are faster compared with other web forming technologies, they are efficient, and they can form a sheet that can be almost perfectly isotropic, an opposed to one that has a high degree of directionality. Webs can be produced as multi-layered structures of different layer compositions. Wet-formed precursor webs can be produced from 10 g/m^2 up to 1000 g/m^2. But for effective entanglement, however, web weights below 30 g/m^2 are too light because there are too few fibers per unit mass [9].

In the past, differences in speed were not allowing a combination of spunbonding and spunlacing since it was not economical. In spunbonding, polymer granules are melted and molten polymer is extruded through spinnerets. The continuous filaments are cooled and deposited on to a conveyor to form a uniform web. Some remaining temperature can cause filaments to adhere to one another, but this cannot be regarded as the principal method of bonding. The spunbonding process has the advantage of giving nonwovens greater strength, but raw material flexibility is more restricted. Co-extrusion of second components is used in several spunbonding processes, usually to provide extra properties or bonding capabilities [1]. The spunbonding technology had already reached high speeds, while spunlacing technology was operating at moderate speeds due to the limited water pressures resulting from the line design. But now, with the development in spunlacing and spunbonding technology, new lines are created to make a combination of both methods, allowing to produce new product qualities. By using these methods, web weights from under 10 to more than 600 g/m^2 can be successfully bonded [10].

Choosing the right web-forming equipment can significantly reduce the number of injectors and associated water quantities, filtration equipment, etc., and consequently reduce the total capital investment required. Today almost all suppliers of carding equipment develop cards capable of producing uniform, isotropic, random webs at high production speeds with three-dimensional formation [8].

2.3. Hydroentangling Process

Hydroentanglement is a mechanical bonding technology that uses water jets (water needling) with high-pressure to entangle and bond fibers together to form a hydroentangled fabric. Figure 2.1 depicts a schematic of a hydroentanglement bonding technology. The main components of the hydroentanglement technology are filtering unit, nozzle unit, forming surface (wire), suction unit and the drying and winding section [11].

2.3.1. Entangling unit

The entangling unit consists of the forming wire and water jets. In the spunlacing process, fiber entanglement is accomplished at the entangling unit by directing fine, columnar, high-energy jets of water from a series of manifolds, arranged perpendicular to the machine direction, against a nonwoven web supported by a porous substrate (forming wire) (Figure 2.3).

The principal components of a hydroentangled system are as follows:

The forming wire (surface) or the web supporter system plays an important role in the formation of hydroentangled fabric. The forming surface in the bonding region decides, among other factors, the properties and aesthetics of the resultant fabric.

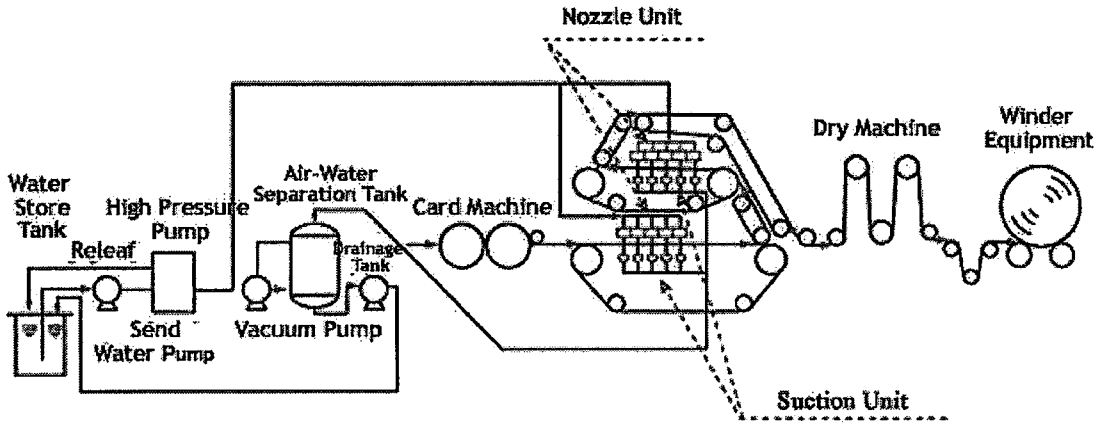

Figure 2.1. Schematic of hydroentanglement bonding (courtesy of Kazen Nozzle)

The supporting substrate is an important variable influencing the fabric end-use characteristics. There are two basic methods using forming wires to make spunlace products: flat and rotary. The rotary concept uses a compact machine design with ease of sheet run that provides entanglement of both sides of the web. Entanglement is seen to be achieved with as little as four meters (in the machine direction) of the material. Where as in the flat concept, the fibers are sometimes driven through the supporting wire, and the wire (along with the fibers) is dragged over the suction box causing difficulty in the removal of the product. In the rotary concept this problem is not encountered because the fibers are not pulled along the machine direction [22].

Commonly used wires for bonding are metal wires in a 70-100 mesh (number of wires per inch) or 28-39 wires per cm range. Figure 2.2 shows the flat view and the cross section of a wire mesh. Recently plastic wires have been introduced both in fine mesh single-layer as well as multi-layer designs. Experience has shown that because plastic wires exhibit somewhat different characteristics than metal wires, some process changes may have to be made when converting from metal to plastic wires [11]. The comparison of metal and plastic wires is given in Table 2.1. The forming wire is directly related to the nonwovens product in spunlace. This means, of course, that the quality and uniformity of the forming wire is very important to the final quality of the produced hydroentangled fabric. The mirror image effect of the nonwovens product from the forming wire means that the quality level for forming wire for spunlace must be exceptional [12].

Table 2.1. Comparison of metal and plastic wires [11,12]

Plastic wire	**Metal wire**
Good flex resistance	Poor flex resistance
Lightweight	Heavyweight
Easy to install	Difficult to install
Corrosion resistant	Corrosion prone
Difficult seams	Nonmarking seams
Shower damage prone	Shower damage resistant
Difficult to control knuckle height	Easier to control knuckle height

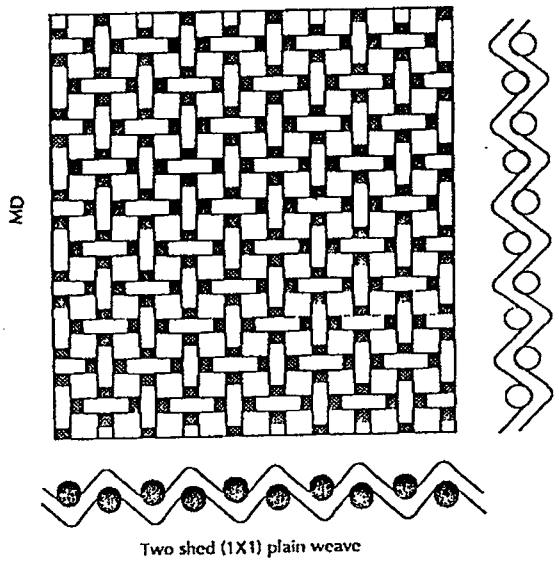

Figure 2.2. A typical weave pattern (two shed (1x1) plain weave) of a forming wire [12]

The number size and pressure level of the water jets depend on the type of fiber(s) being processed and the amount of entanglement desired [3]. Series of injectors with typical nozzle size of 100-120 μm in diameter arranged in single or multiple rows with a 3-5 mm spacing and 1-2 jets per mm. 200 bar pressure is very common in modern hydroentangling machines [14]. More typically on heavy duty machines, 400 bar injectors are installed, reaching outputs of 4000 kg an hour, but in some specific applications, new modeling techniques have been developed to offer water jet injectors with the highest efficiency and jet quality, currently reaching 1000 bar [4]. Various machine parameters from different hydroentanglement manufacturers are given in Table 2.2.

Table 2.2. Examples of machine parameters for web bonding by hydroentanglement [15]

Designation	***Manufacturer***	***Working width (m)***	***Pressure (bar)***	***Web weight (g/m^2)***	***Production speed[1] (m/min)***
Jetlace 2000	ICBT Perfojet	3.5	400	20-400	300
Aquajet	Fleissner	4.2	600	10-600	600[2]
Hydrolace 350	Spunlace Technologies	3.5	200	till 450	200

[1] with lowest possible web weight
[2] with lightweight spunbonded nonwovens

Water jet specific energy is the energy required to produce one kilogram of hydroentangled fabric. Specific energy input is a function of the number of

T.C. YÜKSEKÖĞRETİM KURULU DOKÜMANTASYON MERKEZİ

entangling manifolds and the web treating pressure as well as machine width, process speed, surface design and basis weight of the hydroentangled fabric. [16]. Specific energy is an independent variable, which significantly affects fabric texture, physical and mechanical hence fabric properties and performance.

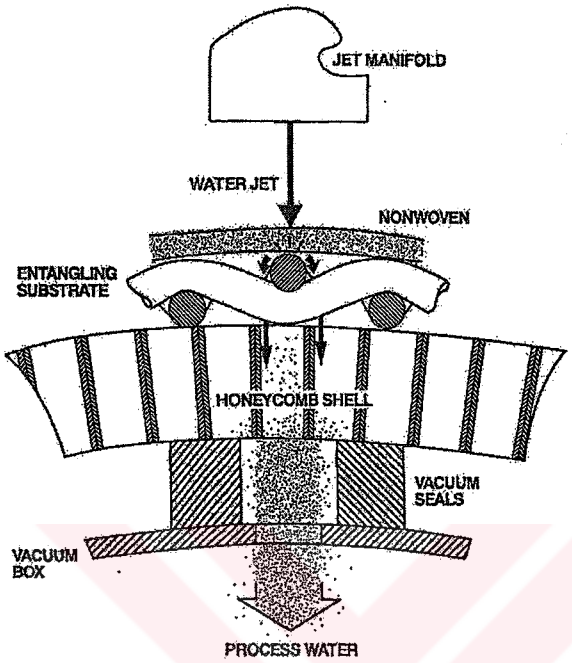

Figure 2.3. Cross-section of a hydroentanglement unit

The total jet specific energy applied to the fiber web is a key process variable. The theoretical formula for specific energy, E, in j/kg applied to the fiber web by water jets in a manifold is given by equation 1.1. [17-19]:

$$E = 6.66\times10^{4}\,\frac{C_d.d^2.N.P^{3/2}}{\sqrt{\rho}.W.S} \qquad (1.1)$$

where C_d is the orifice coefficient , d is the diameter of jet orifice (m), N is the number of jets/m per manifold, P is the water pressure (N/m^2) in each manifold, ρ is water density (kg/m^3), W is the basis weight of the web (g/m^2), and S is the line speed in m/min. The total specific energy applied to the fabric (j/kg) is calculated by equation (1.2). This formula neglects the energy losses in the pumps and the water supply channel (simply it is assumed that there is no viscosity and friction in the process of flowing). It also excludes the energy required for water extraction.

Total Specific Energy, $E_t = \sum_{i=1}^{p}\sum_{j=1}^{m} E_{ij}$ (1.2)

where E_{ij} is the specific energy applied to the fiber web by manifold, j (j=1,2,....m), calculated by equation (1.1.), in the pass (i= 1,2,.... p), where m and p are the number of manifolds and passes respectively. It is a common practice to hydroentangle webs on the first side using low hydraulic pressures on a fine, wire mesh substrate. Sometimes there is a second-side entangling treatment. This would maximize strength, eliminate two sidedness, minimize fiber loss associated with a one side treatment, or create apertures or patterns. Two sided means one side is entangled and exhibit texture and the other is "fuzzy". Passing a fabric through the entangling zone twice so that the side against the forming screen on the first pass becomes the water jet manifold side on the second pass eliminates two-sided entanglement.

2.3.2. Water extraction

Separate vacuum slots are provided underneath the needling substrate for each jet manifold to remove water penetrating the web. Insufficient water removal at any stage in the needling process can result in flooding and loss in entangling efficiency. Additional water may be removed to reduce the drying load by high-vacuum flat belt or rotary vacuum extraction systems or mangle rolls and situated before the drying section.

2.3.3. Water circulation and filtration

The water handling system is the heart of the entanglement process. Immediate removal of the spent water from the entanglement site is necessary to avoid fiber floating. This is accomplished by means of vacuum slots positioned directly under the supporting member at the jet impact point. The water is collected and recycled.

The water handling system is extensive. It consists of pumps, water reservoirs for high pressure pump intake, cleanse and makeup of water, or a filtration system, vacuum separators and bacterial control units. Commercial lines use centrifugal pumps to supply high water volume at pressures up to 140 bar [7].

Normal non-deionized water is commonly used. The filters are also simpler since the extremely fine filtration is believed to be vital in the past, but is not really necessary. In fact, it is mentioned that most of the defects attributed in the past to the filtration system were actually problems in the high-pressure piping, injector, and high-pressure pumps [8]. The volume of the water for the entanglement is high. It takes 600-900 liters of water to entangle one kg of fiber [20]. While some of the water exits with the fibers or is washed out, most of the liquid is recycled.

The recycled water contains fiber finish and debris that needs to be filtered out. Excessive debris in the water can lead to jet plugging and jet erosion, while fiber finish that is washed out during the entanglement can foam or otherwise generate scum that blinds the filters. The degree of filtration depends on the types of fibers. Cellulosic fibers that are subjected to high and medium energy treatment generate a relatively high level of fiber debris, while synthetic fibers do not. This is why elaborate filtration systems are used in lines that are intended to handle cellulosic base fibers.

Similarly, the water systems must be designed to prevent bacterial growth in the water. Bacterial growth can contaminate the product and can clog the filters. Adding biocides to the water and having an ultra violet system in line achieve control. The selection of fiber finish to minimize nutrients can lessen the bacterial growth problem.

2.3.4. Drying

Once the fabric entanglement is completed, the fabric that contains several times its weight in water is dried. In many cases a vacuum or a mechanical dewatering system first removes the excess water. The fabric is then dried in a conventional manner using steam cans or dryers.

2.4. Hydroentanglement Lines

Fleissner's Aqua Jet systems and ICBT's Perfojet/JETlace have emerged as the two principal equipments for this technology. Both suppliers offer specific lines to make fabrics for specific markets. They both have entered the hydroentanglement of pulp-

based air-laid systems and are offering bonding of spunlaid and meltblown webs through hydroentanglement.

Needlepunching technology was the only practicable technology for heavy basis weight applications. However, by raising pressures up to 1000 bars, hydroentanglement technology also appears to be compete with needlepunching in producing heavy fabrics. Fleissner manifolds are now capable of handling water pressures of 600 bars, whereas ICBT/Perfojet claims 1000 bars. In addition to improving the efficiency of hydroentangling, the jet strips have multiple row of orifices. Also, ICBT uses perforated smooth rolls as supporting substrate for getting better entanglement. The underlying reason for raising the bars is just to hydroentangle heavy-basis weight webs from 15 to 600 g/m^2 at claimed production rates of 300-600 m/min.

Figure 2.4 illustrates typical configurations of some of the hydroentanglement section of the lines offered by Fleissner. With the exception of the one step process (not shown), the configurations are designed to conserve energy in hydroentangling both side of the fabric in one unit. There is a continuous development in the hydroentangling unit, since there was up to three steps in ITMA '99, but now multiple steps are produced. It is seen that manifolds are replaced apart from each other when constructing multiple steps unit, for distributing the energy on the fabric more uniformly on the other hand, mostly microporous shell drum without any additional support is used to carry the web [21].

Additionally, different line configurations are available according to the end-use purpose. Spunlace system are available for dry-laid, wet-laid, and spunbonded nonwovens and composites. Different line configurations are shown in Figure 2.5.

One or more cards can be used in hydroentangle line. Usually for manufacturing heavy-weight fabrics, at least two cards and a crosslapper is used. Crosslappers are used to ply the webs and make a web with bimodal fiber orientation. For light or medium weight fabrics, however, one card is enough. Using a crosslapper decreases the speed of the line. The production speed in spunlace nonwovens is not dependent on the entanglement unit. Since manifolds can be added to the machine theoretically the entanglement unit does not have a limit in the speed, but the cost of the machine

then increases. On the other hand, one can also use a spunbond before hydroentanglement for much higher speeds (up to 600 m/min). Another application is the production of high quality nonwovens from micro denier splittable fibers from spunbonded or staple fibers. Air laid machines can be also added in the lines for composite production. It is obvious that, limitless configurations are possible in a spunlace line. All web formation techniques can be used depending the purpose. Web formation technique and hence web structure, has a major impact on the fabric characteristics, and spunlace technology offers a variety of options for the fabric manufacturer. When investing in a spunlace line, the line configuration should be planned not just for today's demand but also for future needs even if the investment costs of the machinery is expensive. Selection of lines, consisting different web preparation systems, can be a wise selection so that one can produce a variety of fabric types for the market. Fabric producers, however, do not reveal their hydroentanglement line(s) configuration due to competition.

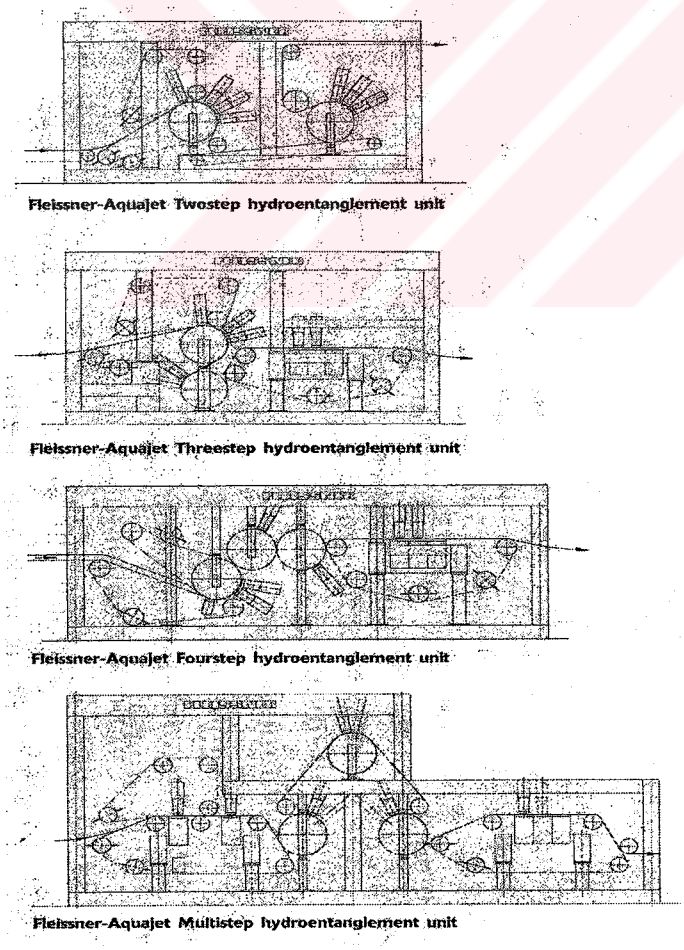

Figure 2.4. Typical configurations of hydroentanglement unit (Fleissner)

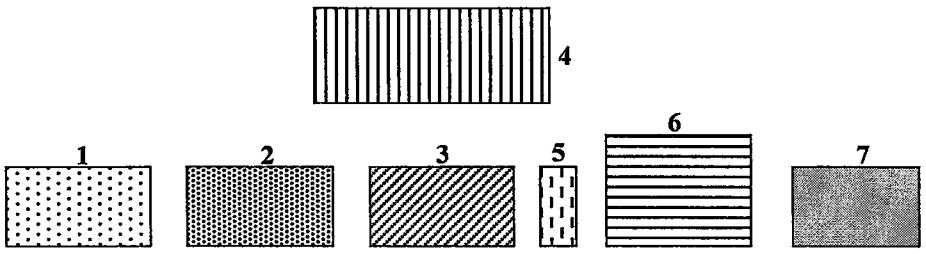

1. card 1
2. card 2
3. spunlace unit
4. water circulation system
5. impregnation
6. dryer
7. winder

Spunlace production line for carded nonwovens – low/medium weight and high speed

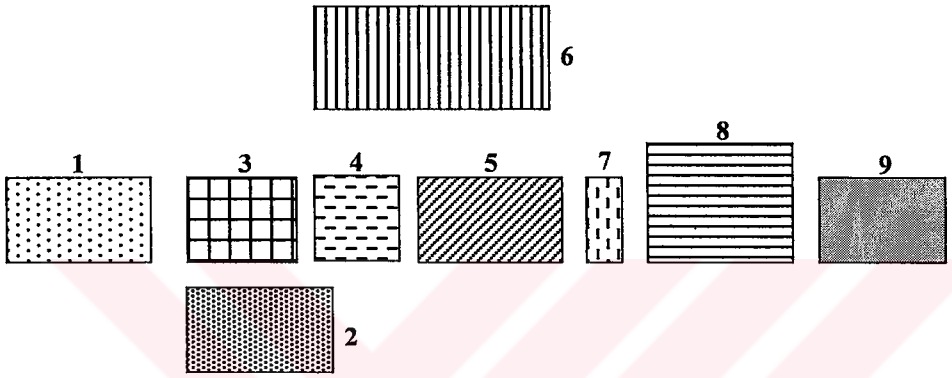

1. card 1
2. card 2
3. crosslaper
4. drafting unit
5. spunlace unit
6. water circulation system
7. impregnation
8. dryer
9. winder

Spunlace production line for carded nonwovens – low/medium/high weight

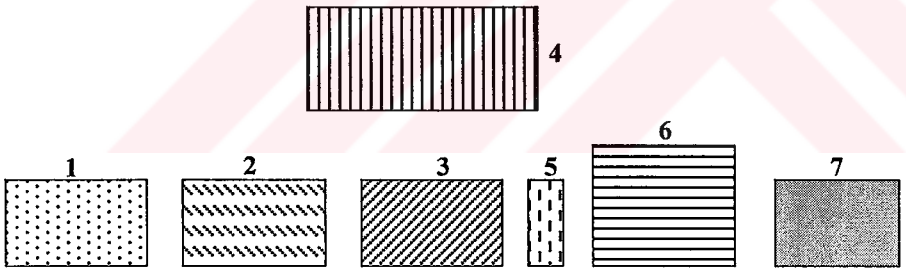

1. card
2. airlaid
3. spunlace unit
4. water circulation system
5. impregnation
6. dryer
7. winder

Spunlace production line for carded/airlaid composite nonwovens – high speed

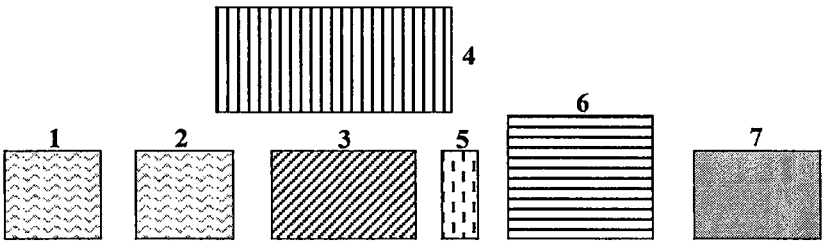

1. spunbond 1
2. spunbond 2
3. spunlace unit
4. water circulation system
5. impregnation
6. dryer
7. winder

Spunlace production line for spunbond nonwovens – high speed 600 m/min, large width up to 5400 mm

Figure 2.5. Various spunlace lines for different purposes (Fleissner)

2.5. Parameters Affecting the Product Performance and Aesthetics

Fiber and web properties have primary effects on the performance of the finished product. These parameters consist of the web material, basis-weight, and web manufacturing method (dry laid, wet laid and spun laid). The characteristics of a good quality precursor web are uniformity, isotropic in-plane and three-dimensional fiber. The degree of fiber entanglement, orientation of fibers in the fabric and resulting properties of the fabric are all determined by the water jet's force acting on the fibers and the fabric forming surface [4].

Bonding of the fabric is achieved by the impact of high-pressure water jets. In the system, the water pressure can reach up to 400 bar before water leaves the nozzle, where the nozzles have a diameter of 0.08 to 0.15mm and are spaced at 40-120 nozzles per inch. The water jets hit the surface at a speed of up to 300 m/sec, penetrate in the fabric and flow to the openings of the forming surface through the suction slots. In spunlace process the fibers are caught, reoriented and entangled, which results in compacting and bonding of the web. Factors that affect the degree of bonding are: fiber type, the impact force of the water jets, the dwelling time of the water jet on the surface unit of the web as a function of the web transport speed and the number of the jet beams (manifolds), the surface structure (degree of opening) of the web and fabric forming screen [4].

The nonwovens producer can utilize spunlace for two entirely different purposes. One method is to make a nonapertured product, which essentially is a way of bonding fibers together. The other method is to make an apertured or patterned end product. The requirements of the forming wires in these two end uses are vastly different. In manufacturing a nonapertured product, the intent is primarily to impart strength to the spunlace product. It can also be used to combine two or more different webs into a composite end product. In this case, little or no mark from the forming wire is desired in the final product. In the apertured nonwovens manufacturing process, a textured product surface with a distinct mark from the forming wire is desired. This is totally opposite to the nonapertured process. The surface topography of the forming wire is extremely important and will have a direct influence on the appearance of the final product [13].

T.C. YÜKSEKÖĞRETİM KURULU
DOKÜMANTASYON MERKEZİ

The fineness of the mesh of the forming screen is also important, it has been shown that the finer substrate yielded a stronger product resulting from that of coarser support when the same energy was imposed to two webs manufactured from different substrate meshes. [22]. The coarser wire support (20 mesh) resulted in a bulkier product with more permeability, but on the other hand lower in strength. The coarser the mesh, the more energy is needed to remove the water. In addition to that, the surface of the fabric can be apertured (textured on the surface) with special designed forming wires [13].

The amount of energy delivered to the web is a crucial parameter influencing the fabric structure and properties since it affects fiber entanglement completeness. 'Completeness' is a term that is defined as the portion of fibers that are tied together. Water pressure is another parameter related to fabric energy intake. There are several water pressure levels used [8].

Table 2.3. Energy requirements for partial or complete entanglement [8]

Level of entanglement	***Water pressure, bars***	***Additional bonding requirement***
Low	30-60	High
Medium	60-90	Medium
High	120-150	Low

Higher energy levels result in stronger fabrics up to a certain point [16-18]. Additionally, shifting the balance of energy input to the second side (low specific energy ratio) can decrease fiber loss significantly. The benefits of different energy ratios are not so clear [16]. Higher water pressure machines are mostly used since energy can be delivered into a web with less water needles and less water consumption which is economically more useful [8].

As the target weight and density of product increases so does the water energy requirement, to a point where web penetration can no longer be achieved without major fiber damage. This results in a fabric of skin-core effect, with fibers bonded at the surfaces but little or no entanglement at the center. Such fabrics easily delaminate and have no commercial value. By selecting the optimum orifice size, shape, concentration and energy distribution, it has been possible to gradually build-up the entanglement with heavy weight webs, to produce unique fabrics of uniform dense structure throughout the cross-section [23].

For lightweight fabrics, the industry trend is to apply the entanglement energy in the form of a multitude of injectors, working at comparatively low pressure. Energy applied in this way to heavy weight webs results in good surface entanglement but weak delaminating core structures [23]. Another basic process parameter having influence on the fabric is the speed of the line. If a constant amount of energy is being delivered to a fabric, the speed of the fabric determines how much energy is going to be absorbed per fabric unit area. Logically, the higher line speeds, the less the energy that is absorbed by the fabric and the lower the fabric strength that is achieved.

2.6. Spunlace Fabric Characteristics

Spunlaced fabrics are unique among nonwoven fabrics because of the balance achieved between strength and shear modulus as shown in qualitative correlation in Figure 2.6. [24].

Microscopic examinations of spunlaced fabric structure reveals that entanglement points are very frequent but the fibers are not tightly entangled. Fibers from the web surface are driven into the web resulting in high Z-direction strength. The combination of jet orifice spacing and screen patterns produces densely spaced, loosely entangled areas arranged in parallel, straight-line patterns joined by unentangled bundles of fibers. This type of structure has low out-of-plane bending rigidity along any axis and low in-plane shear, tensile and compressive moduli resulting in the following fabric characteristics [3]:

- Soft, limp, flexible hand
- High drape
- Conformable and Moldable
- High bulk
- Stretchable without thickness loss
- High strength without binders
- Delamination resistance
- Low linting
- Pattern possibilities

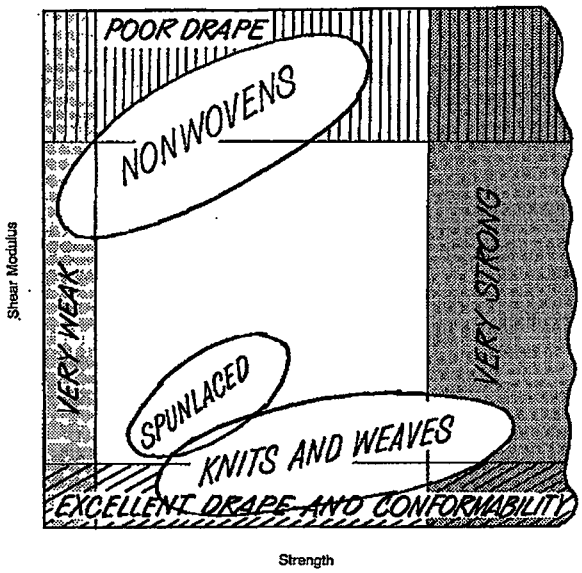

Figure 2.6. Shear modulus-strength of fabrics [24].

2.7. Advantages and Disadvantages of Hydroentanglement Technology

The hydroentanglement technology has the following advantages:

- It uses efficiently the majority of all types of fibers, from long fibers up to 6 cm, to the shorter type such as cotton or wood pulp. Recently it has been shown that fiberwebs of continuos filament can be hydroentangled.
- For a similar web basis weight and fiber composition, the tensile strength of a hydroentangled nonwoven could achieve some 70-80% of that of equivalent woven or knit.
- Addition of binder is not needed, and thus spunlace fabrics are easy to recycle.
- The technology can produce composite materials by hydraulic interlacing of the fiber web with reinforcement scrims and yarns [25].
- The process is environmentally friendly.
- The system protects the inherent fibers without damage to them.
- Good for long runs (high production efficiency and low cost)

The disadvantages of this technology are:

- Lack of acceptable physical properties in regards to strain recovery and abrasion resistance.

- Appearance of the spunlace fabrics is fuzzy and less defined when compared to woven and knits.
- A critical fiber length is needed.
- Can not produce lightweight fabric as compared weaving technology
- High water consumption.
- Fluid recycling and clogging problems of the jets.
- Simple designs compared to knits and wovens.
- Not good for short runs.
- Poor wash durability.
- High initial investment costs.

2.8. Applications and Future

Hydroentanglement process is very suitable way of converting not only the textile fibers, but also new generation and high performance fibers and their blends into nonwovens without damaging them and without the need for binder. The physical characteristics of hydroentangled nonwoven fabrics e.g. softness, flexible hand, high drape and bulk, conformability and moldalibity, high strength without binders and delamination resistance make this process unique among the nonwovens process. The characteristics of fabrics can be engineered according to the end use requirements.

Application areas of spunlaced nonwoven fabrics cover a wide range of product weights, from 20 to 600 g/m^2. A significant part of the hydroentangled fabrics are used for disposable medical products (single use surgical gowns and drapes; breathable, fluid and bacterial barrier fabrics, medical dressings –60% of the market) due to lint-free and clean nature of fabric. Other applications include household products and wipes from cellulose and its blends (20%), fusible textiles and textile interlinings (15%) and other applications (5%) such as thermal apparel insulation, heat resistant fabrics, insulation (glass fiber webs), roofing, filtration, hydrophilic and hydrophobic laminates. Versatility of the process also opens up endless opportunities for its industrial applications. Current industrial applications include aircraft seat fire-blocking, auto hood veiling, high temperature and corrosive filter fabrics, fire-fighter turn out jackets from high performance aramid fibers that have

high melt temperature and chemical resistance. Other applications include insulation and roofing, floppy disc liners and pultrusion from polyester fabrics. Glass fiber is another candidate, as well as Kevlar and Nomex for hydroentangled composite fabrics [14].

Hydroentangled fabrics' tensile strength, resistance to tear, and bending behavior are comparable to those of woven and knits, however they exhibit low initial modulus, poor tensile recovery and wash durability. Additionally, spunlace fabrics are limited in variety of designs, patterns, and their appearance is fuzzy and less defined as compared with woven and knits. To expand the markets for spunlace fabrics beyond their traditional end uses, improvements in initial modulus, stretch recovery, wash durability, and aesthetics are needed. These classes of fabrics can be formed with texture that resembles woven and knits. It is expected that this technology will strongly compete with weaving and knitting in the future in the commodity fabric enduses.

3. PREVIOUS STUDIES

3.1. Hydroentanglement Research

Hydroentanglement fabric producers consider information about this process highly proprietary [16]. This is the reasons behind the fact that many articles published in trade journals about hydroentanglement process and products but very few articles are published in the scientific literature in the area of the impact of processing and fiber parameters, and their interactions on the aesthetics and the performance of the spunlace fabrics [14, 16, 17, 26-28].

The limited published research work has focused on the influence of the specific energy on fabric properties and reducing process energy consumption. Connolly and Parent [16] have investigated the influence of the specific energy on fabric properties. They selected polyester and rayon blend fabrics containing fibers of similar deniers and staple lengths. They have produced fabrics with varying weight and entangled them under various energy levels. They found that higher energy levels result in stronger fabrics up to a certain point fibers produced with low specific energy ratio (shifting the balance of energy input to the second side of the fabric) decreases the fiber loss significantly. From the strength point of view, however, the benefits of energy ratio is not so clear. They have also showed that simple carded and cross-lapped spunlaced fabrics can be comparable in strength to conventional woven and knitted fabric with the exception of washing durability. Timble and Gilmore [17], and Timble and Allen [18] have also reported the influence of specific energy on spunlace fabric properties. They have used different fibers: unbleached, bleached and low micronaire unbleached cotton [17]; and polyester-unbleached cotton blends [18] in their studies. Timble and Gilmore [17] have shown that the weight loss on hydroentangled unbleached cotton fabrics increases with increasing specific energy level. They also found that strength, stiffness and tear strength had an increasing tendency whereas fabric elongation decreases with increase in specific energy level. Unbleached and bleached hydroentangled cotton fabrics had almost the same tensile

strength, but hydroentangled unbleached cotton fabric had better tear strength compared to bleached ones. Fabrics from lower micronaire unbleached cotton fabrics were stiffer and stronger than higher micronaire cotton fabrics. In another study, Timble and Allen [18] used polyester and unbleached cotton blends to investigate the effect of blending polyester fiber with cotton on hydroentangled physical properties and to investigate the effect of various specific energy levels on tensile strength. They concluded that increasing of the polyester content in the fabrics results in increased cross direction strength, increase in machine direction elongation, increase in tear strength and decrease in stiffness of polyester-cotton blended fabrics. The absorption capacity occurred suddenly at higher energy levels with increase in polyester content. In another study, Hwo and Shiffler [27] used PTT (polytrimethylene terephthalate), Polyester and Nylon investigated the impact of fiber type on fabric properties. They showed that inherent low fiber bending rigidity of the PTT fiber has provided the following characteristics in the fabrics: break strength significantly developed at very low specific energy levels (80 kJ/kg), the flexural rigidity of the fabrics did not increase with specific energy and tear strength also significantly developed at 40 kJ/kg. PTT showed comparable tensile strength, tensile elongation and tear strength at meaningful lower energy levels when compared to PET, Nylon and PET/Nylon blends. In addition PTT provided a favorable strength – flexural rigidity balance, which should result more drapeable fabric, and PTT fabrics are rated softer than the other fabrics subjectively. Acar et al [14] produced composites from glass and aramid fibers (Kevlar and Twaron), for industrial and composite applications. They concluded that by selecting the right combination of fibers, adjusting pass rate and water pressure, there is a big potential to manufacture composites using hydroentanglement technology. More recently, Ghassemieh et al [26] reported on the improvement of the efficiency of energy transfer in the hydroentanglement process. They have produced Viscose-PET blend fabrics from different web weights. Additionally PET and Twaron fabrics were formed and studied. They have investigated the relationship between fabric strength, water jet pressure and hydraulic energy consumption. They reached a conclusion similar to Connolly et al [16] that fabric strength increases as energy increases to a certain point and then levels off. They called this point as the critical water jet pressure. They found that critical pressure increases with the web density and can be correlated with fiber properties. They suggested that pass speed has little effect on

strength at a pressure lower than critical pressure except for Twaron fabrics. They concluded that the quality of the fabric produced and the efficiency of the energy transfer are highly dependent on the energy distribution over the fabric. Different efficiencies can be obtained by different pressure profile schemes. In order to reduce energy consumption, while maintaining the strength and modulus of the product, one should identify the optimum pressure profile, which depends on the web and fiber properties.

There are some other works in the open literature on hydroentanglement research that deals on theoretical and experimental analysis on the tensile mechanism of these nonwovens [29] and improving the spunlace fabrics by foamed latex bonding [28]. From the analyses on the tensile mechanism [29], it was found that increasing of the fiber compactness (ratio of hole area per unit area) showed higher slippage and the frequency of fiber orientation distribution is gradually increase at the machine direction. The tensile strength increased as fabric is consolidated and they obtained a considerably good agreement with the theoretical and experimental stress-strain data. On the other hand, Shahani et al [29], investigated the effect of foamed latex bonding of spunlace fabrics to improve physical properties. They used polyester, acrylic and cotton fibers. They have applied very low levels (less than 5%) of acrylic latex binder as foam to hydroentangled fabrics. The addition of the binder significantly increased the break strength, load at 5% strain, abrasion resistance, strain recovery and the bending rigidity.

3.2. Image Analysis in Textiles

Image analysis is a technique concerned with extracting useful measurements, data, or other information from an image field. The results of image content analysis are usually expressed numerically or in the form of quantitative descriptions of the image contents. But the original image is not always in a proper form for an analysis; it must often be enhanced to improve its appearance or to be converted into a form that is better suited to human or instrumental analysis. Such enhancement or conversion procedures are called image-processing [30].

Digital image processing first involves capturing a video image of a scene and converting it into digital (or numerical) form. Thus the scene is represented by a

digital image comprising many tiny picture elements (or "pixels"). Each pixel has a number assigned to it by the digitizing process as a measure for the intensity of light at a specific location in the scene. For 8-bit images this number is in the range 0-255. Pixels that represent the darkest parts of the scene have values close to 0, while the brightest pixels have values tending towards 255. By connecting the video camera to a personal computer, using a special "framestore" board as the interface, the computer can be programmed to treat the information in the scene as an array of numbers, much like a giant spreadsheet. Calculations can be carried out on these numbers to determine various features associated with the original scene[31].

In the textile field, image analysis is mainly used for textile product structures such as carpets, woven and knitted fabrics, and nonwovens. Various studies have been made on these structures that are shown in Table 3.1.

Table 3.1. Studies on textile structures using image analysis

Carpets	**Woven and Knitted Fabrics**	**Nonwovens**
Appearance characteristics [30,33-35, 36-42, 80]	Pilling [43-47]	Fiber Orientation analysis [61-70]
	Fuzziness, hairiness [48-50]	Pore analysis [70-75]
	Smoothness (wrinkling, creasing) [43, 51-54]	Fiber diameter measurements [70, 76-78]
	Roughness [55-60]	Web uniformity analysis [70, 79]

3.2.1. Carpet texture studies

The application of image analysis to appearance measurements in carpets is firmly established in the literature [30,33-35, 36-42, 80], and digital image analysis offers the most promising avenue to the future development of a rapid and reliable instrumental method for measuring carpet texture. Researchers at the University of Maryland at College Park (UMCP) and the Wool Research Organization of New Zealand (WRONZ) had given considerable effort to investigate carpet texture [30, 32-39, 41, 42]. In these investigations, researchers tried to identify and investigate the parameters that reliably discriminate between different carpet textures or different levels of wear in carpets. Two conclusions have been reached: First, carpet appearance parameters derived using different image processing algorithms may be

quite highly correlated, implying that they actually measure the same characteristic. Second, no unique parameter exists that is capable of completely describing the appearance characteristics of all carpet types. Rather, a set of parameters is required to fully specify appearance, with the relative importance of individual parameters depending on the sort of carpet being considered. The unique nature of carpet pile texture and the reasons for measuring it mean that the general approach must inevitably be pragmatic. There is no "right" or "wrong" way to tackle the problem of measuring carpet texture. If a particular algorithm provides a measure that agrees well with human perception of the level of wear treatment and is versatile across a wide range of carpets, then it might be regarded as successful and useful [41,42]. Xu summarized carpet appearance characteristics and corresponding image analysis techniques as shown in Table 3.2. [40].

Table 3.2. Carpet characteristics and applied image analysis techniques [40]

Tuft definition	Tuft Geometry	Tuft placement	Periodicity	Texture	Pile lay Orientation	Roughness
Local intensity variation (LIV) [33]	Size measurements [30]	Tuft evenness [30]	Two-dimensional Fourier transform [35]	Run length matrix [81]	Flow-field analysis [82]	Normalize relief [38]
Image moments [38]	Shape Analysis [30]	Distance measure [39]	Auto correlation function [35]	Neighboring gray level dependence statistics [81]		Fractal dimension [38]
		Spatial density [39]	Image covariance [37] co-occurrence matrix [36]			

Jose et al started analyzing actual carpets and their photographs using computerized image analysis at UMCP. They had simply correlated gray level histograms with changes in appearance, differences in tuft spacing and related carpet properties [32]. Lee et al also analyzed carpets by using image analysis at WRONZ and applied four texture matrix methods to carpet texture measurement: gray level run length matrix (GLRLM), spatial gray level dependence method (SGLRDM), neighboring gray level dependence matrix (NGLDRM), and gray level difference matrix at (GLDM) [81], and later on, another technique, based on an edge detection filter such as a Sobel filter, named local intensity variation (LIV) is preferred for determining a

T.C. YÜKSEKÖĞRETİM KURULU DOKÜMANTASYON MERKEZİ

relative (and bulk) measure of carpet texture [33]. Wu et al reported however, that the LIV or other bulk techniques yielded mixed and unpredictable results [34].

Wu et al have attempted to use colored images to analyze carpets. Color imaging offers distinct advantages over gray level imaging in evaluating soiling, staining and wear, with their concomitant changes in carpet color as well as texture. They used the histograms of the red, green, and blue (RGB) color components and the luminance (L) component to depict the colors of nylon and polyester carpets and changes in these colors due to wear [34]. The shifts in the mean values of these histograms depend on the illuminant used and the nature of the wear treatment, i.e., floor-worn or machine-worn (Vetterman drum). The magnitude and the direction of the shifts were different for the three color components, but the trends were similar for all carpets studied. This work concluded that the color image processing has distinct advantages over monochrome images for carpet appearance characterization, but interpreting color shifts from RGB histogram data is not particularly easy. Also the use of full-color images requires more elaborate control of the illumination and camera characteristics. The color temperature of the light source and the spectral response of the camera assume greater importance in full-color imaging. Also, measures of pile lightness may be readily derived from monochrome images of carpets and these correlates closely to luminance. For these reasons, color change in carpets due to wear (in absence of soiling) is believed to be essentially a lightness change [83]. So, researchers used monochrome (gray level) images for carpets which are much more easier to process comparing to color images.

Another approach for characterizing carpet appearance is tuft geometry and tuft displacement [30, 39]. Wu et al introduced concepts of evenness, or tuft spatial distribution and shape of individual tufts, and demonstrated the effectiveness of these approaches using image enhancement, valley mapping, and tuft isolation techniques on both nylon and polyester carpets [30]. Pourdeyhimi et al also measured tuft spatial distribution using the gravity centers of local intensity maxima to indicate the position of tuft centers. The placements of these points are then analyzed with respect to average distance, density, and spatial pattern [39].

The periodic attributes of carpet images are robust indicators of texture[36]. Researchers have explored the periodicity of texture from different perspectives. The

regular periodic nature of many textile patterns permits Fourier transform techniques in image processing to be used to measure their visual characteristics. In carpets, the patterns may be due to either the arrangement of the pile or the repetition of a colored design. Wood investigated carpet texture using two dimensional Fourier transform techniques [35]. The Fourier power spectrum provides a useful description of the spatial frequency content in a digital image, and in particular the coarseness of any texture present. The techniques have been considered to be very appropriate for their conceptual and computational simplicity as well as good discrimination. Sobus et al used two different techniques for measuring periodicity: co-occurrence analysis [36, 39] and image covariance method [37]. Co-occurrence methods have the advantage of no preprocessing of individual image objects that is required. Although covariance method is computationally more quick and efficient than co-occurrence analysis, binary conversion is essential as a preprocessing step. The results of covariance method for period length estimation were comparable but not identical to gray level co-occurrence analysis. The discrepancies were due to information loss in the binary operation; both methods should yield very similar results for high contrast images. However, the results have been qualitatively consistent with those obtained by co-occurrence analysis [37].

Another parameter of measuring carpet characteristic is surface roughness. It is determined on surface relief or fractal dimension for carpets [39]. A truly fractal surface shows the same degree of roughness at all magnification levels; natural surfaces may exhibit fractal properties for a restricted magnification. Pourdeyhimi et al used reticular cell counting method for fractal analysis as described by Rao [84] who recommends it for its computational efficiency. They assumed that their natural surfaces played fractal properties over the range of the scale employed, but Rao notes that while different methods for estimating D (fractal dimension) produce similar rankings, they differ numerically, and the estimations of the fractal dimension is considered in their study in a relative sense [39]. They found that both normalized area and fractal dimension decreased (smoothed) as the surface became flatter and therefore more reflective. Mean intensity and fractal dimension appeared to be a consistent indicator of texture change in their study. Pourdeyhimi et al [82] also explored the application of image analysis to quantify pile lay orientation using flow-field analysis described by Rao [84]. In flow-field analysis, a gray–scale carpet

image is split into series of small windows. The average of each window is then computed, and the resulting orientation data can be used to derive the dominant orientation of the texture. These data can also be used to visualize flow by creating a flow map that employs short line segments to indicate the directions of oriented components [84]

3.2.2. Evaluation of nonwovens using image analysis

Fiber orientation is clearly an important structural characteristic that influences many physical and mechanical properties of web. As indicated by Hearle et al, the properties of a nonwoven fabric will depend on the nature of the component fibers as well as the way in which the fibers are arranged [85]. Experimental methods for measuring fiber orientation extend back to 1963 when Hearle and Stevenson explored the utility of a micro-densitometer as well as a projection microscope [86]. They used direct fiber counting method, which is tedious and time consuming, later, researchers discovered indirect techniques [62]. Indirect techniques, however, are highly dependent on the validity of assumptions and theories employed in fiber orientation. For this reason, although fiber counting is tedious and time consuming, the reliability of most indirect methods is evaluated by comparing the results to fiber counting. Since fiber counting is considered to provide reliable fiber orientation results, a way to speed up and automate fiber counting would remove a major obstacle that limits its use.

Later on, workers have used image analysis techniques to evaluate nonwoven structures. Huang and Bresee [62] developed a random sampling algorithm and a software to analyze fiber orientation in thin webs. In this algorithm, fibers are randomly selected and traced to estimate the orientation angles; then a diameter-based distribution is generated, based on the measurements of the lengths, diameters, and orientation angles of measured fibers. The test results showed an excellent agreement with results from the visual measurements. Pourdeyhimi et al used a direct tracking algorithm [65], Fourier analysis [66], and flow field [68] analysis technique to characterize a series of simulated nonwoven fabrics where fiber orientations were known. At the images they present, direct tracking algorithm remained the optimal choice in terms of off-line accuracy. The Fourier method was fairly accurate and

reliable but tended to slightly overestimate the standard deviation of the distribution, although the proper windowing and removal of unwanted frequencies were done prior to any measurement. The results of the flow field analysis showed that, for the most part, the method was fairly accurate and reliable, but was aimed at obtaining the mean orientation angle, not the orientation distribution function, and hence ranked behind both the direct method and the Fourier method for this purpose. They had also similar results with real webs [69]. Xu, et al [67] used Hough transform (HT) for determining fiber orientation distribution and they compared their results with those obtained from zero-span tensile testing method. The principal of using HT is that it is robust in suppressing image noise and is able to deal with fibers containing gaps and breaks. Measurements with HT method have shown good correlation compared with the zero-span tensile testing.

Pore size and shape is another important characteristic that influences the mechanical and physical properties of nonwoven fabrics. Conventional methods of determining pore size, such as sieving and hydrodynamic filtration, are time consuming, however, often reliable. A number of theoretical methods have also been developed for estimating pore size and distribution, but their utility and general applicability remain suspect. Pourdeyhimi et al used geometrical methods for both size and shape measurements on simulated images. They also used Fourier methods to measure shape and granulometry method for size measurements. In these methods, geometrical methods have provided exact measures of pore size and shape, however morphological methods did not provide sufficient measurement of pore size while Fourier methods provided reliable measures of shape [72, 73]. Nonetheless, it must be kept in mind that image analysis methods were only limited to thin webs for pore measurements.

Fiber diameter has a role in determining nonwoven web properties, including porosity, web uniformity, filtration efficiency and mechanical properties. It is therefore important to quantify fiber diameters in webs. Measurements of fiber diameters are often obtained by manual methods. A typical procedure involves acquiring web images (or photographs) by an optical microscope or scanning electronic microscope, drawing one or two diagonals on each image and measuring the diameters of fibers intersecting diagonal lines using a ruler or pointing device (e.g. computer mouse). This method is time consuming, it produces results that differ

among operators and causes results that are influenced by human fatigue. Moreover, it is difficult to obtain enough measurements to provide statistical meaningful results from such a tedious procedure if webs have large diameter variations. Manual measurements can often be improved by automation. Huang et al [76] and Pourdeyhimi et al [77,78] determined fiber diameter distributions using image analysis. Pourdeyhimi et al [77,78] applied distance transform technique to estimate fiber diameter distribution in nonwovens. They used a binary image to create a "distance map" of the image, which recorded the distance from each pixel to the background. From the distance map, the fiber diameter at any pixel location was determined. They tested their technique both with simulated nonwoven images and real webs, and if the image quality is good enough to allow reliable automatic thresholding of the images, then distance transform can be adapted to determine fiber diameter distributions in nonwoven webs [78].

Web uniformity can be categorized three ways: weight (mass) uniformity, structural uniformity and visual uniformity. Huang et al [79] have investigated web uniformity by image analysis, and derived a connection between mass uniformity and optical uniformity characterized in both cases by the coefficient of variation. They have employed different techniques to characterize uniformity. These were non-uniformity spectral analysis and non-uniform texture pattern extraction. Their results have showed that web mass was linearly related to optical density and the coefficient of weight variation was linearly related to the coefficient of optical variation. Militky et al measured visual uniformity to quantify surface appearance irregularity of nonwovens. They have used microscope and a CCD camera to capture the images. They used software named LUCIA-M for image processing. Optical uniformity is measured both subjectively by human eye and objectively by the image analysis. The evaluation of appearance uniformity has been based on the variation coefficient estimation and on the ANOVA (analysis of variance) model. They have concluded that their proposed methods can be used for lightweight nonwovens without any problem [87].

3.2.3. Objective evaluation of woven and knitted fabrics

For the textile industry, the comfort properties of fabrics -handle and appearance- have become a very important sales issue. The characteristics of textile fabrics in general, and of technical textiles in particular, are dependent on their geometry and surface contours. These are determined in a complex manner by the surface structure of the fibers and the yarn and fabric construction. This statement applies both to subjective characteristics such as appearance and handle, and to technical usage characteristics [55].

Surface texture, and thus fabric appearance, traditionally evaluated by observers following the procedures set in a number of standardized methods [88, 89]. But, these methods are now characterized by poor accuracy because of their subjective nature. It is therefore desirable to create a new objective fabric evaluation systems for the textile and related industries based on more advanced technologies.

Fabric appearance can be characterized from the following perspectives: wrinkle, stain, pill, crease, smoothness, and color [43]. A wrinkle is defined under standard ASTM D123 as an undesirable crease or a short and irregular deformation in a fabric. There have been attempts to automate this characterization process using image analysis [51-54]. Wrinkling is quantified easily using different image analysis techniques. One way of acquiring surface data from a fabric specimen is by a laser probe to measure surface height variation [53]; these devices have excellent resolution in order of microns. However fabric has to be scanned in two directions and this makes data acquisition too slow to be suitable for industrial applications. Na et al [51] used power spectral density to determine the degree to which the replicate surface is distorted from a plane. The results were consistent with the degrees of wrinkling and their associated subjective ranking. They used also, co-occurrence method for randomness, and surface area, normalized relief, and surface fractal dimension for roughness measurements. The results showed that wrinkling correlated well with roughness and surface area. The methods that are used in this study are applicable to simple fabrics. Xu et al have used a video camera with a lighting system [54], although these systems produce good resolution, they are sensitive to color, further the system can not analyze fabrics with constructed or printed designs. Xu et al [52] also developed an instrument for fabric wrinkle grading based on a laser

triangulation technique. Due to the rotation of the sample, the system is insensitive to fabrics uni-directionally wrinkled, and it is also insensitive to color differences on the fabric.

Pilling on textile fabrics is a well-known problem. Pilling is affected by numerous textile structure variables, including fiber, yarn, fabric, and finishing treatments. Many of these variables have been carefully controlled to reduce pilling, but it continues to be a problem. Pilling is also affected by abrasion related problems [45]. More than 20 methods have been developed to evaluate pilling, but no method in wide spread use detects pills conveniently and objectively or describes them completely [45]. Pills are described according to ASTM as "bunches or balls of entangled fibers that are held to the surface of a fabric by one or more fibers". Since the unaided eye possesses poor spatial resolution, one would expect to experience difficulty in distinguishing low-density pills from fuzz. Konda et al [44] have developed a method of comparing images of pilled samples taken by a video camera with corresponding images of standard photographs to determine a fabric pilling grade. The method was useful for plain-colored fabrics, but is lack for patterned ones because the camera could not distinguish between pills and dark regions of fabric. Ramgulam et al [47] measured laser-light scattering from fibers on fabric surfaces to obtain a surface profile of the test fabric. By selecting a suitable threshold value of height, they segmented each sample surface into two separate zones-pills and background. Once pills were detected, the number, projected area, and height of pills were computed. His et al [45], have used fluorescent illumination, and thresholded their images using a technique that called brightness-thresholding reported by Huang et al [71]. Pills were located by run-length encoding, and images were size-thresholded. This process has provided an image displaying pills without displaying the base fabric. They also compared their results with visual pill ratings, and concluded that image-analysis technique may provide a wealth of detailed information about pilling but their system is limited to uncolored or lightly colored solid shade fabrics that are not highly textured [45]. Recently, Sirikasemlert, et al [90], have used laser triangulation technique to study pilling of knitted fabrics. They have investigated a number of data analytical techniques for this purpose, including roughness, statistical, fractal, two dimensional Fourier, and wavelet analysis. Among

these techniques, wavelet energy has given the highest correlation coefficient with subjective grades.

Fabric fuzziness refers to the severity of hairiness of a fabric caused by untangled fiber ends protruding from the surface, and indicates fabric deterioration in structure and appearance after repetitive abrasions in service. Although the average height and density of protruding fiber ends are the information that can be directly used to evaluate fuzziness, fiber ends are too short and too fine to permit reliable measurements of fiber heights and density over a large area. In practice, visual examinations are often used for fuzziness evaluation despite the subjective nature of the method. Hairiness is important in giving a textile fabric a characteristic structure. It makes the effective surface three dimensional with many hidden areas. Lin et al [49] applied wavelet transform to quantifying fabric fuzziness in a customized image analysis system. They have constructed an index from the average powers of the components from different frequency bands, finding index did not require information about the height or density of individual fuzz fibers, and have demonstrated to be indicative of fabric fuzziness. His et al [48] and Bueno et al [58] have developed devices to measure fabric fuzziness. His et al [48] also developed an image analysis-based software to detect in-focus fibers elevated from fabric surfaces and to describe these fibers in substantial quantitative detail. The key feature of their instrument was an algorithm to detect out-of-focus fiber segments in individual images in order to delete them from the images before fuzz was described. A procedure has been developed to allow the results of out-of-focus fuzz detection/deletion to be visualized. A comparison of the measurements for fabrics with intuitively known fuzz attributes have shown that the fuzz analysis instrument have provided reasonable results, they have also concluded that the instrument could be used for assessing the influence of the yarn interlacing pattern, mechanical abrasion, and a fuzz-reducing finish on fuzz. Bueno et al [58] have developed a hairiness meter for fabrics which directly measured the hairiness quantity on fabric surface. They have used a laser diode that is placed tangentially to the material. They have captured both the structures (the interlaced threads) and the surface hairiness, the structure information contained in the transmitted ray has been stopped with a direct current filter. The measured hairiness parameter has found to be proportional to the fabric hairiness meter. Kim et al [50] have characterized fuzz in nonwovens by

using a cylindrical lighting system. Fuzz in nonwovens is affected by the inherent anisotropy of their structure resulting from the orientation distribution of fibers as well as the bond patterns. They have captured the images by their new cylindrical lighting system, and have demonstrated the usefulness of the system. They have concluded that this lighting system is also very useful for determining the degree of pilling in woven and knitted fabrics.

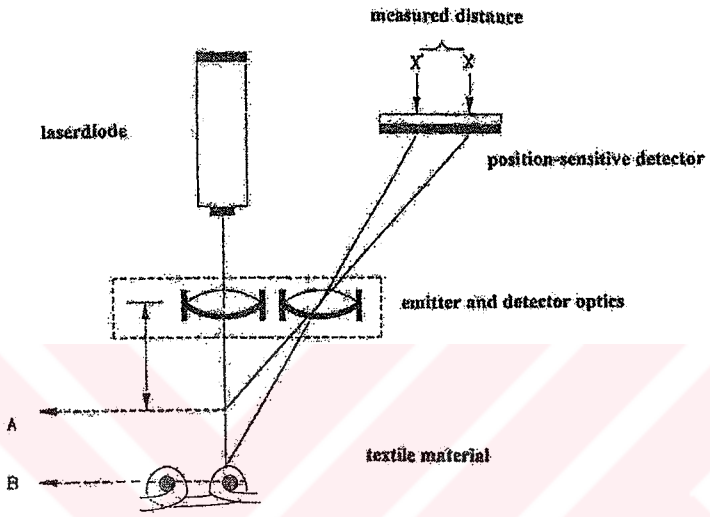

Figure 3.1. Principle of laser triangulation technique [57, 59]

Fabric smoothness or roughness is a desirable appearance for most garments. AATCC Test Method 124 (ISO 7768) specifies procedures and provides the three dimensional standard replicas for assessing smoothness of fabric appearance. These replicas are similar to those used for assessing smoothness of fabric appearance. Several studies characterize surface texture by non-contact methods, using different surface acquisition and signal processing methods. Some authors take one-dimensional measurements with a profilometer based on laser triangulation technique (Figure 3.1) [57,59]. The acquisition device is a sensor that may scan in only one direction or in all the surface directions if one rotates the sample in its plane between measurements [59]. Or the acquisition can be two dimensional [35, 41, 45] or a scanner [60]. Several types of signal processing are possible. If the surface is not periodic, topographical parameters are usually employed [55, 56, 59] in texture analysis for both optical and mechanical parameters, such as vertical parameters (mean roughness, centerline averaging etc.), or parameters of the profile height

distribution (root mean square, standard deviation, skewness, kurtosis, etc.). Fractal dimension is used as a mean of measuring surface roughness of a fabric [38]. The fractal dimension of a surface has proven highly consistent with the perceived smoothness of the surface. One algorithm for computing surface fractal dimension is reticular cell counting [38, 84].

Bueno et al [58] have developed an optical multidirectional roughness meter (Figure 3.2) to measure periodic and quasi periodic fabric roughness. They have used diode laser to scan the fabric surface and have studied the signal obtained from the reflected ray by Fourier analysis. Results from different fabrics were not comparable, and the system was sensitive to fabric color. This method was practical for light colored fabrics.

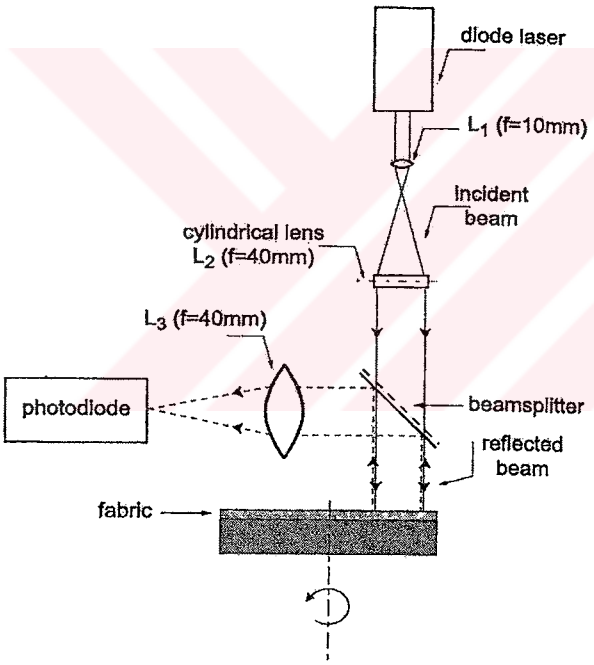

Figure 3.2. Diagram of the optical roughness meter [58]

4. OBJECTIVES

Hydroentanglement technology is one of the leading technologies in the nonwovens sector. Manufacturers aim to produce textiles alike conventional textiles whereas they have to overcome some difficulties in the technology. Many researchers have used image analysis techniques for objective evaluation of fabrics and carpets however hydroentangled nonwovens' texture analyses are not studied so far.

From this point, the intention in this research is to develop an optical method and a turnkey imaging system for classifying texture in hydroentangled fabrics. So as to compare the texture similarity of hydroentangled fabrics and those of fabrics they are to replace objectively by measuring surface properties for the purposes of developing a reliable and efficient objective evaluation method for assessing hydroentangled fabrics.

Consequently, the main objective of this research is the systematic experimental investigation of the textural properties of hydroentangled fabrics with a view to determine:

- the influence of abrasion on texture change
- how closely the texture is reproduced
- the efficiency of the texture transfer from the forming belt to the fabric as a function of the process parameters
- how reliable the jet streaks are determined.

5. EXPERIMENTAL

5.1. Methodology

Texture is observed in the structural patterns of surfaces of objects such as wood, grain, sand, grass, and cloth. The term texture originates from the Latin word textura, which means, "to weave". The term texture generally refers to repetition of basic texture elements called texels. A texel contains several pixels, whose placement could be periodic, quasi-periodic or random. Natural textures are generally random, whereas artificial textures are often deterministic or periodic. Texture may be coarse, fine, smooth, granulated, rippled, regular, irregular, or linear [91]. In image analysis, texture is broadly classified into two main categories, statistical and structural [92].

The texture of an image is characterized by its spatial distribution of the gray levels and tonal features (i.e., connected pixels of similar gray level). Where a small area of an image has little variation in the level of tonal features, the dominant property of that area is its gray level. On the other hand, if the area has a wide variation of features of distinct gray level, its dominant property is texture.

Another way of considering textures is a continuum between two extremes. At one end is the deterministic texture, which has a regular pattern and is suitable for the structural method of analysis. In this approach, a texture is considered to be defined by elements "textels" that occur repeatedly according to placement rules. The chessboard pattern is a simple example of a deterministic texture. The other extreme is the stochastic (or random) texture, well exemplified by white noise on a television screen. Observable textures occur somewhere between these two. All sorts of textures can be analyzed by the statistical approach, where texture is regarded as a complex pictorial pattern defined by statistics [33].

A different approach for defining texture is from Rao who proposes three elemental categories that may be used to classify naturally occuring textures (Figure 5.1). Strongly ordered textures are composed of repeating features that are distributed in a

regular fashion throughout the image, and may be characterized by specifying feature geometry and spatial distribution. An important category of textures, which can neither be modeled statistically nor structurally is that of weakly ordered, or oriented textures. Such textures are characterized by a dominant local orientation at each point of the texture, which can vary arbitrarily, and disordered textures are those that show neither repetitiveness nor orientation. A statistical model is appropriate for this type of textures [84].

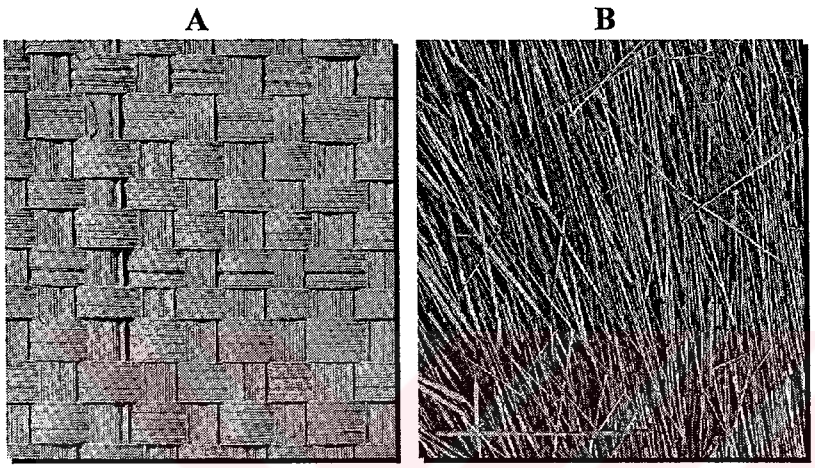

Figure 5.1. An example for strongly ordered (A) and disoriented texture (B)[84]

There are a number of ways that one may quantify texture. The choice of the method depends however on the information sought. Two aspects of texture are very critical. These are texture periodicity and texture definition. Texture periodicity is the repetition of texture elements in a region, where as the texture definition is the strength or amplitude of the texture. These attributes may be measured by: spatial co-occurrence, morphological co-variance, fourier transform, autocorrelation, etc. Studying fabric surface texture requires a study of fabric periodicity or what it has been referred to as macro texture. Though it is shown that spatial co-occurrence method is the most effective method for texture classification and the viability of several approaches are firmly established in literature for determining carpet appearance changes due to mechanical wear [30, 32-42]. Here, in this research, the application of this method is extended for fabrics (especially hydroentangled nonwovens).

Co-occurrence analysis is a "global" technique, which summarizes weighted inputs from the entire image. This technique does not require serious image preprocessing but must be interpreted with care. For the understanding of the technique, assume a discrete (i.e. digitized) X by Y picture I(x,y) on the x,y plane with XY sample points, each of them having G possible gray level values.

Spatial co-occurrence examines the second-order, joint-conditional probability density function, $f(i,m|d,\theta)$ for the probability of sampling a pair of pixel positions with intensity values i and m, separated by distance d in direction θ. In practice, an image is systematically sampled by examining every pixel of an image for which a neighboring pixel exists d units away in direction θ. The intensity of the current pixel, i, and that of its neighbor, m, constitute a single co-occurrence of i and m for given sampling parameters d and θ. The frequency of all co-occurrences are stored in a matrix, $\boldsymbol{M}$, of dimensions N by N. Thus, entry i, m in the matrix is the number of i, m pairs sampled in the image. Typically, these frequencies are normalized by the sample size. For a rectangular raster, there are eight directions: 0 (right), 45 (up right), 90 (up), 135 (up left), 180 (left), 225 (down left), 270 (down) and 315 (down right).

For example, an image is composed of 3 gray levels (0,1 and 2). If a matrix M is defined by dividing every element in Matrix C by the total numbers of point pairs, i,m is an estimate of the joint probability that a pair of points will have gray levels i, m. Here the co-occurrence matrix is defined in a given distance (d=1) and a given direction (θ =0 right) (Figure 5.2).

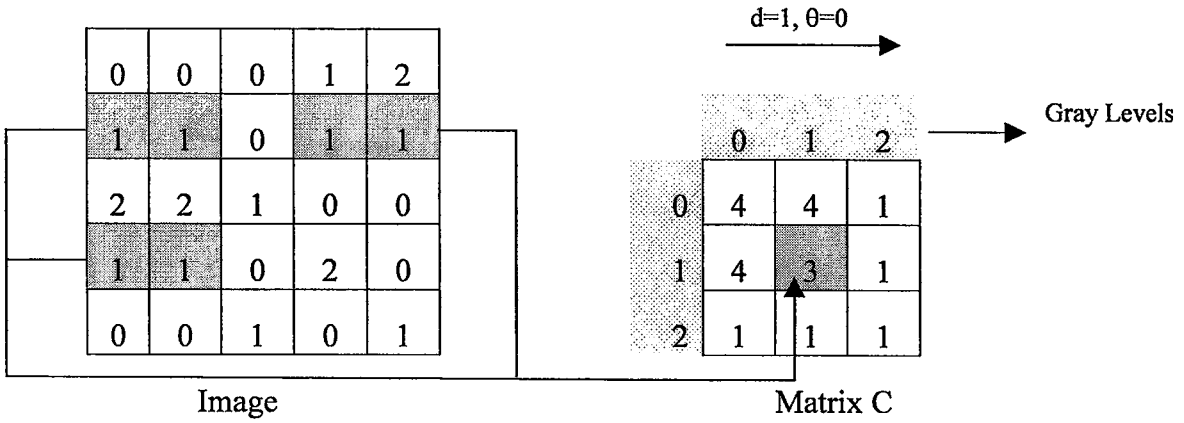

Figure 5.2. Construction of co-occurrence matrix.

The degree of spatial correlation will be reflected in the co-occurrence matrix. If the intensities change over short distances, the frequencies will be spread more evenly across the matrix than if intensities change gradually over distance. A number of statistics have been devised to describe this spread, or moment, away from the main diagonal, where $i=m$ (a full description of this technique is detailed elsewhere [36]). It is concentrated here on *contrast* (otherwise known as *inertia*), defined as :

$$\text{Contrast} = \sum_{i=0}^{n}\sum_{m=0}^{n}\{(i-m)^2 M_{i,m}\} \qquad (5.1)$$

Contrast is a moment statistic and is proportional to the degree of spread away from the main diagonal of $\boldsymbol{M}$ (Figure 5.3).

Spatial co-occurrence may also be utilized to investigate periodic patterns since aspects of texture periodicity (amplitude, frequency, direction) will be reflected in the co-occurrence matrix [39]. For example, a repeating pattern with a period θ for which $\theta > d$ implies that sampled pairs will have similar intensities, thus increasing the frequencies about the diagonal of $\boldsymbol{M}$. If $d \sim \theta$, sampling will generate a relatively uniform $\boldsymbol{M}$. Each $\boldsymbol{M}$ is defined for a given set of d and θ, but one may compute a series of matrices for a range of d, say 1 to 100. Such a series would represent changing texture features over 100 pixels.

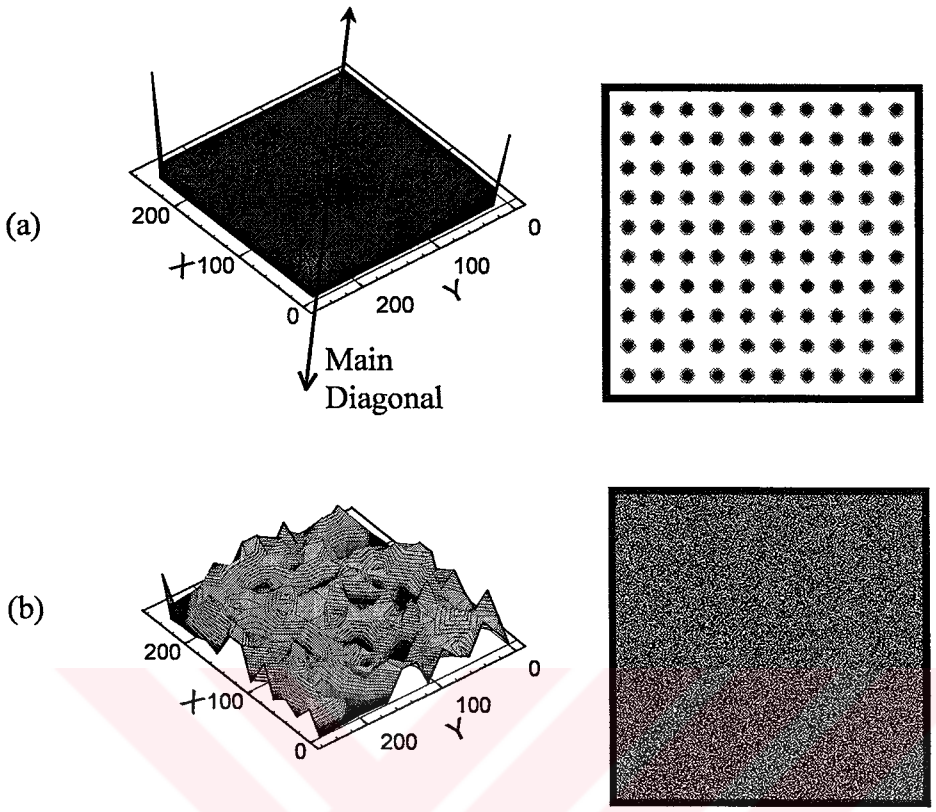

Figure 5.3. Co-occurrence matrix of images in three dimensional space. X and Y are the number of pixels, Z is the gray level. ((a)Uniform and (b) random image respectively)

The contrast statistic is used in order to measure texture differences. One may compute the contrast of matrices for a range of *d*. Contrast then becomes a function of distance. For an image generated by randomly sampling a uniform distribution, this function assumes a constant mean value. Conversely, an ordered texture produces a periodic function as the spatial correlation alternately falls and rises with distance. It has been previously shown that the period of such a function is the period of the texture, and that the amplitude is an indication of the relative strength of the signal in terms of periodicity [36, 39] (Figures 5.4, 5.5, 5.6, and 5.7).

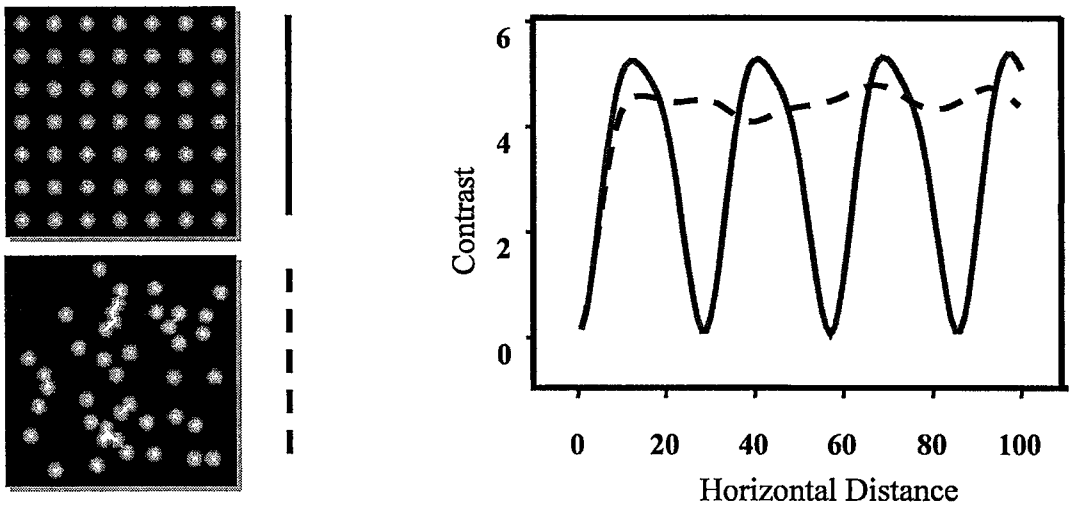

Figure 5.4. Typical co-occurrence functions

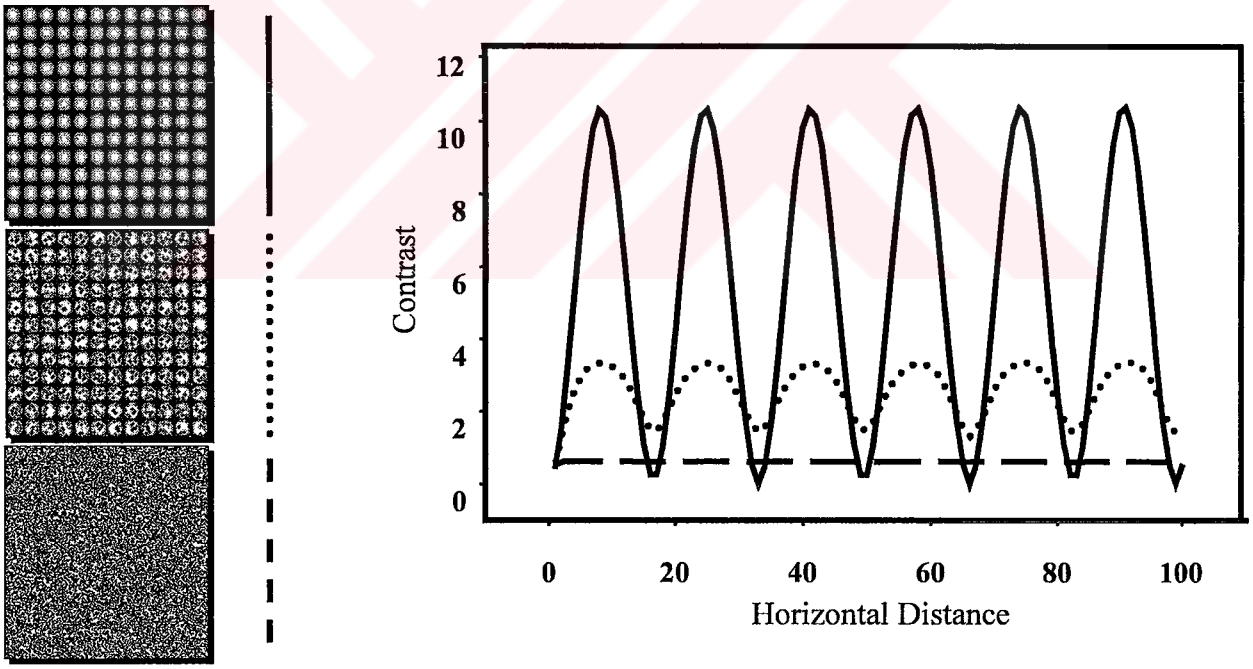

Figure 5.5. The change of co-occurrence functions with the addition of random noise

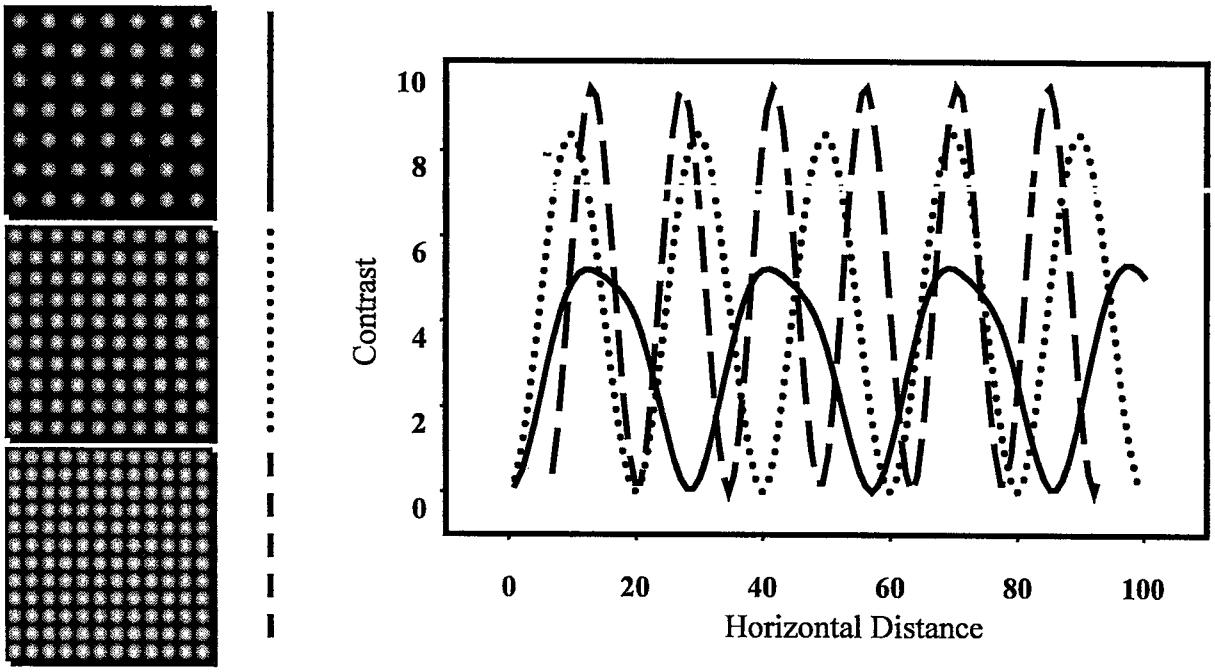

Figure 5.6. The change of co-occurrence functions with different texture coarseness

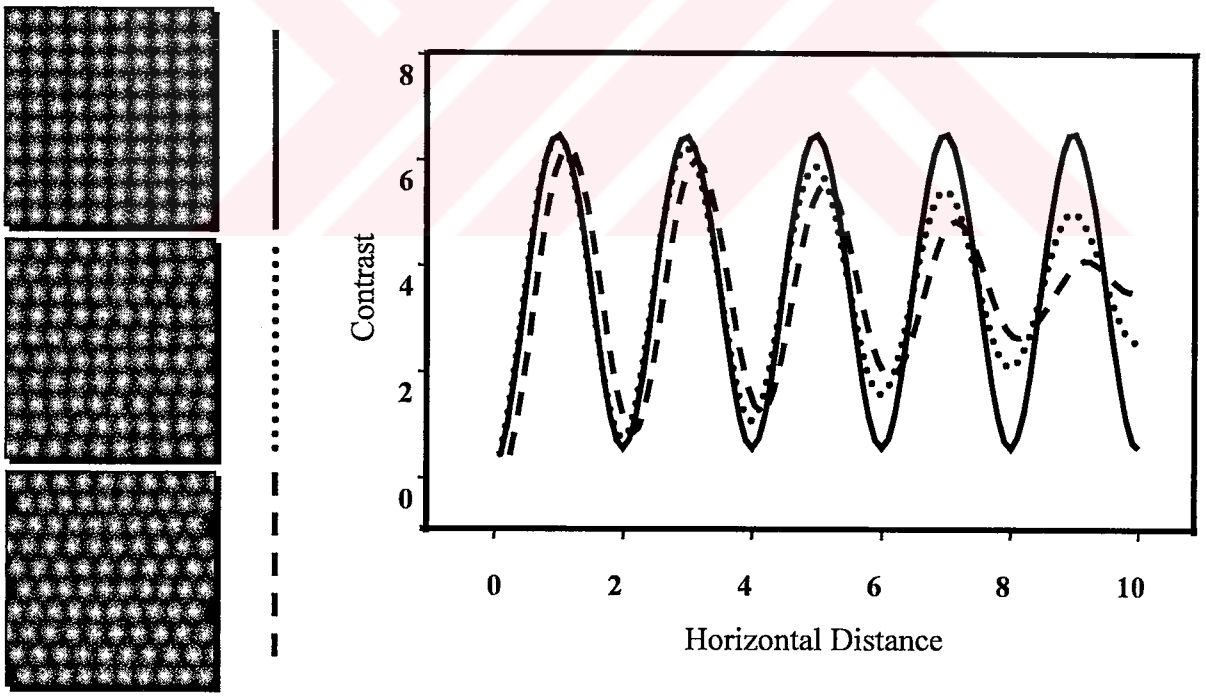

Figure 5.7. The change of co-occurrence function with fixed increment deviation in X direction

In this research, the contrast statistics for spatial co-occurrence matrices were computed for the horizontal and vertical directions, for $d = 1$ to 256. The latter value of d was chosen to facilitate spectral analysis of the contrast function.

Sobus and Pourdeyhimi have shown that the spectral densities can be used by using a finite Fourier transform to compute the periodogram or power spectrum and that the magnitude of the periodogram indicates the statistical 'strength' of the indicated frequency or the texture period [36, 37]. The Fourier transform theorem can be stated in one or multiple dimensions, depending on the number of independent variables used in the transformed function. It provides the link between a waveform in the time (or spatial) domain ad its spectrum in the frequency domain. The Fourier theorem states that any signal can be represented as the sums of squares of the sine and cosine waves of various frequencies and amplitudes. The contrubition of each frequency to the total effect (i.e., the signal) is determined by the amplitude of its Fourier coefficient.

If a function f(x) in the time (or spatial) domain is known, its Fourier transform F(u) is defined as

$$F(u) = \int_{-\infty}^{\infty} f(x) e^{-j2\pi ux} dx \tag{5.2}$$

where u is the variable frequency and $j = \sqrt{-1}$. It is clear that F(u) is a complex function. If the real and the imaginary components in F(u) are denoted as $F_r(u)$ and $F_i(u)$, then the magnitude M(u) and phase $\phi(u)$ can be calculated from equations 5.3 and 5.4.:

$$M(u) = |F(u)| = \sqrt{F_r^2(u) + F_i^2(u)} \tag{5.3}$$

$$\phi(u) = \tan^{-1}\left[F_i(u) / F_r(u)\right] \tag{5.4}$$

F(u) is often presented in the polar form by equation 5.5.:

$$F(u) = M(u) e^{j\phi(u)} \tag{5.5}$$

The square of the magnitude function $|F(u)|$ is a real function and is commonly referred as the "power spectrum" P(u) of f(x) from equation 5.6.

T.C. YÜKSEKÖĞRETİM KURULU
DOKÜMANTASYON MERKEZİ

$$P(u) = |F(u)|^2 = F_r^2(u) + F_i^2(u) \tag{5.6}$$

For digital computation of the Fourier transform, a discrete version of the integrals is needed. Suppose f(x) is sampled at N points, a distance Δx apart, so that x now assumes the discrete values 0,1,2,....N-1. The discrete Fourier transform pair that applies to sampled function is given by equations 5.7 and 5.8.

$$F(u) = \frac{1}{N}\sum_{x=0}^{N-1} f(x)e^{-j2\pi ux/N} \tag{5.7}$$

for u = 0,1,2,....N-1, and

$$f(x) = \sum_{u=0}^{N-1} F(u)e^{j2\pi ux/N} \tag{5.8}$$

for x = 0,1,2,.....N-1.

In the discrete case, the values u = 0,1,2,....,N-1 correspond to samples of the continuous transform at values 0, Δu, $2\Delta u$, ...(N-1) Δu. The sampling increments Δu and Δx are related by the equation 5.9.

$$\Delta u = 1/N\Delta x \tag{5.9}$$

Unfortunately, the Discrete Fourier Transform (DFT) is an extremely slow process, especially when the data set is large. In 1942, Danielson and Lanczos developed an algorithm to enhance the efficiency of the DFT. This algorithm and the other variants now known as the Fast Fourier Transform (FFT) and are widely used in various applications. The basic idea of the FFT is that a DFT of an N data set is the sum of the DFTs of two subsets: even-numbered points and odd-numbered points. The data set can be recursively split into even and odd until the length equals one. Since the DFT of one point is equal to itself, the DFT of the data set becomes a series of simple operations. The FFT algorithm can reduce N^2 operations in the DFT to $N\log_2 N$ operations in the FFT. If N=1000, the FFT is about 100 times faster than DFT. In this research, an FFT procedure was used.

Since the resulting transform of a function is a complex function, the magnitude and phase have to be displayed seperately. For a function f(x), the square of the magnitude M(u) is called the power spectrum P(u). The power spectrum is often

displayed against frequency to show the contributions of each frequency to the function. Power spectrum is useful to identify the periodicity in a function. The power spectrum shows one or several peaks corresponding to the fabric structure and it is range (or power) corresponds to texture definition (Figures 5.8, 5.9 and 5.10). The number of peaks in the spectrum depends on the structure of the fabric (for example the kind of the weave), and the frequency depends on the fabric density. The magnitude of each peak yields information on the fabric structure.

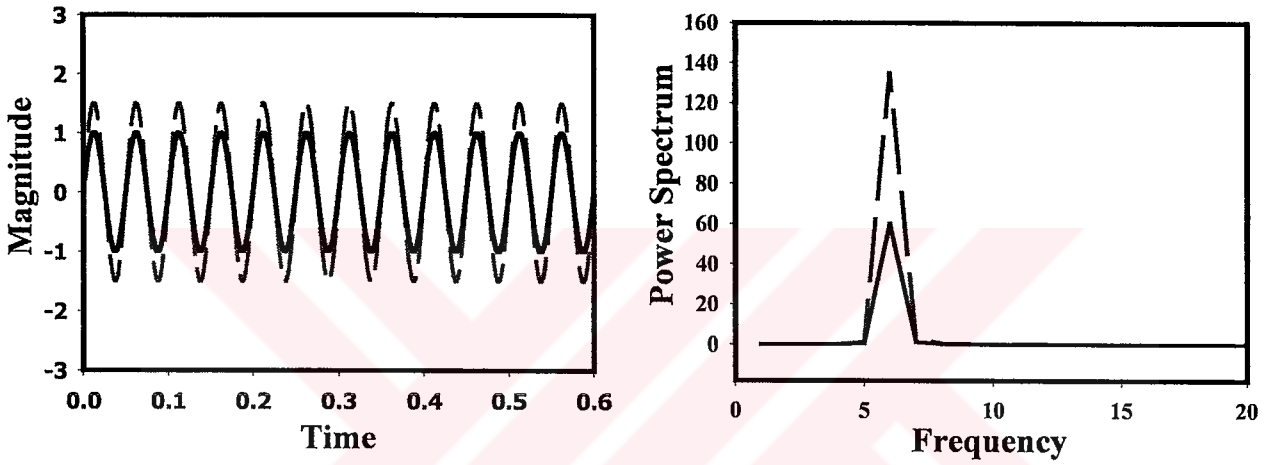

Figure 5.8. Analysis of a function with the same period but different amplitude

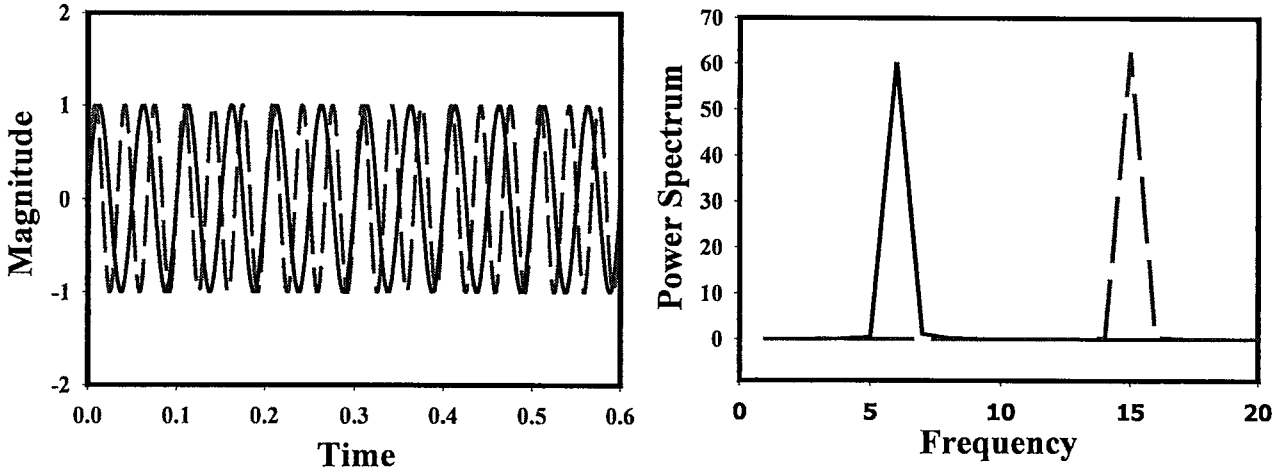

Figure 5.9. Analysis of a function with a different period but same amplitude

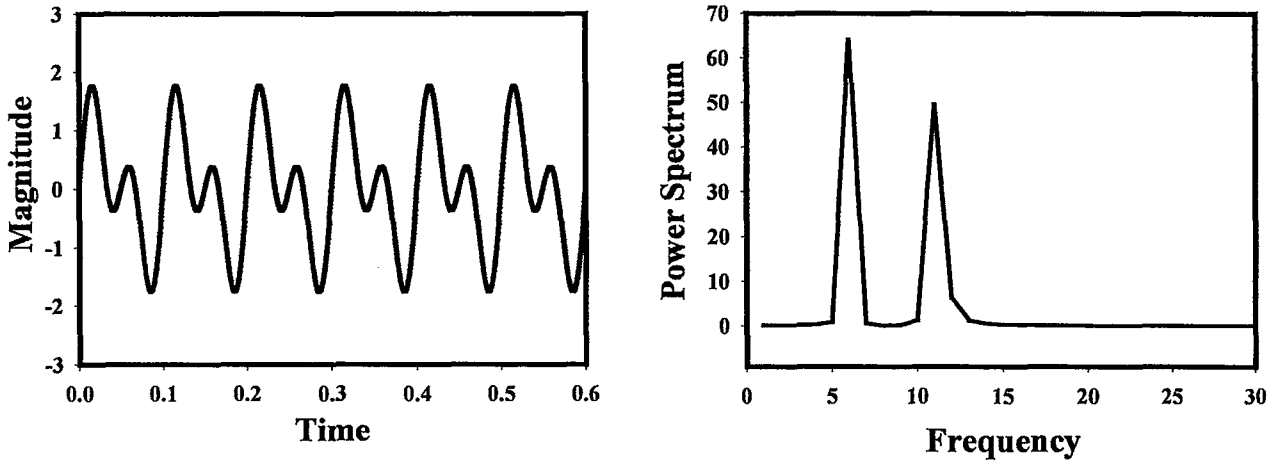

Figure 5.10. Decomposing textural elements in a function with two periods and amplitudes

5.2. Raw Materials

Polyester fibers of 1.7 dtex and 38 mm length were provided in bale form.

5.3. Sample Production

Samples are produced at NC State College of Textiles' Nonwoven Laboratory.

5.3.1. Formation of fiberweb

The polyester fibers were first opened, carded (by a flat top card)(Figure11), and cross-lapped for obtaining webs with bimodal fiber orientation. In the carding process, individual staple fibers are separated from clumps of fibers and they are more or less oriented in one direction. In general, flat and roller carding machines used in the spinning process can provide carded web to be converted into fiber layers to produce nonwovens. Nonetheless, roller cards are more common for higher productivity, width and versatility. Productivity of older roller cards is about 30-50 kg/hour at the width of 1.5-2 m. Nowadays the performance of the roller cards can reach up to 1000 kg/hour in 2.5-3m width. Flat carding machines are usually 1 m wide and give 5-50 kg/hour. Recently, high-speed carding machines of width up to 5 m have been developed for nonwovens.

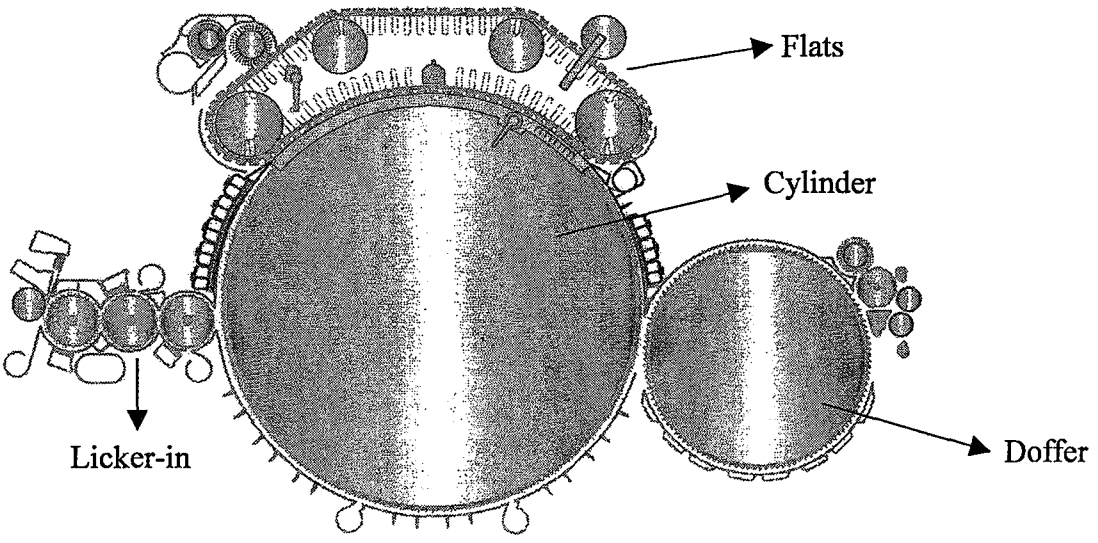

Figure 5.11. High speed flat card used in the nonwoven industry (Trutzchler DK903)

Carded webs are light fiber assemblies of basis weight usually 5-30 g/m^2. The carded webs are needed to be layered to get the desired weight. Cross lapping is a good way of folding the webs, also crosslapped webs are characterized by their bimodal fiber orientation that is required to enhance crossmachine fabric properties as compared to unimodal fiber orientation obtained by carding only. The function of the crosslapper is clear in the Figure 5.12. A crosslapper similar to Figure 5.12 is used in this study.

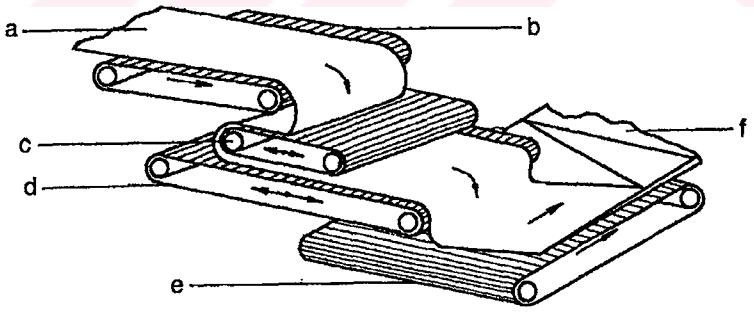

a. Web
b. Feed belt
c. Upper conveyor belt
d. Lower conveyor belt
e. Delivery belt

Figure 5.12. Crosslapping process [93]

5.3.2. Hydroentangling

After forming the web, a pilot-scale Honeycomb hydroentangling machine (see Figures 5.13-5.15) was used to produce fabrics under varying pressures and number of passes. The machine has three manifolds (Figure 5.14). The pressure of manifold can be independently controlled. The jet strips have two lines of orifices. The orifice diameter is 0.127 mm and the density of the jets is 16 orifices/centimeter. The pressure can be as low as 13 bars for pre-wetting, and as high as 110 bars for hydroentangling. In this study, two different kinds of textures were produced with two different forming wires. One was an apertured fabric formed with a twill forming wire, another type was a herringbone designed wire to produce textured fabric and two of the various fabrics were produced at the same respective energy levels. However different lightning systems were used for apertured textured fabrics and so the image of the forming wire could be captured, and the results of the apertured fabrics are given separately.

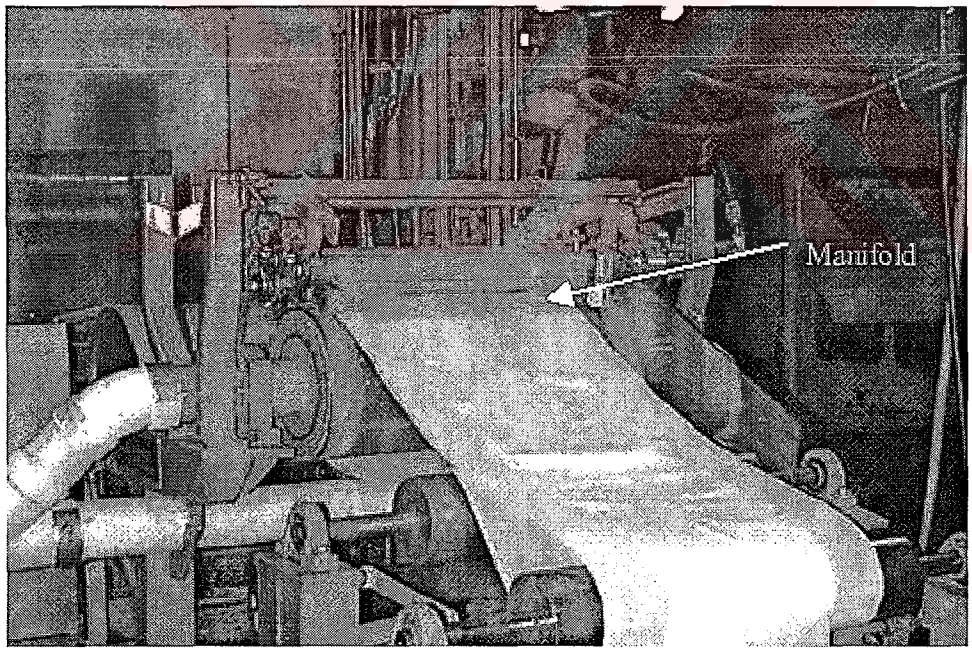

Figure 5.13. Pilot scale Honeycomb hydroentanglement machine employed

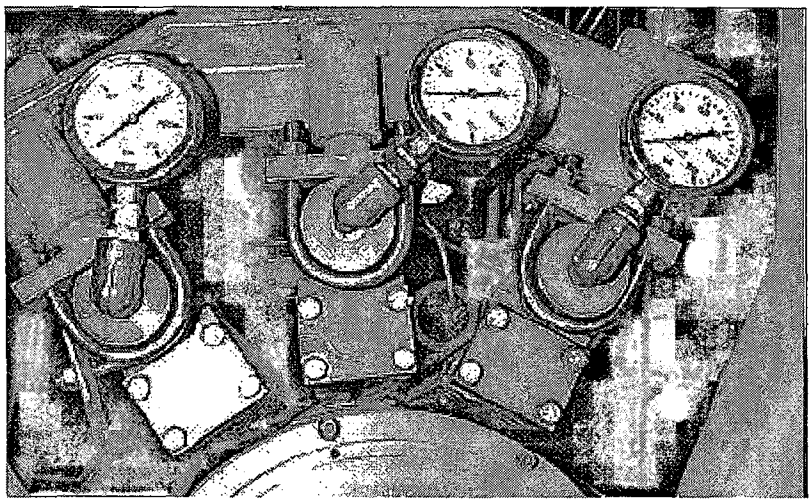

Figure 5.14. Jet manifolds of the Honeycomb hydroentanglement machine

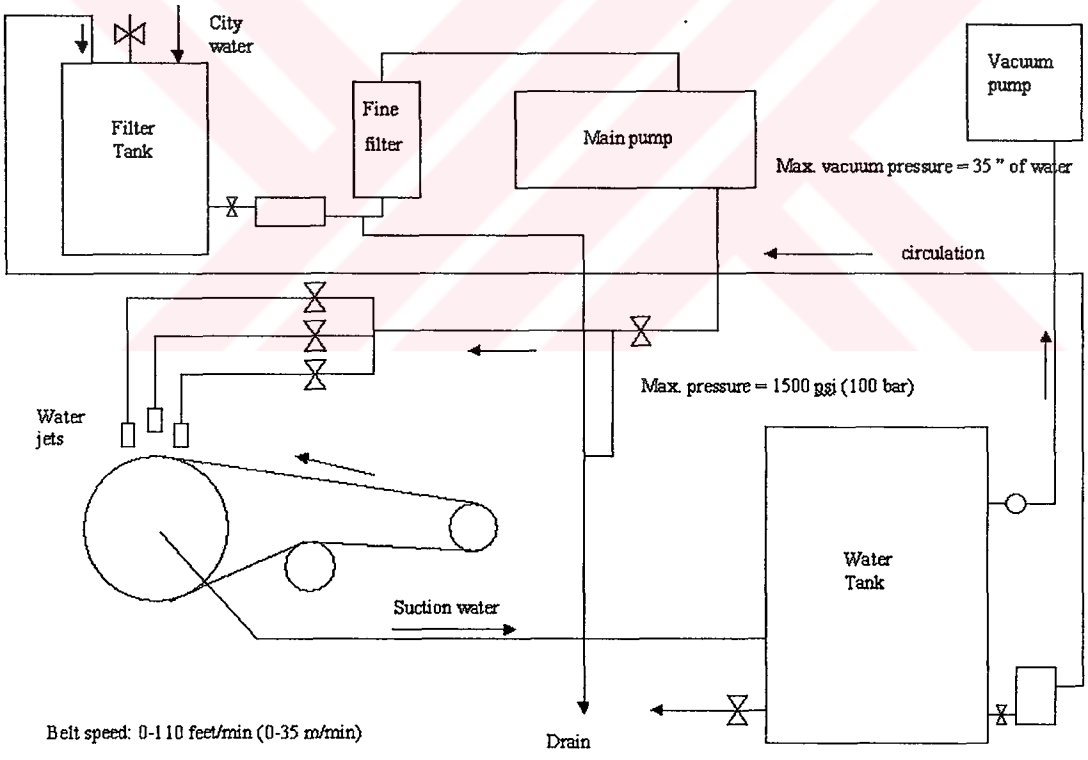

Figure 5.15. Sketch of the Honeycomb hydroentanglement machine

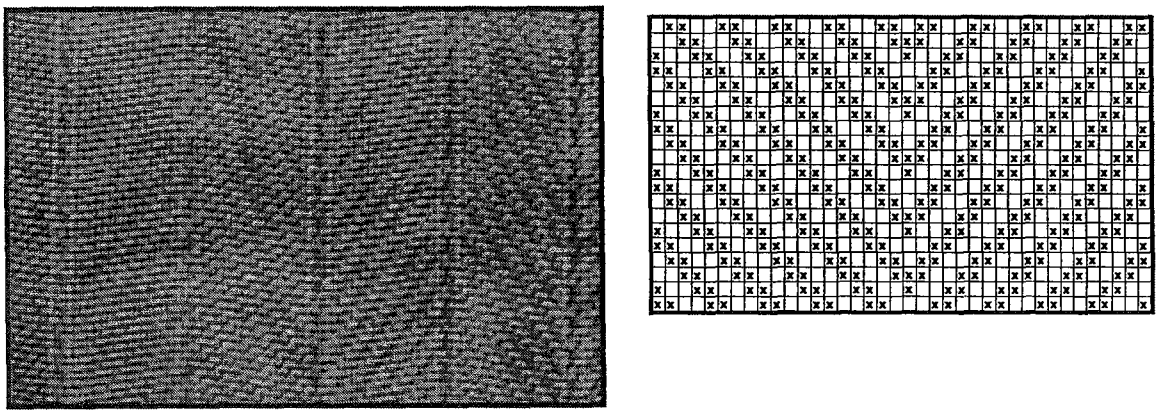

Figure 5.16. Herringbone designed forming belt.

One of the forming belts was a plastic herringbone-designed wire for manufacturing textured fabric (Figure 5.16). The open area of this belt was 27.2% and the diameter of the filaments both in weft and warp direction was 0.63 mm.

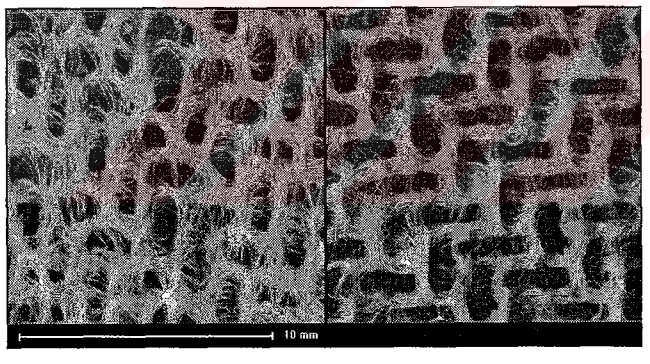

Figure 5.17. Trials using a 50-g/m^2 web at a pressure of 96.5 bars by herringbone designed belt (1 pass and 2 passes respectively)

Initially, a web of nominal basis weight of 50 g/m^{2}was used. However it was observed that, a light fiber web without any consolidation does not give satisfactory results, due to the destruction of its texture at higher pressures and number of passes. An example is given in Figure 5.17. It is clear that in the absence of any consolidation, the water jets displace the fibers. Thus, better texture can evolve if the web is consolidated to some degree first before it is subjected to higher pressures. Consequently, it was decided to use heavier webs and two sets of fabrics were

produced, respectively from nominal basis weights of 100 g/m^2 and 150 g/m^2 carded and croslapped webs. These webs were first consolidated at a pressure of 55 bars. Table 5.1. shows the processing parameters utilized to produce the final samples.

Apertured fabrics with a twill-forming belt were also produced. Forming surface was a 1 by 2 twill design and a 2.8 mm thick plastic belt (see Figure 5.18). The open area of the surface was 15%. The same webs and same energy levels are used as mentioned above.

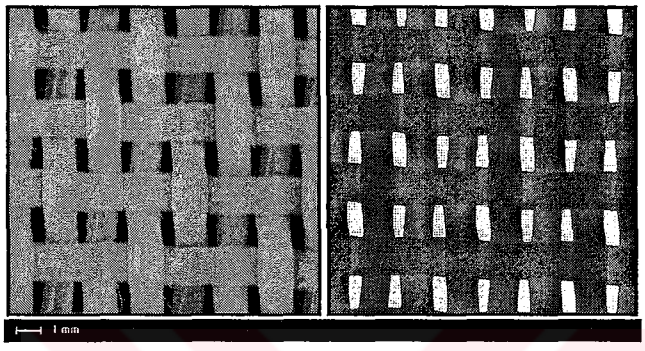

Figure 5.18. Twill designed forming belt.

5.3.2.1. Calculation of specific energy

Nominal basis weights of 100 g/m^2 and 150 g/m^2 webs are first consolidated under 55 bars (note that: it was a two-sided consolidation). There were three manifolds on the machine. The manifolds were first adjusted to 13.8, 55 and 55 bars respectively for consolidation of the web. 13.8 bars are usually used for pre-wetting before hydroentanglement. Then, the resulting web is used for textured fabric production. The following formula (previously explained) was used for calculating the specific energy of the fabric per kilogram.

$$E = 6.66\times10^{4}\,\frac{C_d.d^2.N.P^{3/2}}{\sqrt{\rho}.W.S} \qquad (5.10)$$

Where C_d = 0.7, d = 1.27.10^{-4} m, N = 1600 jets/m per manifold, P is the water pressure (N/m^2) in the manifold, ρ = 1000 kg/m^3, W = 100 g/m^2, and S =4.57 m/min.

And the total specific energy applied to the fabric (j/kg) is calculated by equation (5.11.).

Total Specific Energy, $E_t = \sum_{i=1}^{p}\sum_{j=1}^{m} E_{ij}$ (5.11)

Where E_{ij} is the specific energy applied to the fiber web by manifold, j (j=1,2,....m), calculated by equation (5.1.), in the pass i (= 1,2,.... p).

So (for example) if this equation is applied for specimen no.4 (100 g/m^2 web):

$$E_t = 6.66\times10^4\left(\frac{0.7\times(1.27\times10^{-4})^2.1600}{\sqrt{1000}\times100\times4.57}\right)\left[(13.8\times10^5)^{3/2}+(5\times55\times10^5)^{3/2}\right]+$$
$$6.66\times10^4\left(\frac{0.7\times(1.27\times10^{-4})^2.1600}{\sqrt{1000}\times100\times4.57}\right)\left[(13.8\times10^5)^{3/2}+(2\times69\times10^5)^{3/2}\right]$$

$E_t = 8525.10^3$ j/kg

Table 5.1. Processing Parameters of Experimental Fabrics

						Web Weight = 100 g/m^2	Web Weight = 150 g/m^2
No	No. of passes	No. of manifolds	Pressure (bars)			Specific Energy (kj/kg)	Specific Energy (kj/kg)
1	1	3	13.8	27.6	27.6	6312	4209
2	1	3	13.8	41.4	41.4	6939	4627
3	1	3	13.8	55.2	55.2	7682	5122
4	1	3	13.8	69	69	8525	5684
5	1	3	13.8	82.7	82.7	9456	6305
6	1	3	13.8	96.5	96.5	10469	6980
7	2	3	13.8 27.6	27.6 27.6	27.6 27.6	7436	4958
8	2	3	13.8 41.4	41.4 41.4	41.4 41.4	9004	6004
9	2	3	13.8 55.2	55.2 55.2	55.2 55.2	10861	7242
10	2	3	13.8 69	69 69	69 69	12968	8646
11	2	3	13.8 82.7	82.7 82.7	82.7 82.7	15297	10199
12	2	3	13.8 96.5	96.5 96.5	96.5 96.5	17829	11887

5.4. Samples Acquired from Industry

In the first and the third part of the study, samples were acquired from the industry. Samples consist of three sets, a woven 3/1 twill fabric, a Miratec® hydroentangled fabric with twill design and a loosely bonded herringbone hydroentangled nonwoven for the abrasion study. The twill fabric was an ordinary cotton twill fabric, which has well defined structure. Miratec® was a new PGI product which was introduced in April 1998 (see "Quality Fabric of the Month," ATI December 1998). It is a proprietary fiber to finished fabric process and can produce light or heavy weight textiles. The other sample was a loosely bonded hydroentangled with herringbone design fabric also produced by PGI.

In the third part, for the study on jet streaks, four different fabrics (A, B, C and D) were received from different fabric manufacturers. Fabrics A, B and C are unfinished and white in color. Fabrics A and C are fairly dense structures composed of micro denier fibers while fabric B is a loosely bonded structure. Fabric D is also made from micro denier fibers but it is finished and dyed. Since the manufacturers wanted to keep their fabric properties confidential, the overall properties are not given for this set of fabrics.

5.5. Image Processing System

A capture device that consists of a high-resolution monochrome camera, a frame grabber and a lighting system was configured to provide a collimated dark-field illumination. The set up is shown in Figure 5.19. The images were captured perpendicular to the focal plane of the camera. The light source consists of a uniform LED light panel. The captured images covered an area measuring 20x20 mm^2. Three images were captured for each sample and the data reported are the mean and the standard deviation for the three replicates.

Images were preprocessed before co-occurrence analysis. A 7x7 Gaussian filter was first used to smooth the edges and wiping of the electronic noise, then a histogram equalization is applied using a standard algorithm [94], where gray level values are reassigned to produce a flattened histogram therefore making a more uniform gray

level distribution, and removing any biases caused by the variations in the overall image intensity [95].

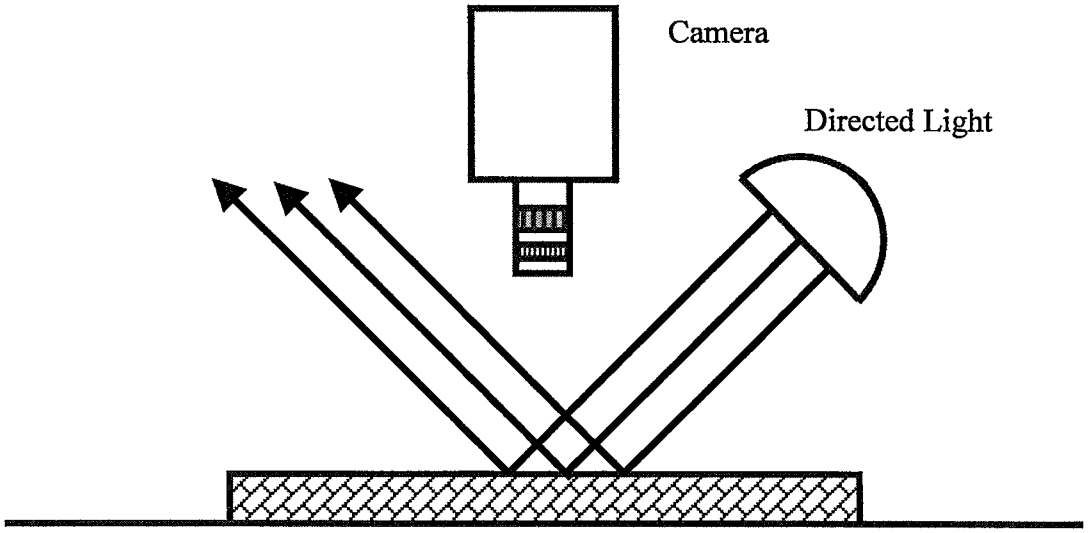

Figure 5.19. Illumination and capture set-up

5.6. Testing and Evaluation

To investigate the changes in appearance brought about by fabric-to-fabric abrasion, a crock meter was used as a wear tester according to ASTM Test Method 8. Crock meter is an abrasion tester generally used for fastness tests. The fabric is abraded usually by a piece of white cloth determining the color fastness of the specimen. In this study, since the fabrics were small to be used at a conventional abrasion tester, a crock meter is used for abrading the fabrics against itself. The fabrics were abraded at varying degrees and imaged on the image analysis system. The fabric characteristics and wear levels are given in Table 5.2.

Table 5.2. Fabrics and wear levels

Fabric type	**Wear degree (cycles)**
Woven twill fabric	Control, 1000, 2000, 2500, 3000
Miratec hydroentangled fabric with twill design	Control, 1000, 2000, 3000
Hydroentangled fabric herringbone design	Control, 200, 500, 1000, 2000

Abrasion levels are selected according to fabric types. Since herringbone hydroentangled fabric was a loose type, it is abraded just after 2000 revolutions. For the other fabrics, specimens are abraded till they lost their texture definition.

All specimens in the research are evaluated by an image analysis system explained in details above, also subjective analysis was used to support the results.

5.7. Statistical Analysis

Three images for each fabric were captured and their average co-occurrence curves are considered through this entire dissertation. Mean and standard error of power values are calculated from Fourier analysis and these values are used in all plots.

6. RESULTS AND DISCUSSIONS

6.1. Texture Retention after Fabric-to-Fabric Abrasion

Changes in appearance brought about by mechanical abrasion may be evaluated with respect to changes in image texture properties, e.g., periodicity. The application of gray-scale image analysis to the measurement of texture periodicity in woven and nonwoven fabrics is discussed in this part. The techniques described here are appropriate for 'ordered' textures with relatively well-defined features such as the Miratec® class of fabrics.

The choice of fabrics studied was arbitrary. A woven fabric normally has well-defined features and is expected to be quite durable. Nonwovens, on the other hand, are considered less durable. The hydroentangled nonwovens studied consist of two very different textured structures. One is a loosely bonded hydroentangled nonwoven with a fairly well defined herringbone texture and the other is a Miratec® fabric with a well-defined twill texture. The intention of the work was not to undertake an exhaustive study of the differences between woven and nonwoven fabrics, but rather to demonstrate the viability of the proposed texture analysis methodology in quantifying different textures.

To investigate the changes in appearance brought about by fabric-to-fabric abrasion, a crock meter was used as a wear tester (method explained in Chapter 5). The fabrics were abraded at varying degrees and imaged using the image analysis system. The fabric characteristics and wear levels are given in Table 5.2.

Texture units in a fabric consist of elements (e.g., ridges in a twill fabric). However, wear (e.g., abrasion) may modify these units through entanglement of fibers and loss of fibers. In consequence, the periodicity (uniformity of texture) will be lost [39].

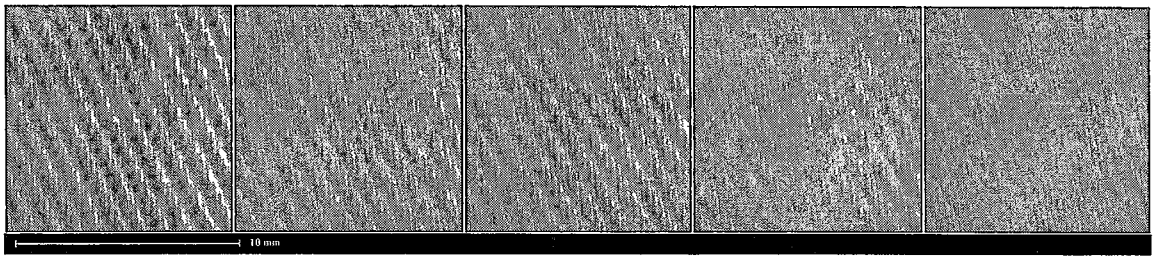

Control Sample 1000 Cycles 2000 Cycles 2500 Cycles 3000 Cycles

Figure 6.1. Images of woven twill fabric before and after abrasion

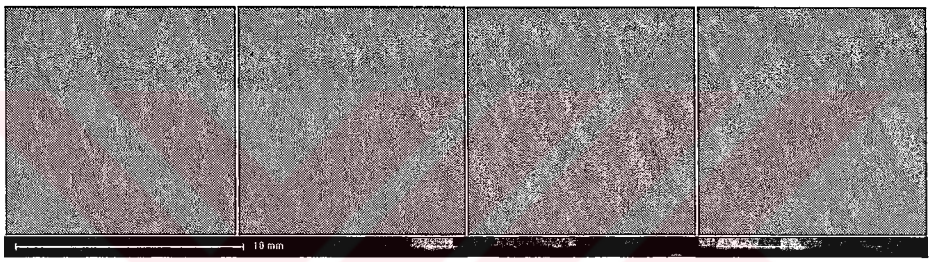

Control Sample 1000 cycles 2000 cycles 3000 cycles

Figure 6.2. Images of Miratec hydroentangled fabric with twill texture before and after abrasion

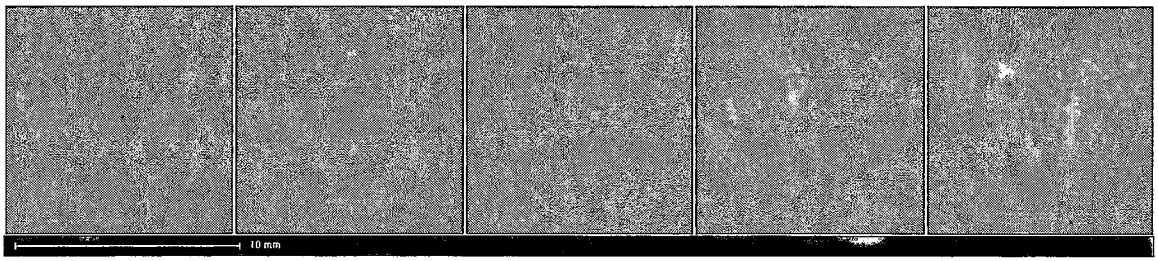

Control Sample 200 Cycles 500 Cycles 1000 Cycles 2000 Cycles

Figure 6.3. Images of hydroentangled fabric with herringbone texture before and after abrasion

The images at various levels of wear are shown in Figures 6.1-6.3. It may be noted that the woven fabric has been abraded and that the texture definition is being lost, and the fabric surface appears to have become somewhat fuzzy. It is clearly seen that fabric periodicity is shifted and the magnitude of the contrast curves has become

smaller as a result of abrasion resulting in reduced texture definition. The Miratec® fabric shows little evidence of wear. In fact, it appears that the marks present in the original control fabric have been covered and that the ridges in the abraded samples appear to be quite pronounced and intact as the number of cycles increased. The loosely bonded herringbone sample however, shows the greatest degree of wear. This is not unexpected as the fabric is lightly bonded to provide bulk and softness. Visual observations are also confirmed by examining the corresponding co-occurrence data for the samples given in Figures 6.4-6.6. For clarity, the co-occurrence data are only shown for the control and the highest level of abrasion; other intermediate levels of abrasion fall between these two extremes. It may be noted that all samples have a periodic texture in both horizontal (cross) and vertical (machine) directions. Note that the vertical data for the herringbone fabric indicates two periods. This is due to the herringbone design. The woven fabric's co-occurrence data decreases in amplitude in both directions fairly significantly as a function of wear. The same is true for the herringbone fabric where the texture is completely lost and the fabric begins to break up. The Miratec®, however, shows little or no evidence of wear. In fact, the samples after 3000 cycles of abrasion appear to be somewhat better defined than the original control samples. This is partly because the abrasion has removed the texture variations between the ridges. This is demonstrated in Figure 6.7 where the intensity profiles are shown for the control and the worn samples. As may be noted, the worn sample shows a smoother profile with a slightly higher degree of contrast. These can in turn result in higher co-occurrence measurements.

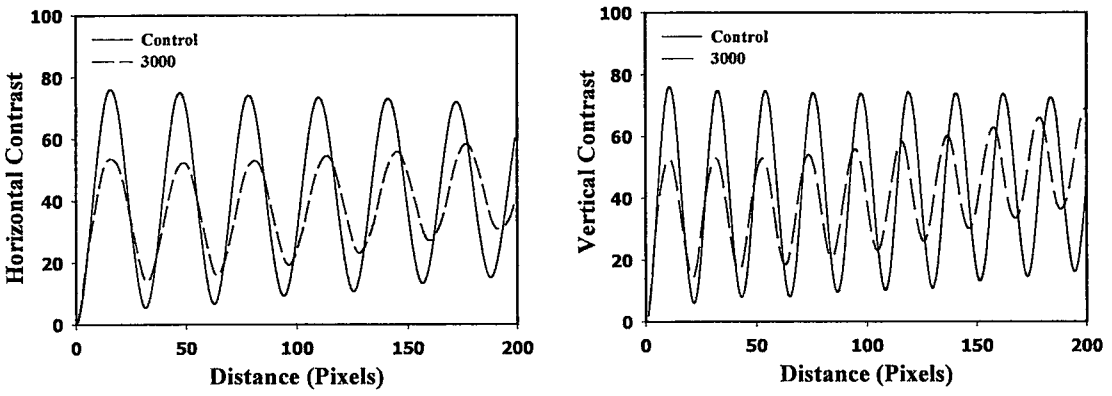

Figure 6.4. Co-occurrence results of woven twill fabric: horizontal (left), vertical (right)

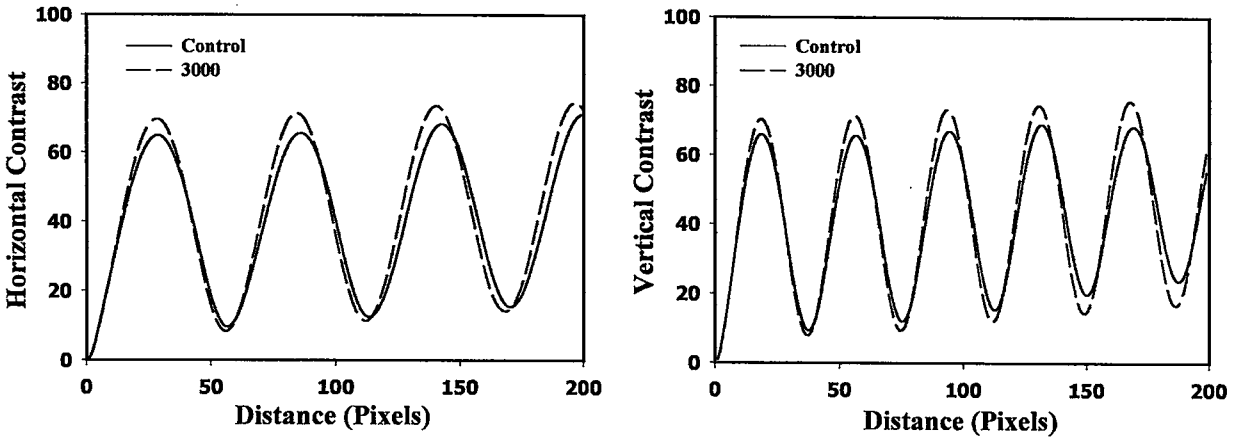

Figure 6.5. Co-occurrence results of Miratec twill fabric: horizontal (left), vertical (right)

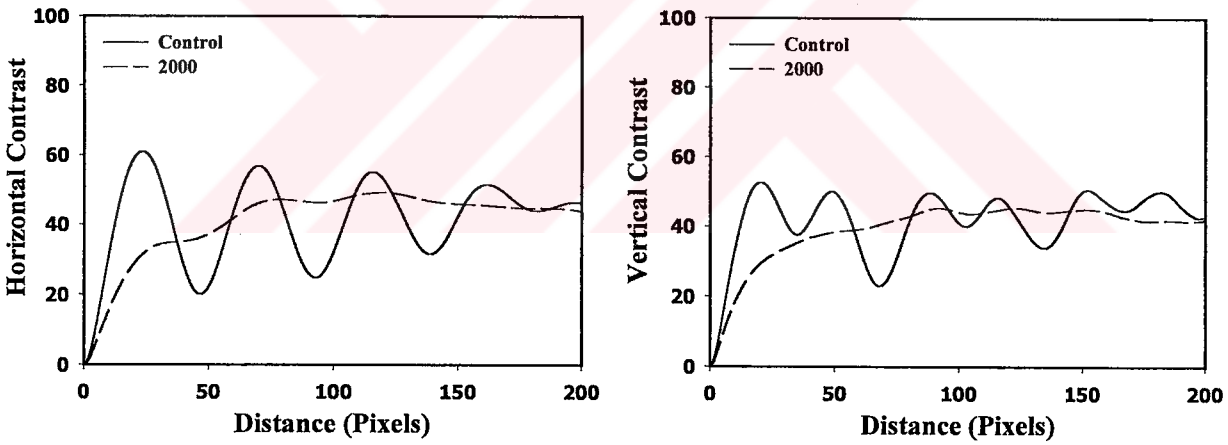

Figure 6.6. Co-occurrence results of hydroentangled herringbone fabric: horizontal (left), vertical (right)

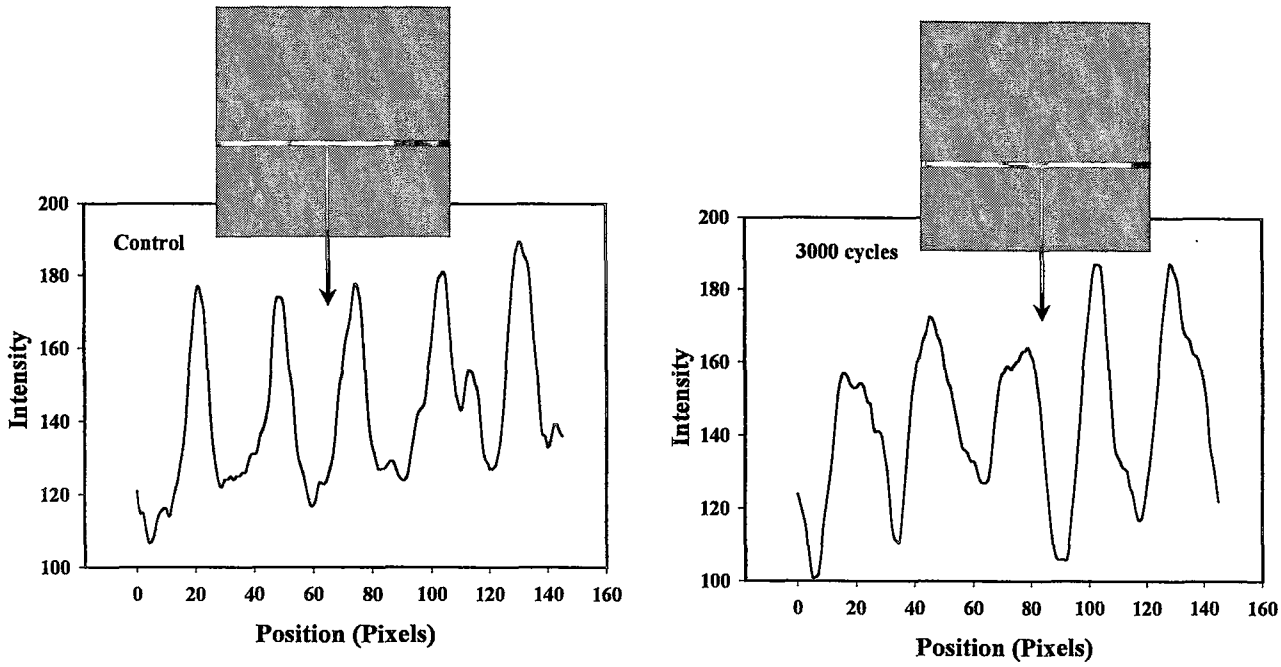

Figure 6.7. Intensity profiles for Miratec twill fabric

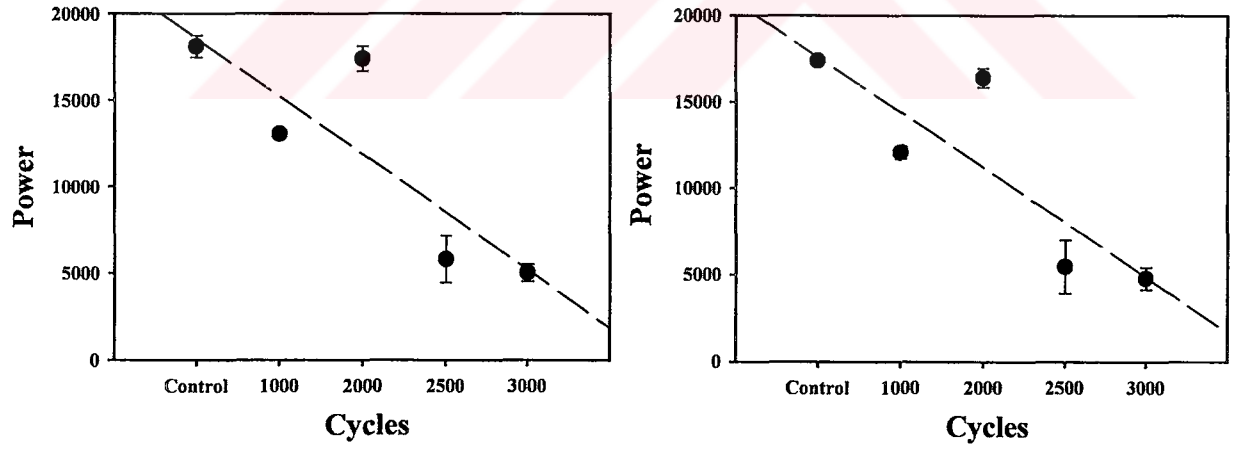

Figure 6.8. Frequency analysis of contrast data for woven twill: horizontal (left), vertical(right)

The data are further corroborated by the magnitude of the power spectra periodograms shown in Figures 6.8, 6.9, 6.10. The woven twill fabric shows a consistent reduction in the periodogram power. The Miratec® shows a slight increase and the loose herringbone nonwoven shows a significant reduction with wear. The surface texture of the herringbone nonwoven is drastically changed by abrasion (see Figure 6.3). The herringbone fabric was the most flexible fabric among the fabrics tested because it was loosely bonded (hydroentangled at low pressure). The appearance change was dramatic even after 500 cycles, and it continued to change significantly at 1000 and 2000 cycles.

These results seem to indicate that co-occurrence statistics used as a function of sampling distance are sensitive to periodic changes of texture and that of the spectral analysis is a good measure of the strength of the periodicity. It should be noted here that investigation was focused on texture retention of each fabric independently rather than comparing their physical structures.

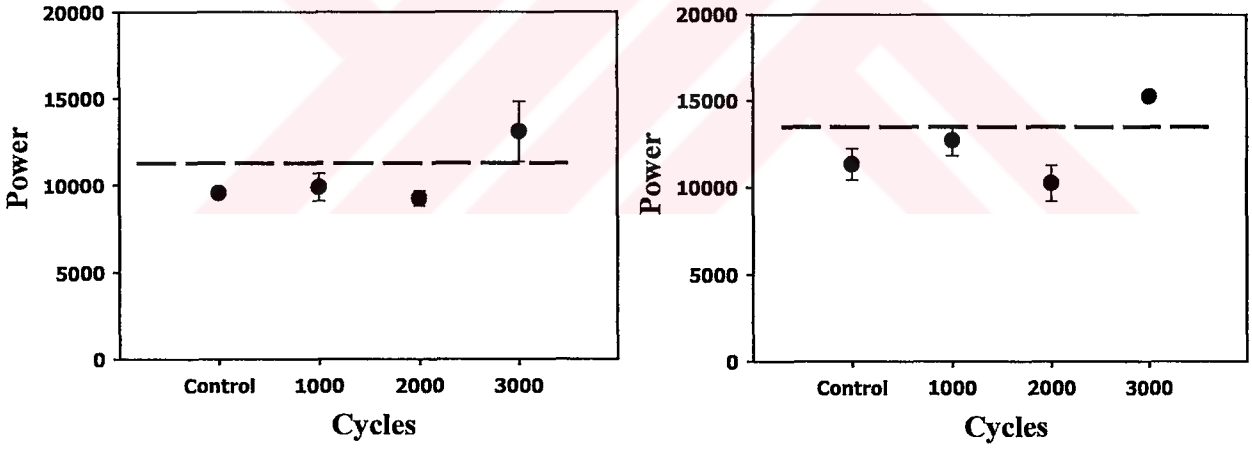

Figure 6.9. Frequency analysis of contrast data for Miratec® twill: horizontal (left), vertical (right)

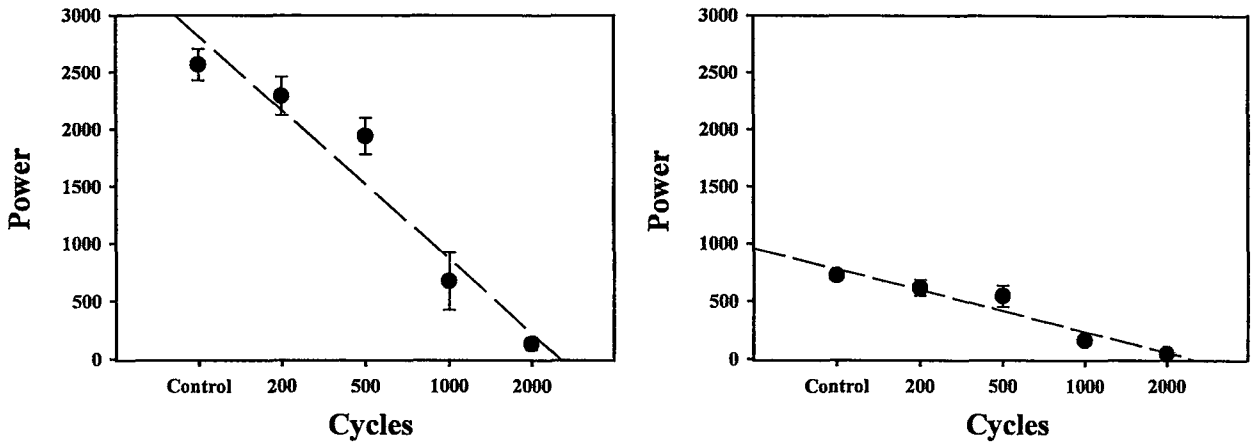

Figure 6.10. Frequency analysis of contrast data for hydroentangled herringbone: horizontal (left), vertical (right)

This was a preliminary study of texture and texture retention in wovens and nonwovens. This study was conducted to assess the suitability of image analysis methods in determining the texture and the loss of texture. The study attempted to demonstrate the viability of co-occurrence analysis for texture retention after abrasion. It is demonstrated that the co-occurrence methods are sensitive enough to structural and textural changes in the fabrics examined. It was mentioned earlier that these methods are reliable in determining the appearance retention in carpets [36,39], and offer a mean to objectively evaluating the textural properties of fabrics.

6.2. Texture Evolution in Hydroentangled Nonwovens

In this part, the proposed texture analysis method is used to examine the development of the texture during hydroentangling as a function of process conditions. This part of the study is focused on the development of texture as a function of hydroentangling energy. Energy was varied by controlling the pressure and number of passes. All fabrics were produced using the same web on the same forming belt substrate. Preliminary data indicate that the degree of texture definition increases as a function of pressure up to a point and then begins to deteriorate.

The total specific energy of water applied to the fiber web is a key process variable responsible for the efficiency of the transfer of the patterns onto the fabric surface.

Naturally, the energy is also going to have a profound effect on the physical and structural properties of the fabrics. The energy transferred to the web can be controlled by : manifold pressure, processing speed and number of manifolds and passes.

Tactile properties and the fabric appearance or surface texture, are also major performance characteristics that influence the consumers like or dislike of the final product. The focus here is on the fabric appearance or surface texture. The texture is evaluated in the context of its periodicity. That is, it is assumed that the texture is periodic and that the level of periodicity is well correlated with how well defined (visually) the texture is. As mentioned earlier, the viability of this approach is firmly established in literature [30, 33, 35-40, 96]. Here, an investigation dealing with the evolution of the surface texture in hydroentangled fabrics formed at varying degrees of specific energy is reported.

All of the textured hydroentangled fabric images are shown in Figures 6.11 and 6.12. However, for the sake of brevity, the contrast results of 4 fabric types are demonstrated. Contrast graphs and their respective powers are illustrated and grouped according to web weight and number of passes.

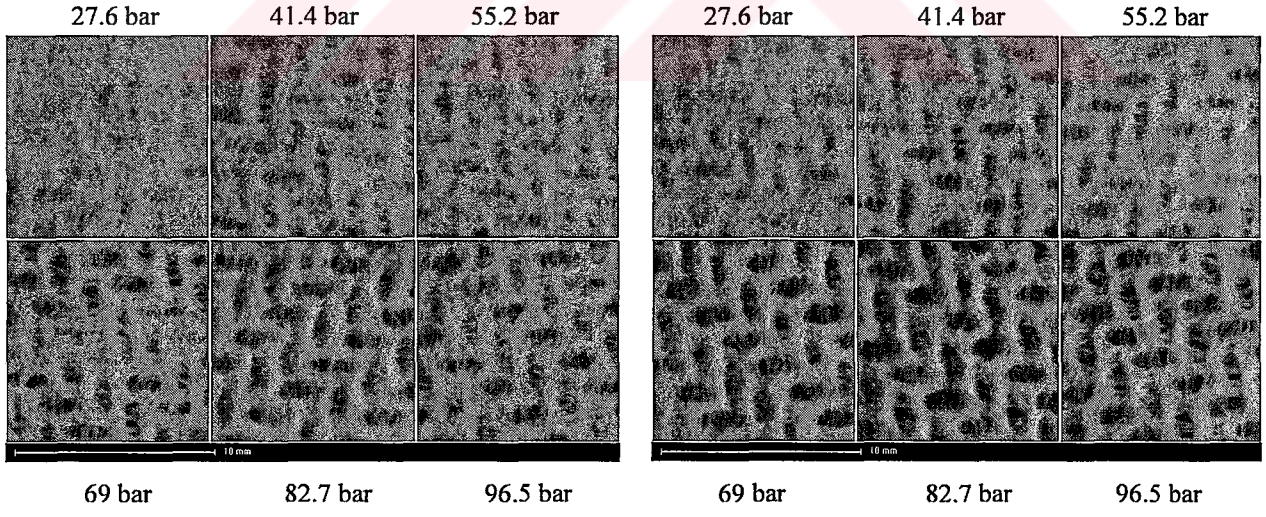

Figure 6.11. Images of Fabrics using a PET 100 g/m2 web - 1 pass (left) and 2 passes (right) under different pressures

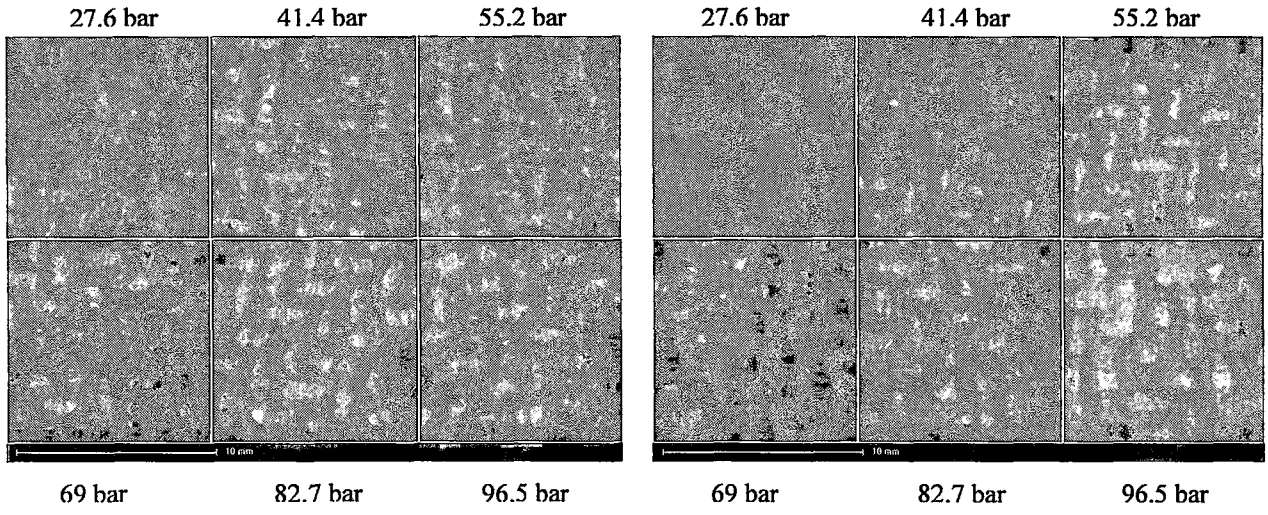

Figure 6.12. Images of fabrics using a PET 150 g/m2 web - 1 pass (left) and 2 passes (right) under different pressures

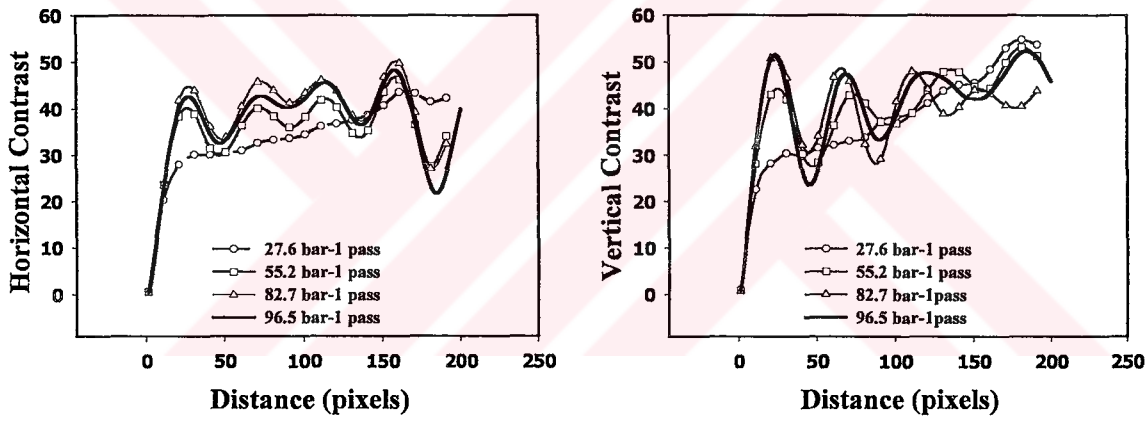

Figure 6.13. Co-occurrence analysis using a PET 150 g/m2 web - 1 pass

Contrast as a function of distance is plotted against pressure for PET 150 g/m^2 webs, 1-pass samples in Figures 6.13. This typifies the results obtained for all samples. Other results are also given in the attachment. (See figures A.1, A.2, A.3 in Appendix). It is clearly seen that the distance function becomes more pronounced as pressure or energy is increased (also see Figure 6.11.) up to a point and then begins to decrease in amplitude. It is possible that at higher pressures, the web is disturbed because it is not sufficiently consolidated. The same behavior is also observed in the spectral analysis of the contrast data for all samples shown in Figures (6.14-6.17). Regardless of the sample or the number of passes or the web basis weight, the trend is consistent. The texture definition increases with pressure and then decreases.

Even in energy vs. power graphs (Figures 6.18 and 6.19) this trend is clear and it seems that in these samples 13000 kj/kg is the threshold energy for the texture loss. As noted above, the loss of texture definition at higher pressures may be due to the lack of web density and consolidation. As shown in Figure 5.17, and also in the last image in Figures 6.11 and 6.12, at high pressures, it appears that the fibers are spread away from the holes created by the knuckles of the screen and the action of the jets, thereby resulting in a lower texture definition.

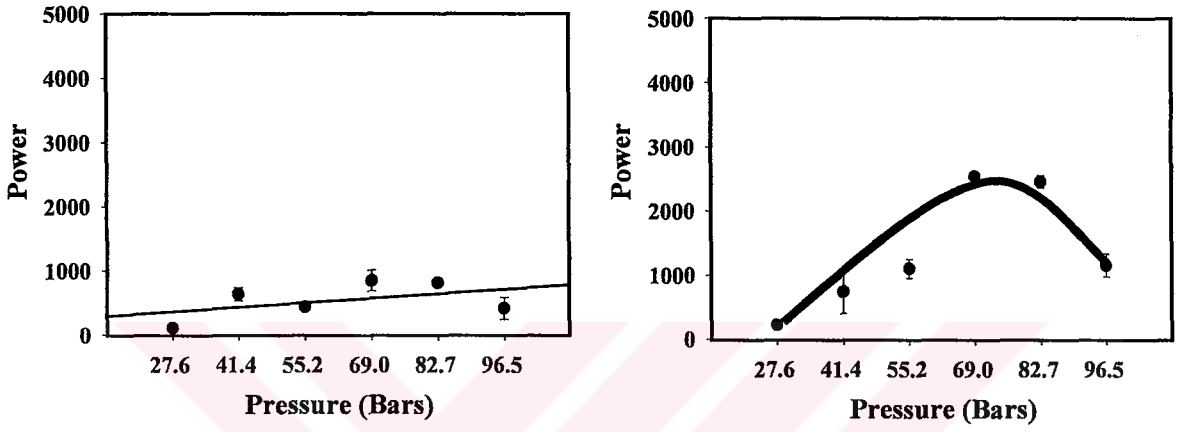

Figure 6.14. Power of PET 100 g/m2 web - 1 pass: Horizontal (left) and Vertical (right) Contrast.

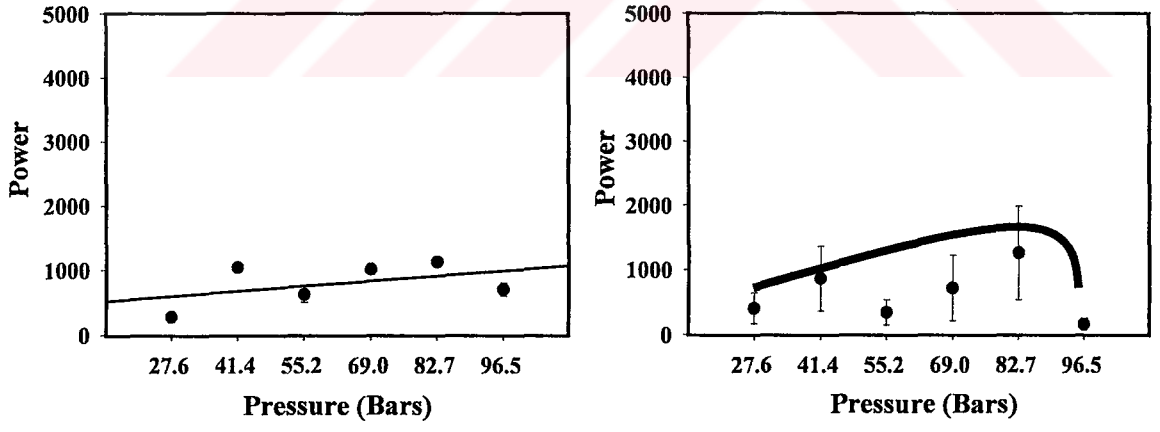

Figure 6.15. Power of PET 100 g/m2 web - 2 passes: horizontal (left) and vertical (right) contrast.

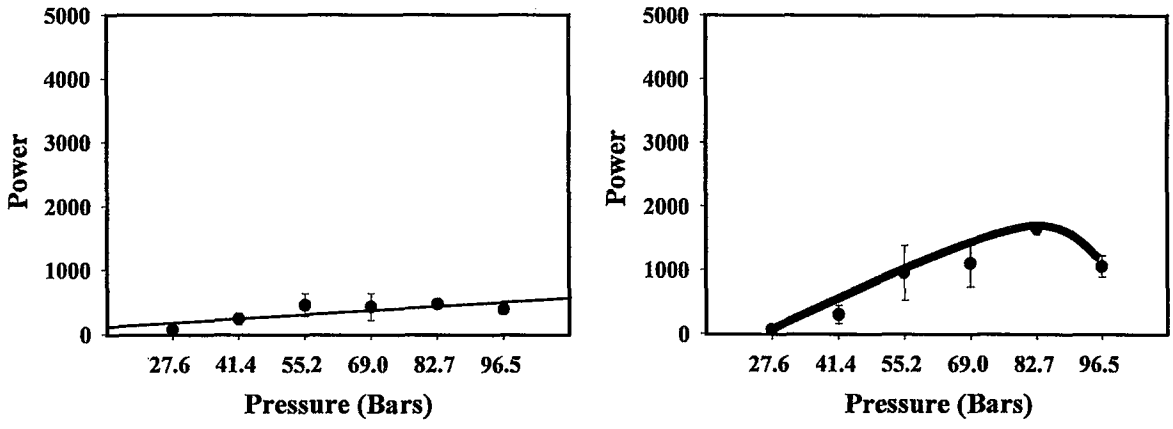

Figure 6.16. Power of PET 150 g/m2 web - 1 pass: horizontal (left) and vertical (right) contrast

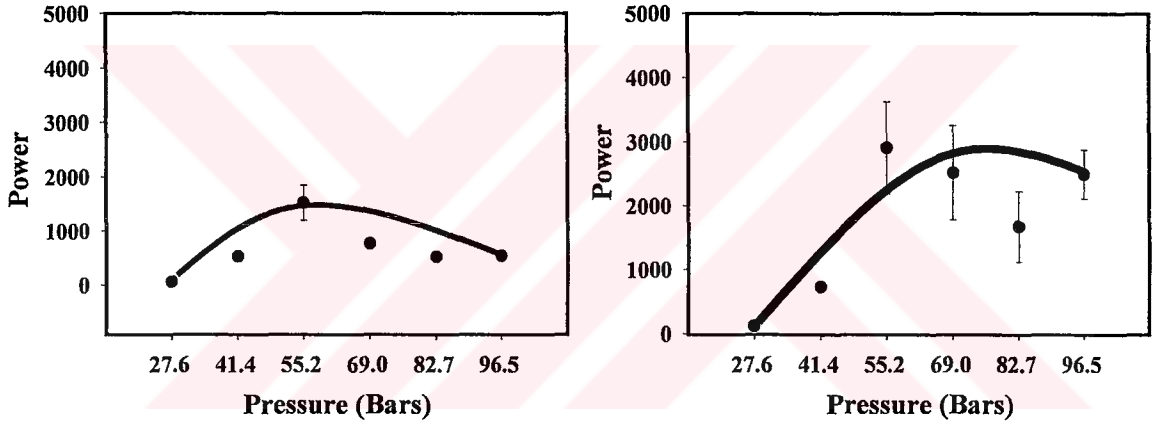

Figure 6.17. Power of PET 150 g/m2 web - 2 passes: horizontal (left) and vertical (right) contrast.

Since there are more fibers to be entangled in a heavier web, the specific energy transferred to the web would be less (see Table 5.1). Thus, it would be expected that the texture definition would not be developed as well by using the same manifold pressures (Figure 6.18 and 6.19). The results however, do not show these differences conclusively. It is felt that this is because the range of pressures available on the pilot equipment is too narrow.

In general, it appears that increasing pressure and the number of passes will result in a better texture definition up to a certain point provided that the web is sufficiently consolidated so that it is not disturbed.

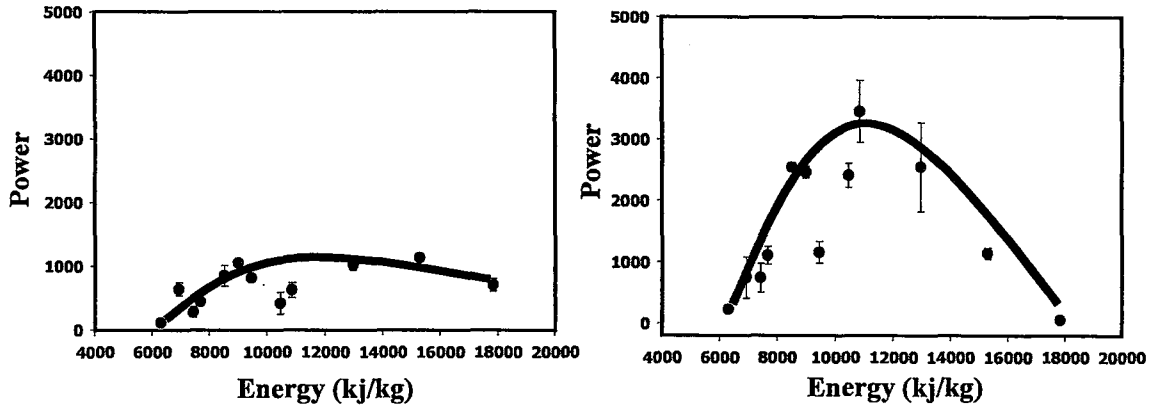

Figure 6.18. Power of PET 100 g/m2 web: Horizontal (left) and Vertical (right) Contrast.

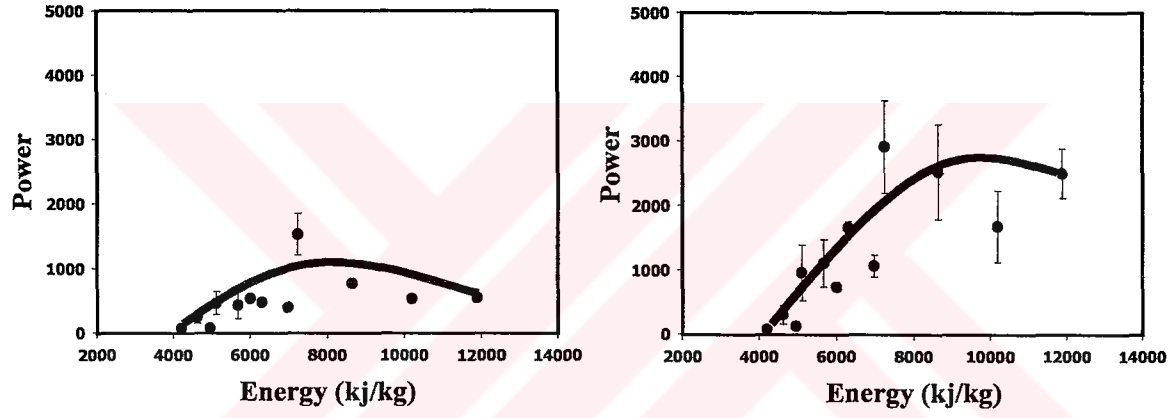

Figure 6.19. Power of PET 150 g/m2 web: Horizontal (left) and Vertical (right) Contrast.

Apertured fabrics were also produced for this part of the investigation. In these fabrics, not only dark field illumination system is used (Figure 5.17.), but also a transmitted lighting system is used (Figure 6.20) to see the apertures better by this lighting system and compare these two lighting systems. The aim here was since the image of the forming wire was captured, both the forming fabric and the apertured fabric can be analyzed separately by co-occurrence analysis.

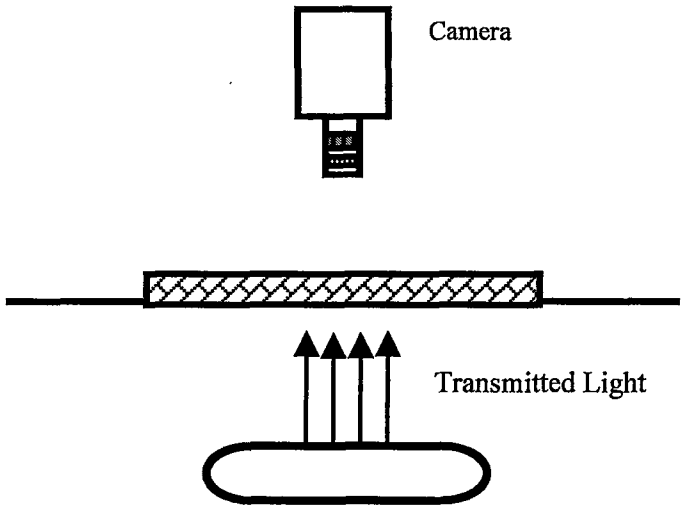

Figure 6.20. Transmitted Illumination Set-up.

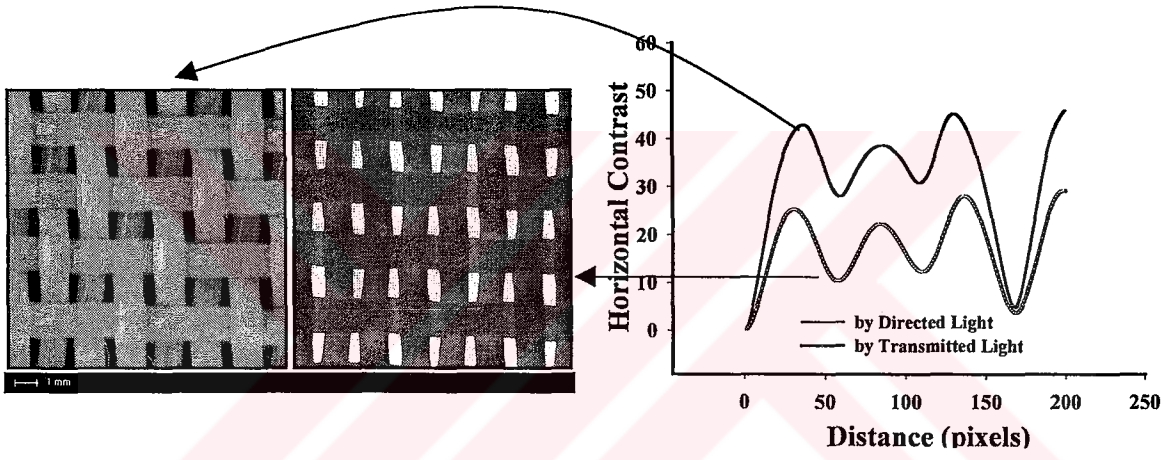

Figure 6.21. Image of the forming wire and its respective co-occurrence analysis.

The periodicity of the apertures on the forming wire can be detected by the co-occurrence analysis (Figure 6.21). However different lighting systems does not show an impact on the curve characteristics, but only the definition of the curves are changed due to lighting. It has been shown in one of the sample images below (see Figure 6.22, and note that all other samples are given in Figures A.4, A.5, A.6). Two different lighting systems are used to capture these images by directed light and transmitted light respectively. The co-occurrence curves shows the distinct periodicity on the fabrics and it is interesting that lighting system does not show any change on the periodicity for the apertured fabrics(Figure 6.23) whereas any meaningful or successful images could not be obtained for textured fabrics. It may be due to the fabric characteristics. Since these were all apertured fabrics, the gray level changes on the fabrics under both lighting systems show the same effect. An interesting result is that co-occurrence curves demonstrate the impact of an

enlargement on the design of the forming surface. The period on the forming wire (Figure 6.21) is more frequent than the respective fabric (Figure 6.23) as expected. The water jets hit the fibers on the fabric and create holes at the knuckles spreading the fibers apart; as the web becomes thinner, and the fabric extends in the width so that the period of the forming wire is decreased on the fabric. The effect of the higher knuckles is seen as a distinct hole on the fabric whereas the lower knuckles creates a more vague aperture formation on the fabric. The development of one by two twill design can be seen clearly on the fabric as one looks at the images diagonally.

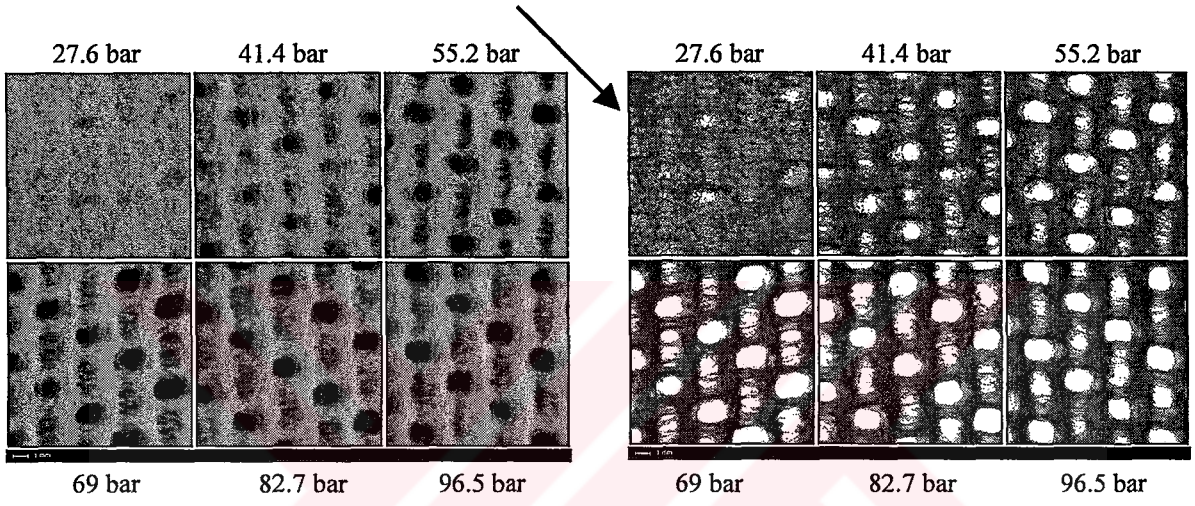

Figure 6.22. Examples from apertured fabrics (PET 100 g/m^2, 2 pass), images by directed light and transmitted light respectively.

The effect of the pressure does not seem to have a significant effect on the periodicity of the fabric except the lowest pressure. Since holes are formed at low pressures and the repetition of the holes is the same in every case (even in all the samples) but just getting more clearer at higher pressures, the formation of the holes can not be differentiated. Whereas the periodicity of the apertures can be clearly detected and the development of apertures can be compared subjectively from the Figures 6.22, A.4-A.6. As is expected, in thin webs (PET 100 g/m^2) apertures are more clear and larger due to the thickness of the web. As the pressure, thus energy, increases more defined apertures are seen but the texture does not change after a certain energy level.

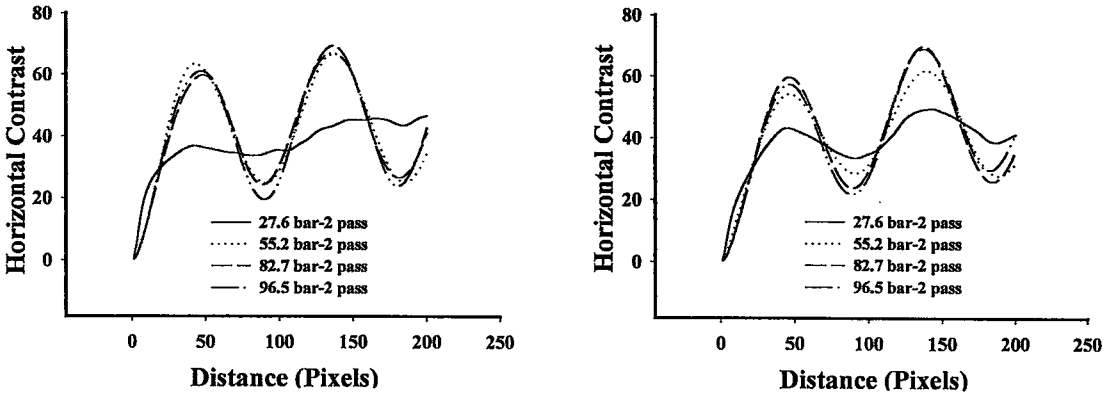

Figure 6.23. Co-occurrence analysis of images respectively from figure 6.22.

In conclusion, it has been shown here that co-occurrence analysis is a good indicator for determining the surface texture properties. It has been demonstrated that horizontal and vertical contrast functions and their respective power spectral analysis data will provide a useful tool for quantifying texture.

It has been demonstrated also that hydroentangling pressure has a marked effect on the manner in which texture develops during the process. In general, increasing pressure and the number of passes will result in a better texture definition up to a certain point provided that the web is sufficiently consolidated. If the web is not consolidated, higher pressures will result in perturbing the web with a concomitantly lower texture definition.

There were several limitations to the current study. The pilot equipment used can only apply pressures of up to 100 bars unlike current commercial equipment allowing 400 bars or more. And the speed of the line was slow.

6.3. Jet Streaks in Hydroentangled Nonwovens

Hydroentanglement is one of the leading technologies in the nonwovens sector [97]. Manufacturers aim to produce textiles alike conventional textiles whereas they have to overcome some difficulties in the technology. One of them is jet streak dilemma. In this part of the study, jet streak periodicity on the nonwovens was investigated by an offline system. Co-occurrence method and Fourier analysis were used for the investigations. These methods have already been used to detect periodicity on textiles in the literature [30,33,35-39].

The quality of fabric mainly depends on two characteristics of fabrics: physical and perceivable properties. Physical properties are imperceptible to a customer but are required for the reliability and serviceability of the fabric. Perceivable properties, however, can be classified as appearance and handle. Purchase decisions are often solely based on the touch and feel and texture of the fabric. It is not surprising that manufacturer place much emphasis on these attributes. In this regard, hydroentanglement is unique in that it can lead to fabrics with unique and distinct textures and can duplicate those found in conventional textiles.

One of the byproducts of using highly collimated water jets, however, is the formation of subtle ridges in machine direction or streaks known as jet streak. It is an inherent result of this process. Collimated, columnar, high-speed jets are necessary for entanglement, but may lead to streakiness. This may be further aggravated by the topography of the forming wire causing periodical watermarks on the fabric. These ridges or streaks are not often desirable. Quantifying the extent to which these are visible is therefore, desirable if one is to adjust the material-process interactions to lower the occurrence of streaks. The vital point for a manufacturer is to determine the magnitude and periodicity of these streaks on the fabric. These two parameters establish the texture quality of the fabric.

Four different fabrics (A, B, C and D) were received from different fabric manufacturers. Fabrics A, B and C are unfinished and white in color. Fabrics A and C are fairly dense structures composed of micro denier fibers while fabric B is a loosely bonded structure. Fabric D is also made from micro denier fibers but it is

finished and dyed. Since the manufacturers wanted to keep their fabric properties confidential, the overall properties are not given for each fabric.

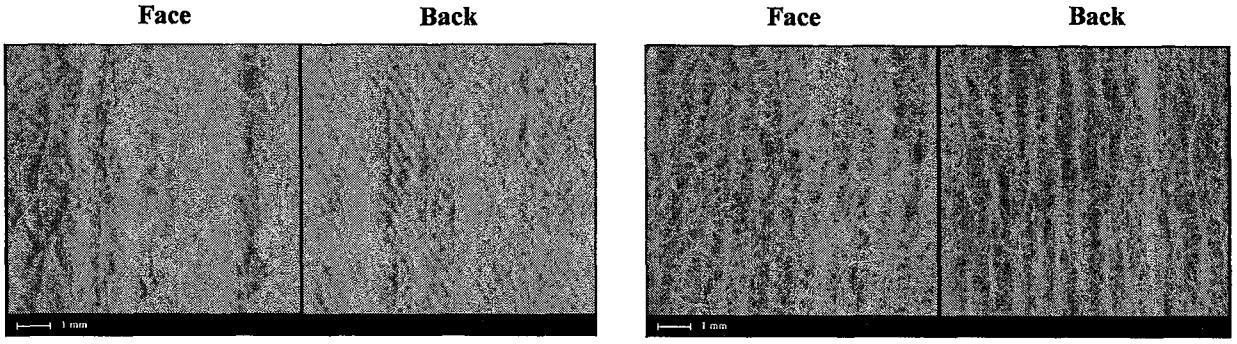

Figure 6.24. Images of jet streaks of fabrics A (left) and B (right)

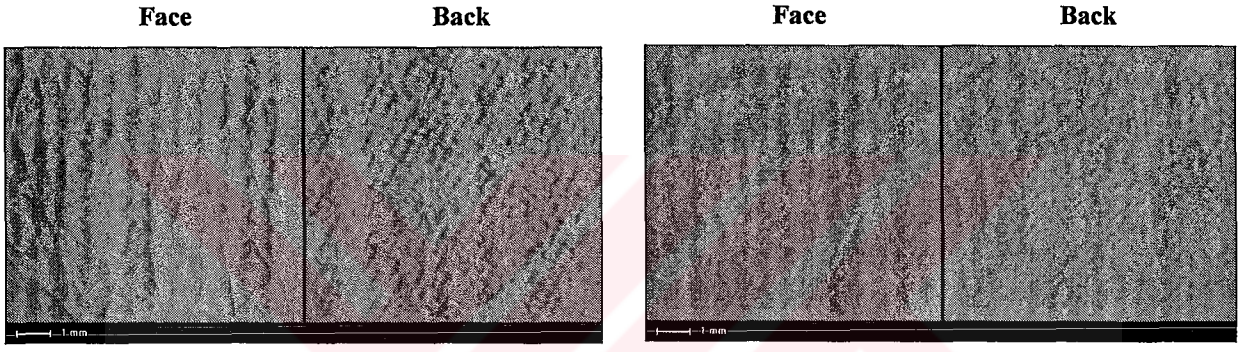

Figure 6.25. Images of jet streaks of fabrics C (left) and D (right)

Images were captured from the face and back of fabrics A,B,C and D. (Figures 6.24 and 6.25). The vertical streaks in Fabric A were not visible to the naked eye and could only be seen when the fabric was viewed at an angle. On the other hand, the streaks in Fabric B are obvious. The ridges of the fabric can be seen from the image of the face of Fabric A, which is the outcome of water jet effect. The co-occurrence curves (Figure 6.26.) indicate some periodicity on the fabrics. However when these data are transformed to the frequency domain (Figure 6.27.), the period of the jet streaks on each fabric is easily recognized (Table 6.1). Challenge in this study was not only just determining the streaks visually but also calculate the periodicity of the streaks by an objective analysis method (Table 6.1). Since period and power of the fabrics correspond to peaks in the spectral density, the period of the jet streaks can be computed from equation 6.1 given below [36]:

$$Period = 2\pi / kF \tag{6.1}$$

k = pixels/mm

F = estimated frequency from spectral analysis

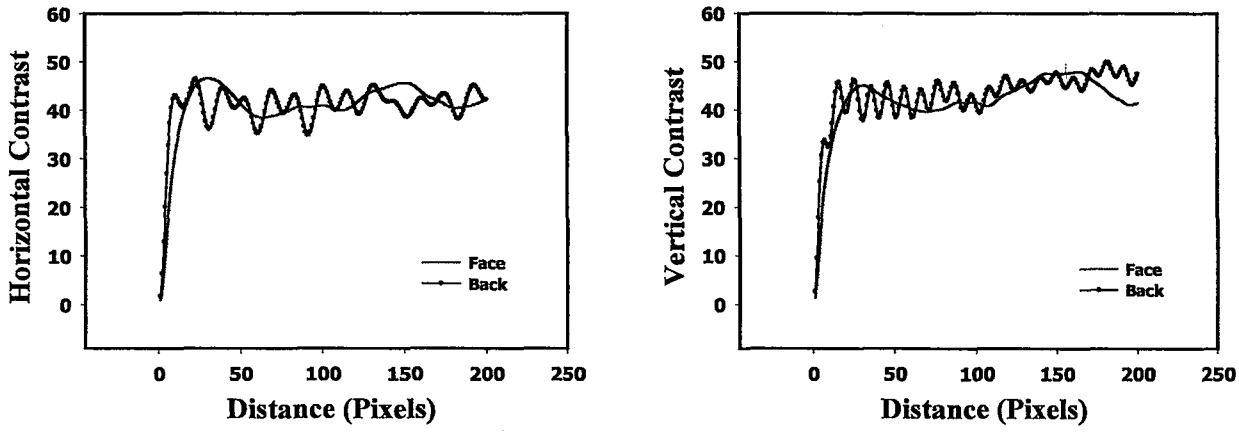

Figure 6.26. Co-occurrence results of Jet Streaks on Fabric A (Horizontal and Vertical)

In the frequency domain, the period of the fabrics can be calculated from the peaks. The highest peak shows the dominant frequency on the fabric (Figure 6.27). The power spectrum shows two peaks at the face of Fabric A (Figure 6.27), where as there are more than two peaks at the back of fabric. It seems that all these textural periodicities do not just come from jet streaks but also is the outcome from the forming fabric. Additionally it is noticed from Figure 6.24 that the fibers in the fabric are placed randomly. Since splittable fibers are used in Fabric A, the fibers are dispersed in the fabric forming a different kind of textural periodicity. All these factors impact the periodicity.

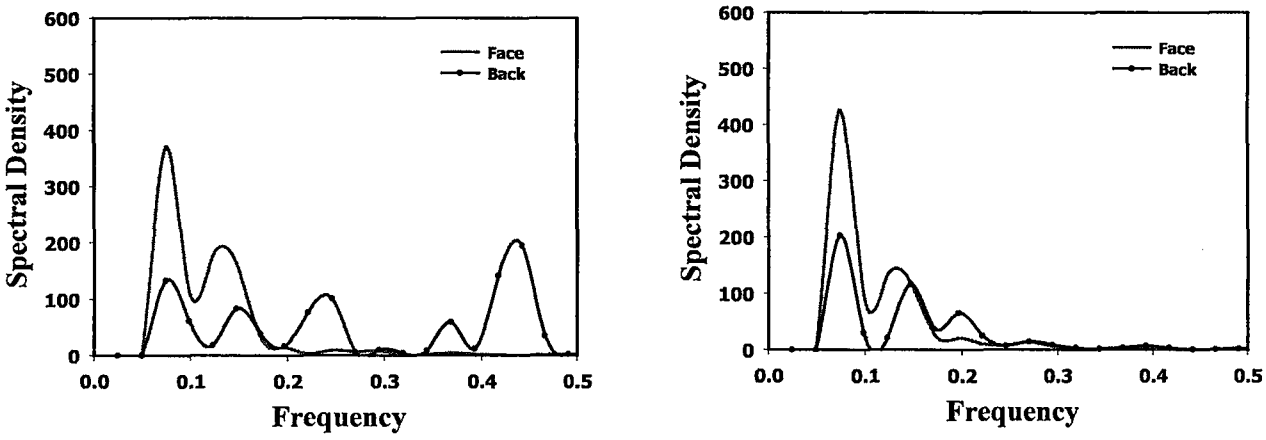

Figure 6.27. Power Spectrum from Fabric A (Horizontal and Vertical)

As is shown in Figure 6.24, jet streaks or ridges on both face and back of Fabric B are easily perceived. Fabric B is produced from homopolymer fibers. The co-occurrence curves from both sides of the fabric almost overlap in the graphs (Figure 6.28), and a similar tendency is also observed from the spectral analysis (Figure A.7). There is only one peak and the power (magnitude) and frequencies are almost the same (Figure A.7) for both sides. Consequently, jet streaks periodicity and magnitude (Table 6.1) can be determined from the co-occurrence graphs (Figure 6.28) and spectral analysis (Figure A.7).

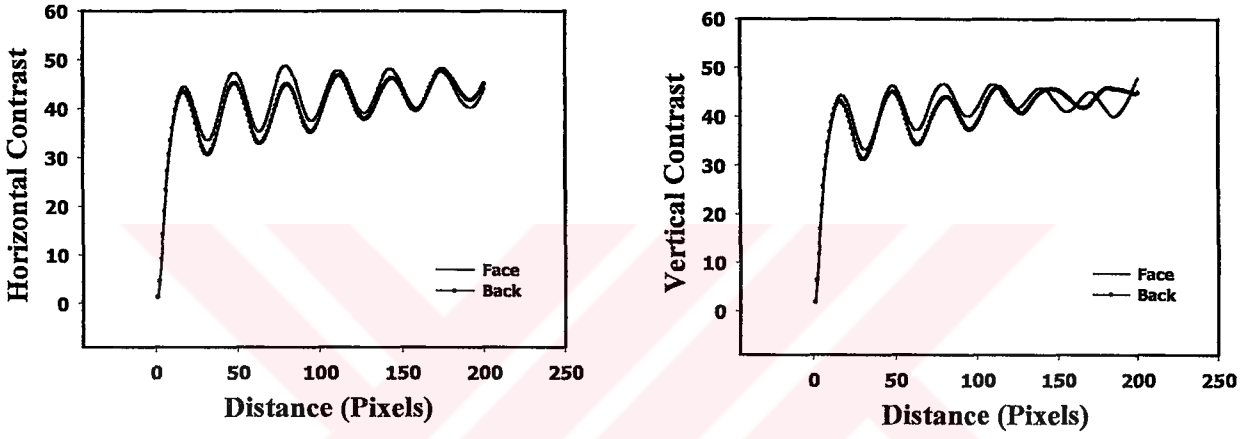

Figure 6.28. Co-occurrence results of jet streaks on fabric B (Horizontal and Vertical)

Splittable fibers are also used in fabrics C and D. The texture of the face of Fabric C is very different from that of the back (Figure 6.25, 6.29) while in Fabric D, face and back seems visually the same. In fabric C, difference in the texture of face and back creates a breaking in the co-occurrence curves as it can be seen in Figure 6.29. Curves for the face of the fabric shows well defined periodicity however periodicity is lost in the back of the fabric. The spectral analysis shown in Figure A.8 in the Appendix also supports these findings. It is clear from the images that the texture of the back is complicated and it is probably the outcome of the forming wire. While the fibers are placed more directional on the fabric face, they are oriented randomly on the fabric back (Figure 6.25)

Image of fabric D is dark due to its color (Figure 6.25). Since the fabric was dyed in blue, brighter images could not be captured. The periodicity of fabric D can not be visually realized due to the limitation of human eye. Since the image is dark, the

gray-level transitions are very hard to be separated by the human eye yet not by the imaging system. This is very clearly seen in contrast graphs and the periodicity on the fabric is shown in Figure 6.30. Especially, the face of the fabric shows a distinct periodicity, but although the back shows a certain periodicity (Figure 6.30), the magnitude of the frequency is very low compared to the face (Figure A.8). This means that there is a hidden frequency in the back, and it may be due to the hairiness at the back of the fabric, which is seen in the image (Figure 6.25). Hairiness can affect the real periodicity and can be a factor for disguising the real periodicity of the fabric. Nonetheless this system and method can determine the periodicity even if its magnitude is low.

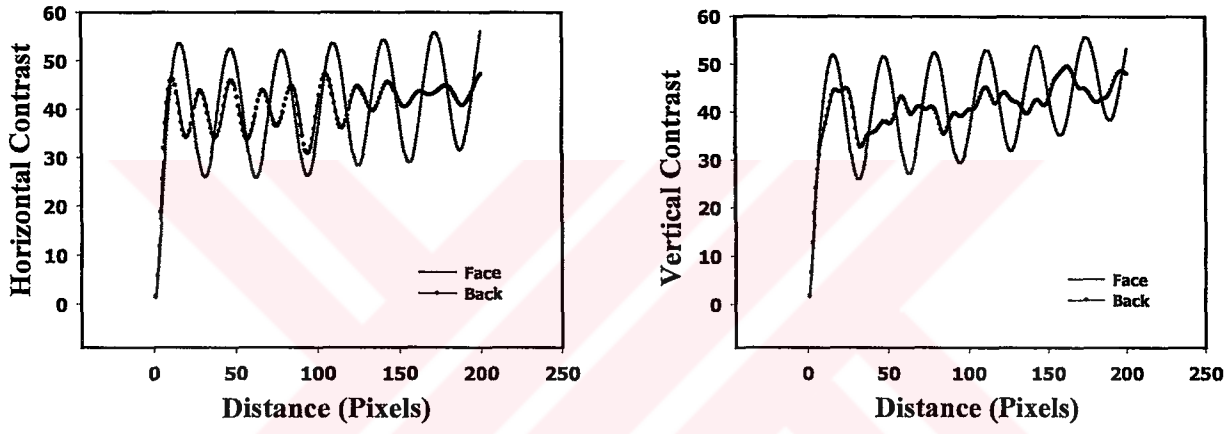

Figure 6.29. Co-occurrence results of jet streaks on fabric C (Horizontal and Vertical)

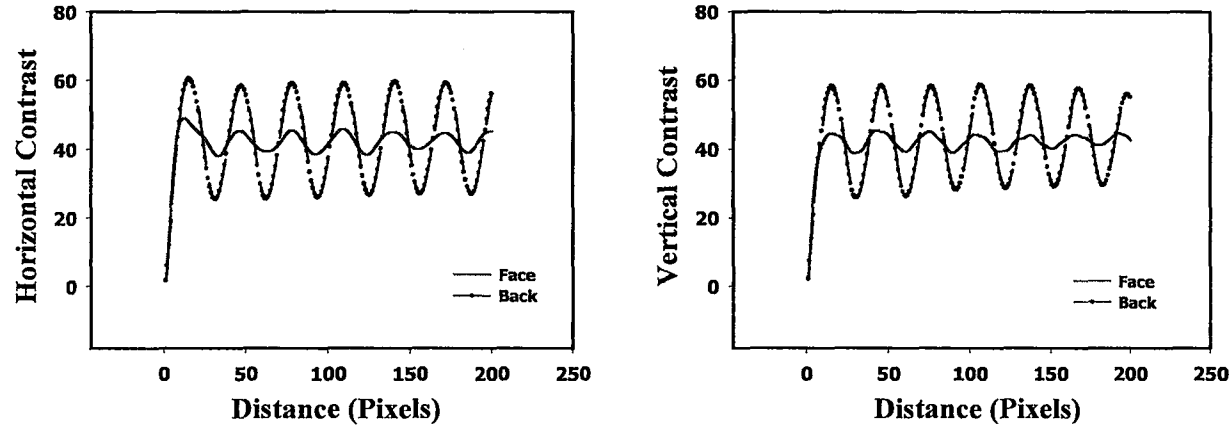

Figure 6.30. Co-occurrence results of jet streaks on fabric D (horizontal and vertical)

The horizontal and vertical contrast function and their respective power spectral analysis data show the periodicity of the ridges on the fabrics. Although, the

periodicity of the fabrics can be detected (from Table 6.1) it can not be exactly said that these findings are the length of the jet streaks. However there are generally 50-60 streaks per inch of a spunlace fabric. Therefore it means that the period of the streaks is between 0.508-0.635 mm. In this study, except Fabric A, all other fabrics have periodicity that generally lies in this range. Since Fabric A has a complex texture structure (Figure 6.24) in both sides, it has more than one dominant frequency. Nevertheless, there is a strong indication for the other three fabrics that the frequencies on these fabrics are caused by jet streaks. It can be concluded then that the textural attributes and defects of hydroentangled fabrics can be objectively determined by the image analysis techniques devised in this investigation.

Table 6.1. Periods of fabrics from their spectral density graphs

Specimen	**Direction**	**Period (mm)**
Fabric A-Face	H Cont.	1.73 0.94
	V Cont.	1.73 0.90
Fabric A-Back	H Cont.	1.73 0.84 0.53 0.31
	V Cont.	0.90 0.67 0.20
Fabric B-Face	H Cont.	0.59
	V Cont.	0.61
Fabric B-Back	H Cont.	0.59
	V Cont.	0.58
Fabric C-Face	H Cont.	0.56
	V Cont.	0.56
Fabric C-Back	H Cont.	0.34
	V Cont.	0.68
Fabric D-Face	H Cont.	0.56
	V Cont.	0.56
Fabric D-Back	H Cont.	0.50
	V Cont.	0.56

7. CONCLUSIONS

In this research, texture classification has been studied in hydroentangled nonwovens. Co-occurrence method has been applied and yet contrast data were determined as a function of sampling distance then afterwards one-dimensional Fourier analysis has been applied on these findings to measure the strength of the periodicity. The relationship between fabric texture, water jet pressure and hydroentangling energy was investigated. In addition to this, jet streaks on the hydroentanglement fabrics are determined. The following conclusions are drawn from the findings of these investigations:

- The viability of co-occurrence analysis is demonstrated for texture retention after abrasion for range of fabrics including a woven fabric. As a result, it was demonstrated that the co-occurrence methods are sensitive enough to structural and textural changes in the fabrics examined. Additionally, the power from Fourier analysis is a good indicator for fabric texture definition.

- The magnitude of the contrast curves has become smaller as a result of abrasion, and spectral analysis results have supported these facts as the power values have decreased.

- Hydroentangling pressure has a marked effect on the manner in which texture develops during the process. In general, increasing pressure and the number of passes (which means energy) will result in a better texture definition up to a certain point provided that the web is sufficiently consolidated. If the web is not consolidated, higher pressures will result in perturbing the web with a concomitantly lower texture definition.

- The use of different lighting system for apertured fabrics does not make a major difference in image capturing and the results obtained. However transmitted lighting gives a better image quality for these kinds of fabrics and better identifies the development of the texture.

- After a certain energy level, the formation of apertures is kept in a certain dimension. There is a threshold energy level for a clear aperture formation.

- Although a pilot scale is used for this study, hydroentangling texture mechanism is understood and the results can be used only as a guide for full-scale production.

- Jet streaks can be determined by the image and analysis systems employed in this research, however, the surface structure of the fabric is complex since there are more than one periodicity on the fabrics. Yet the dominant frequencies for most of the fabrics are found to be approximately 0.57 mm. Since the periods are found between 0.508-0.635 mm, it is a strong indication that these results are very probably belongs to the jet streaks.

- The results has indicated that co-occurrence statistics used as a function of sampling distance are sensitive to periodic changes of texture and that of the spectral analysis is a good measure of the strength of the periodicity.

- Co-occurrence analysis is a good indicator for determining the surface texture properties. It is demonstrated that horizontal and vertical contrast functions and their respective power spectral analysis data will provide a useful tool for quantifying texture. All results are consistent with subjective analysis from the fabric images. This method has given reliable results for both texture and periodical analysis.

8. SUGGESTIONS FOR FUTURE STUDIES

The following are suggestions for future studies:

- While this study provides basic understanding of texture evaluation, the pressure levels and speeds used are significantly lower than today's hydroentangled machines. A systematic study considering high pressures and speeds is proposed.

- An image analyses system with laser based lighting or a surface profiler could provide a way to capture more details than the system used in this study.

- The vital point for a spunlace fabric manufacturer is to determine the magnitude and periodicity of jet streaks on the fabric. This work has shown that jet streaks can be detected with an off-line system. It would be extremely beneficial to industry if an online system is available.

REFERENCES

[1] www.edana.org

[2] **Nonwoven Fabrics Handbook-INDA,** 1999. INDA Association of the Nonwoven Fabrics Industry.

[3] **Medeiros,** F.J., 1996. Spunlace/Hydroentanglement Methods&Products, The Proceedings of Inda-Tech.

[4] **Wilson, A.,** 2000. Blurring the Boundaries, Nonwovens Report International, 30-38, April.

[5] Fibre Know-how the Key to the Machine Developments, 1998. Nonwovens Report Yearbook, 12-16, August.

[6] **Medeiros, F.J.,** 1997. Spunlacing Offers Utmost Versatility, American Textiles International, 34-36, November.

[7] **Turi, M.,** 1988. The Outlook for Spunlaced Nonwovens. Nonwovens Industry, pg. 30-36, November.

[8] **Vuillame, A.M.,** 1991. A Global Approach to the Economics and End-product Quality of Spunlace Nonwovens, Tappi Journal, 149-152, August.

[9] **White, C. F.,** 1990. Hydroentanglement Technology Applied to Wet-formed and Other Precursor Webs, Tappi Journal, 187-192, June.

[10] **Watzl, A.,** 2000. Spunbonding and Spunlacing: Two Leading Technologies Coming Together, INTC 2000, Dallas, Texas, 26-28, September.

[11] What's new in textiles, 1991. Textile Horizons, pg 22-23, October.

[12] **Widen, C. B.,** 1988. Forming Wires for Hydroentanglement Systems, Nonwovens Industry, 39-43, November.

[13] **Widen, C. B.,** 1991. Forming Fabrics for Spunlace Applications, Tappi Journal, 149-153, May.

[14] **Acar, M., and Harper J.,** 2000. Hydroentangled Nonwoven Fabrics for Industrial Applications and Composites, 80th Textile Institute World Conference, Manchester, April.

[15] **Bottcher, P.,** 1999. Machines for Mechanical Web Bonding, ITB Nonwovens Industrial Textiles 3/99.

[16] **Connolly, T. J., and Parent, L. R.,** 1993. Influence of Specific Energy on the Properties of Hydroentangled Nonwoven Fabrics, Tappi Journal 76, No. 8, 135-141.

[17] **Timble, N. B., Gilmore, T. F., and Morton, G. P.,** 1996. Spunlaced Fabric Performance for Unbleached, Bleached and Low Micronaire Unbleached Cotton at Different Specific Energy Levels of Water, The Proceedings of Inda-Tech.

[18] **Timble, N. B., and Allen, C.,** 1997. Hydroentangled Fabric Performance for Polyester/Unbleached Cotton Blends at Various Levels of Specific Energy Levels, The Proceedings of Inda-Tech.

[19] **Gahide, S. F.,** 2000. Combination of Hydroentanglement and Foam Bonding technologies for Wood Pulp and Polyester Fibers in Wet Lay Nonwoven Fabrics, Master Thesis, North Carolina State University..

[20] **Turi, M.,** 1993. Product and Process Development of Spunlace Fabrics, The Prooceedings of Inda-Tech.

[21] **Buchanan, D.R.,** 2000. ITMA 99:Review, Textile Progress, Vol.30, No:1/2, 62-66.

[22] **Jaussaud, J. P.,** 1987. Rotary Hydraulic Entanglement Technology, Nonwovens in Medical and Healthcare Applications Conference, Nov 10^{th}-12^{th} , Brighton.

[23] **Chowdhury, M. D. H.,** 1996. The Hydrolace System and Its Ability to Optimize Modern Fibre Properties in the Development of Unique Properties, Proceedings of Inda-Tech.

[24] **Shivers, J. C., Popper, P., and Saffer, H. W.,** 1976. ' The Mechanical and Geometric Properties of Spunlaced Fibrous Structures', INDA Technical Symposium.

[25] **Vuillame, A.M.,** 1993. Spunlace Nonwovens:The Bridge Between Nonwovens and Textiles, The Proceedings of Inda-Tech.

[26] **Ghassemieh, E., Acar, M., and Versteeg, H.K.,** 2001. Improvement of the Efficiency of Energy Transfer in the Hydroentanglement Process, Composites Science and Technology, vol.61, 1681-1694.

[27] **Hwo, C. C., Shiffler, D.A.,** 1998. Nonwovens from Polytrimethylene Terephthalate Staples, Special Report, NCRC.

[28] **Park, T.Y., Joo, C.W.,** 1993. Theoretical and Experimental Analysis on the Tensile Mechanism of Spunlace Nonwovens, Proceedings of the 2^{nd} Asian Textile Conference, vol.1, 383-388.

[29] **Shahani, A., Shiffler, D. A., Batra, S. K., Cannon, C. C.,** 1999. Foamed Latex Bonding of Spunlace Fabrics to Improve Physical Properties, International Nonwovens Journal, Fall.

[30] **Wu, Y., Pourdeyhimi, B., and Spivak, S. M.,** 1991. Texture Evaluation of Carpets Using Image Analysis, Textile Res. J., 61 (7), 407-419.

[31] **Sonka, M., Hlavac, V., and Roger B.,** 1999. Image Processing and Machine Vision, Second Edition, Brooks/Cole Publishing Company.

[32] **Jose, D. J., Hollies, N. R. S., and Spivak S. M.,** 1986. Instrumental Techniques to Quantify Textural Change in Carpets, Part I: Image Analysis, Textile Res. J., (56), 591-597.

[33] **Wood, E. J., and Hodgson M. R.,** 1989. Carpet Texture Measurement using Image Analysis, Textile Res. J., (59), 1-11.

[34] **Wu, Y., Pourdeyhimi, B., Spivak, S. M., and Hollies N. R. S.,** 1990. Part III: Colorimetric Image Analysis, Textile Res. J., (60), 673-686.

[35] **Wood, E. J.,** 1990. Applying Fourier and associated Transforms to Pattern Characterization in Textiles, Textile Res. J., 60, 212-220.

[36] **Sobus, J., Pourdeyhimi, B., Gerde, J., and Ulcay, Y.,** 1991. Assessing Changes in Texture Periodicity Due to Appearance Loss in Carpets: Gray Level Co-Occurrence Analysis, Textile Res. J., 61(10), 557-567.

[37] **Sobus, J., Pourdeyhimi, B., Xu, B., and Ulcay, Y.,** 1992. Evaluating Loss of Texture Definition in Carpets Using Mathematical Morphology: Covariance, Textile Res. J., 62(1), 26-39.

[38] **Pourdeyhimi, B., and Sobus, J.,** 1993. Evaluating Carpet Appearance Loss: Surface Intensity and Roughness, Textile Res. J., 63(9), 523-535.

[39] **Pourdeyhimi, B., Xu, B., and Wehrle, L.,** 1994. Evaluating Carpet Appearance Loss: Periodicity and Tuft Placement, Textile Res. J., 64(1), 21-32.

[40] **Xu, B.,** 1994. Assessing Carpet Appearance Retention by Image Analysis, Textile Res. J., 64(12), 697-709.

[41] **Wood, E.J.,** 1996. Objective Measurement of Carpet Appearance by Image Analysis- Part I: Principles and Methodology, Melliand English 7-8/96.

[42] **Wood, E.J.,** 1996. Objective Measurement of Carpet Appearance by Image Analysis- Part II: Applications, Melliand English 12/96.

[43] **Xu, B.,** 1996. An Overview of Applications of Image Analysis to Objectively Evaluate Fabric Appearance, Textile Chemist and Colorist, Vol 28, No 5., 18-23.

[44] **Konda, A., Xin, L., Takadersa, M., Okoshi Y., and Torichimi, K.,** 1988. Evaluation of Image Pilling by Computer Image Analysis, J.Textile Mach. Soc. Jpn. 36(3), 96-107.

[45] **His. C.H., Bresee, R.R., and Annis, P.A.,** 1998. Characterizing Fabric Pilling by Using Image-analysis Techniques, Part I: Pill Detection and Detection, J.Text.Inst., 89 Part 1, No. 1.

[46] **His. C.H., Bresee, R.R., and Annis, P.A.,** 1998. Characterizing Fabric Pilling by Using Image-analysis Techniques, Part II: Comparison with Visual Pill Ratings, J.Text.Inst., 89 Part 1, No. 1.

[47] **Ramgulam, R. R., Amirbayat, J., and Porat, I.,** 1993. The Objective Assessment of Fabric Pilling, Part I: Methodology, J.Text.Inst., 84, 221-226.

[48] **Hsi, C. H., and Bresee, R. R., Annis, P. A.,** 2000. Characterizing Fuzz on Fabrics Using image Analysis, Textile Res. J., 70(10), 859-865.

[49] **Lin, S., and Xu, B.,** 2000. Evaluating Fabric Fuzziness Using Wavelet, Opt.Eng., 39(9) 2387-2391, September.

[50] **Kim, H. S., Latifi, M., and Pourdeyhimi, B.,** 2000. Characterizing Fuzz in Nonwoven Fabrics, INDA J., 18-22, Spring.

[51] **Na, Y., and Pourdeyhimi, B.,** 1995. Assessing Wrinkling Using Image Analysis and Replicate Standards, Textile Res. J., 65(13), 149-157.

[52] **Xu, B., and Cuminato, D. F.,** 1998. Evaluating Fabric Smoothness Appearance with a Laser Profilometer, Textile Res. J., 68(12), 900-906.

[53] **Amirbayat, J., and Alagha, M. J.,** 1996. Objective Assessment of Wrinkle Recovery by Means of Laser Triangulation, J. Text. Inst., 87, 349-355.

[54] **Xu, B., and Reed, J. A.,** 1995. Instrumental Evaluation of Fabric Wrinkle Recovery, J. Text. Inst., 86, 129-135.

[55] **Fuchs, H., Magel, M., Offermann, P., Raue, P., and Seifert, R.,** Surface Characterization of Textile Fabrics, Part I: Surface Characterization of Parameters, Meilland Textilberichte, E13, 1/1993.

[56] **Bahners, T., Schollmeyer, E., Magel, M., Fuchs, H., Seifert, R., Raue, P., and Offermann, P.,** 1994. Surface Characterization of Textile Fabrics, Part II: Modern Mathematical Profile Evaluation Process, Meilland Textilberichte, E46, 3/94.

[57] **Seifert, R., Raue, P., Offermann, P,** 1995. Surface Characterization of Textile Fabrics, Part 3: Profilometric Surface Measuring Systems, Meilland Textilberichte, E164, 9/95.

[58] **Bueno, M-A, Durand, B., and Renner, M.,** 2000. Optical Characterization of the State of the Fabric Surfaces, Optical Engineering, 39(6) 1697-1703.

[59] **Ramgulam, R. B., Amirbayat, J. and Porat I.,** 1993. Measurement of Fabric Roughness by a Non-contact Method, J. Text. Inst., 84 No 1.

[60] **Xu, B.,** 1996. Identfying Fabric Structures with Fast Fourier Transform Techniques, Textile Res. J., 66(8), 496-506.

[61] **Pourdeyhimi, B.,** 1993. Assessing Fiber Orientation in Nonwoven Fabrics, INDA J., Vol 5, No.4, 29-36.

[62] **Huang, X., and Bresee, R.,** 1993. Characterizing Nonwoven Web Structure Using Image Analysis Techniques Part II: Fiber Orientation Analysis in Thin Webs, INDA J., Vol 5, No.2, 14-21.

[63] **Gong, R. H., and Newton, A.,** 1996. Image-analysis techniques Part II: The Measurement of Fibre Orientation in Nonwoven Fabrics, JTI, 87: (2), 371-388.

[64] **Xu, B., and Ting, Y-L.,** 1995. Measuring Structural Characteristics of Fiber Segments in Nonwoven Fabrics, Textile Res. J., 65(1), 41-48.

[65] **Pourdeyhimi, B., and Ramanathan, R.,** 1996. Measuring Fiber Orientation in Nonwovens, Part II: Direct Tracking, Textile Res. J., 66(12), 747-753.

[66] **Pourdeyhimi, B., Dent, R., and Davis H.,** 1997. Measuring Fiber Orientation in Nonwovens, Part III: Fourier Transform, Textile Res. J., 67(2), 143-151.

[67] **Xu, B., and Yu, L.,** 1997. Determining Fiber Orientation Distribution in Nonwovens with Hough Transform Techniques, Textile Res. J., 67(8), 563-571.

[68] **Pourdeyhimi, B., and Dent, R.,** 1997. Measuring Fiber Orientation in Nonwovens, Part IV: Flow Field Analysis, Textile Res. J., 67(3), 181-187.

[69] **Pourdeyhimi, B., Dent, R., Jerbi, A., Tanaka, S., and Deshpande, A.,** 1999. Measuring Fiber Orientation in Nonwovens, Part V: Real Webs, Textile Res. J., 69(3), 185-192.

[70] **Yan, Z., and Bresee, R.,** 1999. Flexible Multifunction Instrument for Automated Nonwoven Web Structure Analysis, Textile Res. J., 69(11), 795-804.

[71] **Huang, X., and Bresee, R.,** 1993. Characterizing Nonwoven Web Structure Using Image Analysis Techniques Part I: Pore Analysis in Thin Webs, INDA J., Vol 5, No.1, 13-21.

[72] **Pourdeyhimi, B., and Xu, B.,** 1993. Pore Size Characterization in Nonwoven Fabrics, INDA J., Vol 5, No.3, 20-27.

[73] **Pourdeyhimi, B., and Xu, B.,** 1994. Pore Characterization in Nonwoven Fabrics: Shape Considerations, INDA J., Vol 6, No.1, 26-30.

[74] **Gong, R. H., and Newton, A.,** 1992. Image-analysis techniques Part I: The Measurement of Pore Size Distributions, JTI, 83: (2), 253-268.

[75] **Xu, B.,** 1996. Measurement of pore characteristics in nonwoven fabrics using image analysis, Clothing-&-Textiles-Research-Journal; 14(1): 81-88

[76] **Huang, X., and Bresee, R.,** 1994. Characterizing Nonwoven Web Structure Using Image Analysis Techniques Part IV: Fiber Diameter Analysis for Spunbonded Webs, INDA J., Vol 6, No.4, 53-59.

[77] **Pourdeyhimi, B.,** 1999. Characterizing Fiber Diameter Variability in Nonwovens, INDA J. 29-35, Spring.

[78] **Pourdeyhimi, B., and Dent, R.,** 1999. Measuring Fiber Diameter Distributions in Nonwovens, Textile Res. J., 69(4), 223-236.

[79] **Huang, X., and Bresee, R.,** 1993. Characterizing Nonwoven Web Structure Using Image Analysis Techniques Part III: Web Uniformity Analysis, INDA J., Vol 5, No.3, 28-38.

[80] **Xu, B., and Pourdeyhimi, B.,** 1993. Assessing Pile Lay Orientation in Carpets Using Flow-Field Analysis, Canadian Textile Journal, 39-48, April/May.

[81] **Lee, H. S., Hodgson, R. M., and Wood, E. J.,** 1988. Texture Measures for Carpet Wear Assessment, IEEE Trans. Pattern Anal. Mach. Intell. 10 (1), 92-105 .

[82] **Pourdeyhimi, B., Xu, B., and Nayernouri, A.,** 1994. Evaluating Carpet Appearance Loss: Pile Lay Orientation, Textile Res. J., 64(3), 130-135.

[83] **Wood, E. J.,** 1993. Description and Measurement of Carpet Appearance, Textile Res. J., 63 (10), 580-594.

[84] **Rao, A. R., 1990.** " A Taxonomy for Texture Description and Identification", Springer Verlag New York Inc.

[85] **Hearle, J. W. S., and Sultan, M. A.,** 1967. " A Study of Needled Fabrics, Part I: Experimental Methods and Properties", J.Text. I., 58, 251.

[86] **Hearle, J. W. S., and Stevenson, M. A.,** 1964. "Nonwoven Fabric Studies Part III: The Anisotropy of Nonwoven Fabrics", J.Text. I., 33, 877.

[87] **Militky, J., Rubnerova, J., and Klicka, V.,** 1999. Surface Appearance Irregularity of Nonwovens, Int. J. of Clothing Science and Technology, vol 11, No 2/3, 141-150.

[88] **AATCC Technical Manual,** 1993. Vol. 65.

[89] **Annual Book of ASTM Standards,** 1993: Textiles-Yarns, Fabrics, General Test Methods, Vol.32.

[90] **Sirikasemlert, A., and Tao, X.,** 2000. Objective Evaluation of Textural Changes in Knitted Fabrics by Laser Triangulation, Textile Res. J., 70(12), 1076-1087.

[91] **Jain, A. K.,** 1989. Fundamental of Digital Image Processing, Prentice-Hall, Inc.

[92] **Haralick, R. M.,** 1979. Statistical and Structural Approaches to Texture, Proc. IEEE 67, 789-809, May.

[93] **Jirsak, O., and Wadsworth, L. C.,** 1999. Nonwoven Textiles, Carolina Academic Press, Durham, NC.

[94] **Pavlidis, T.,** 1982. "Algorithms for Graphics and Image Processing", Computer Science Press, Rockville, MD.

[95] **Haralick, R.M., Shanmugam, K., and Dinstein, I.,** 1973. Textural Features for Image Classification, IEEE Trans.Syst.Man, Cybernet. 3 (6), 610-621.

[96] **Berkalp, O.B., Pourdeyhimi, B., Seyam, A., and Holmes, R.,** 2002. Texture Retention after Fabric-to-Fabric Abrasion, accepted for publication for TRJ.

[97] **Wubbe Ellien,** 2002. Spunlace Soaks Up The Spotlight in Nonwovens Technology Nonwovens industry, March.

ATTACHMENTS

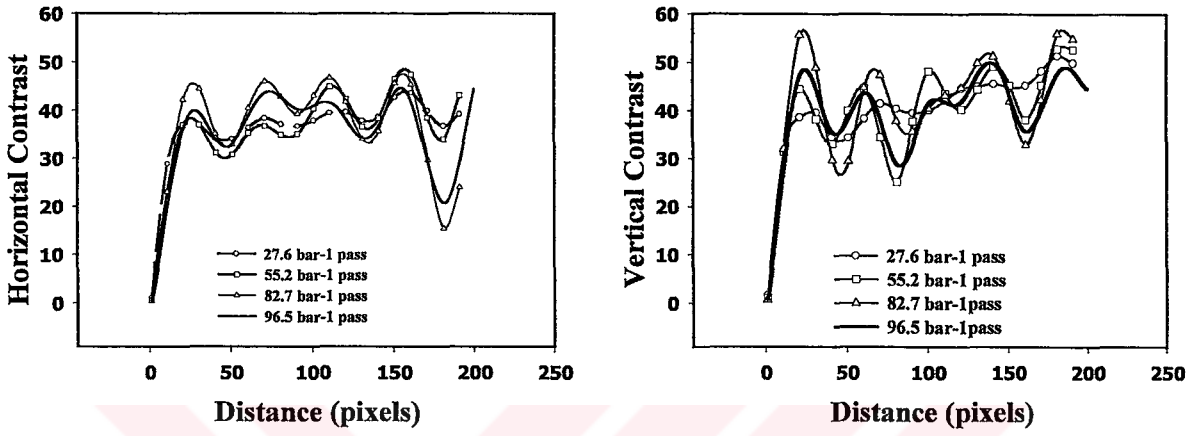

Figure A.1. Co-occurrence analysis using a PET 100 g/m2 web - 1 pass

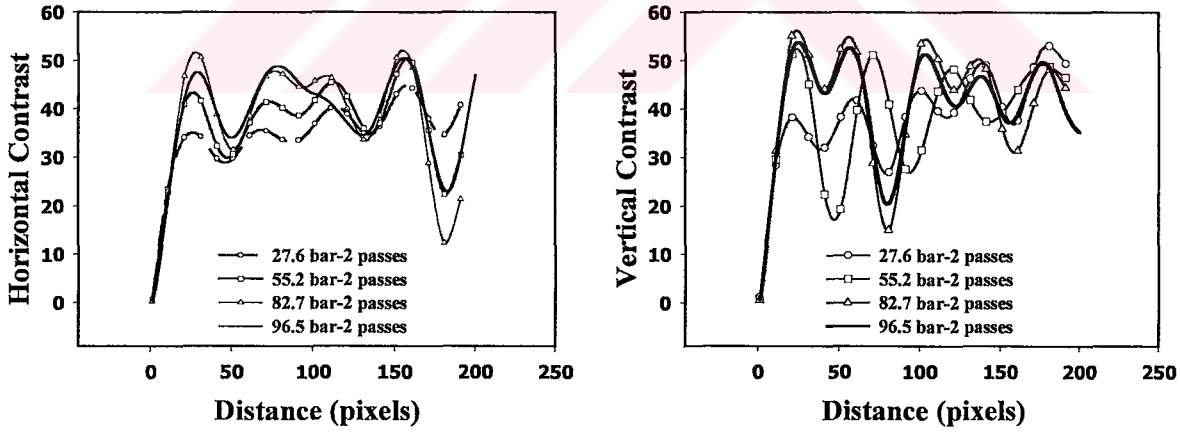

Figure A.2. Co-occurrence analysis using a PET 100 g/m2 web - 2 passes

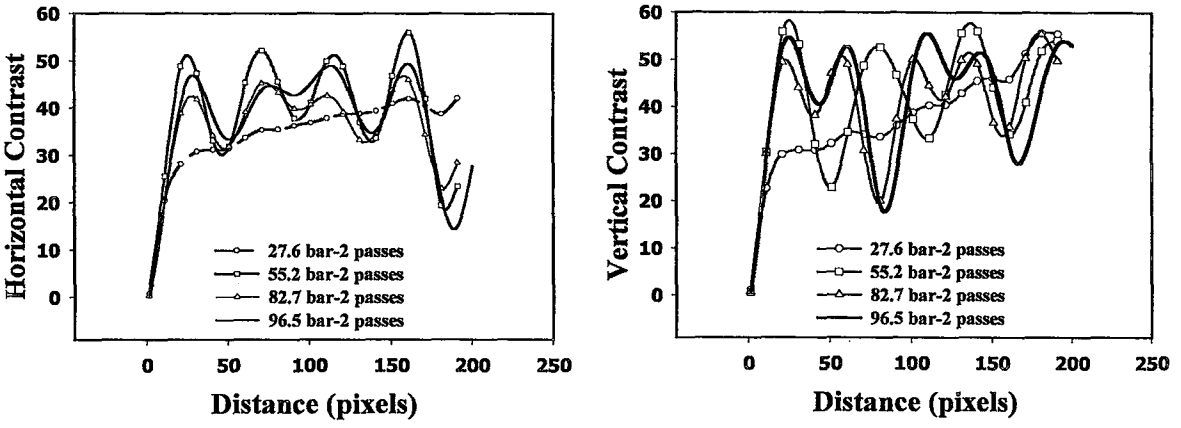

Figure A.3. Co-occurrence analysis using a PET 150 g/m2 web - 2 passes

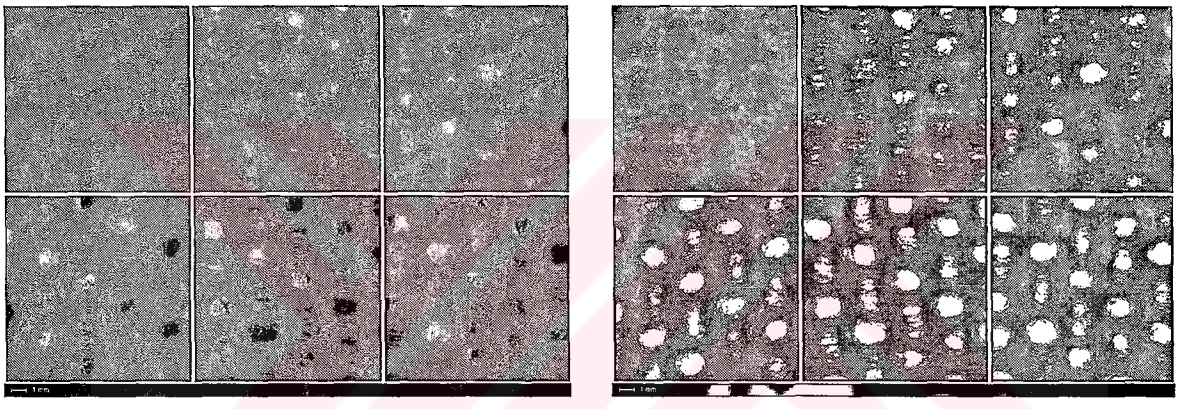

Figure A.4. Examples from apertured fabrics (PET 100 g/m^2, 1 pass), images by directed light and transmitted light respectively.

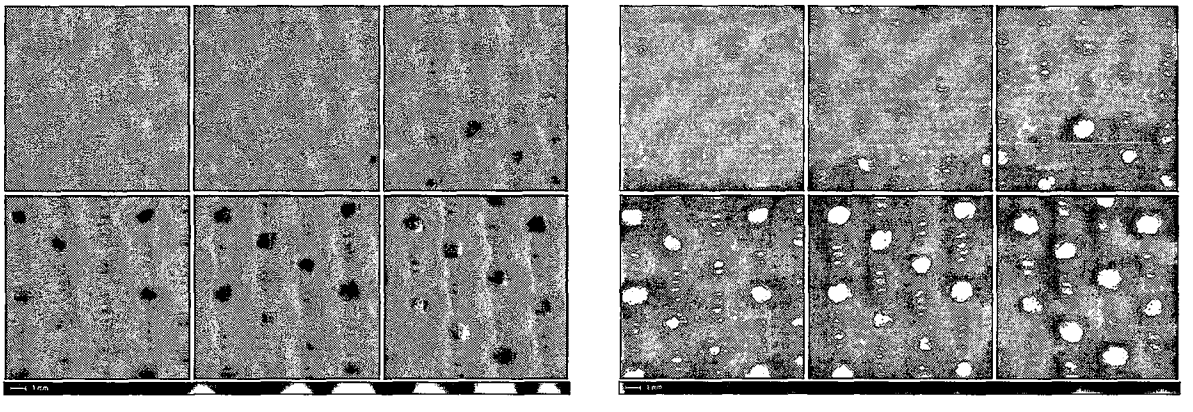

Figure A.5. Examples from apertured fabrics (PET 150 g/m^2, 1 pass), images by directed light and transmitted light respectively.

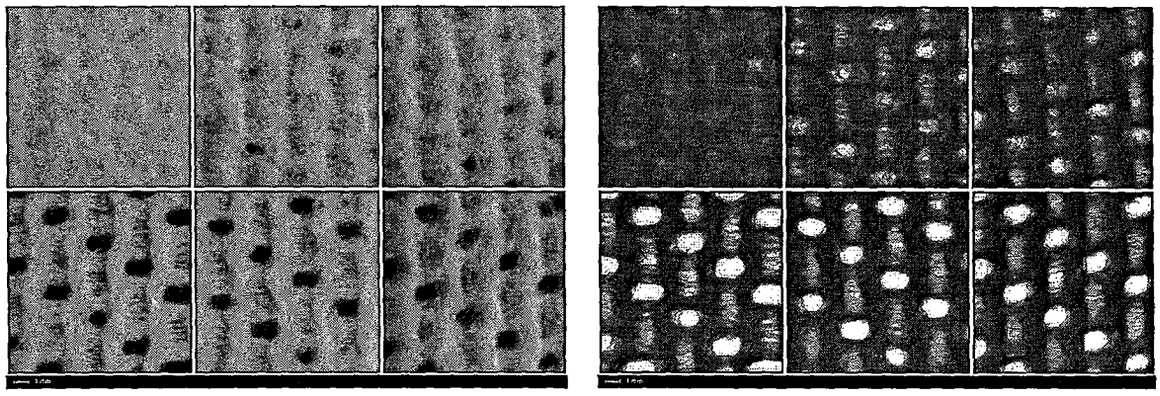

Figure A.6. Examples from apertured fabrics (PET 150 g/m^2, 2 pass), images by directed light and transmitted light respectively.

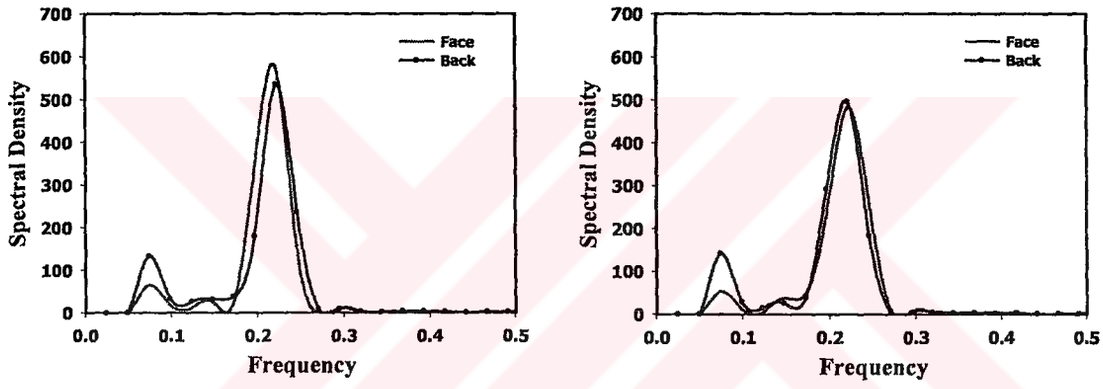

Figure A.7. Power Spectrum from Fabric B (Horizontal and Vertical)

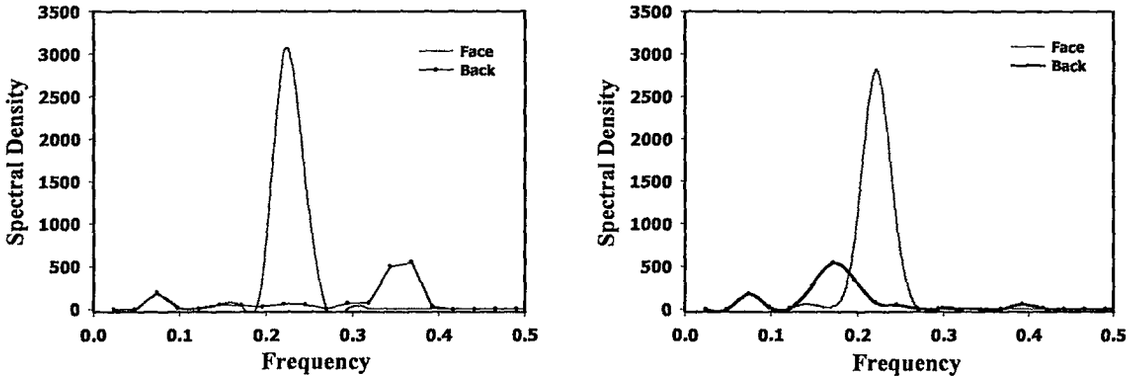

Figure A.8. Power Spectrum from Fabric C (Horizontal and Vertical)

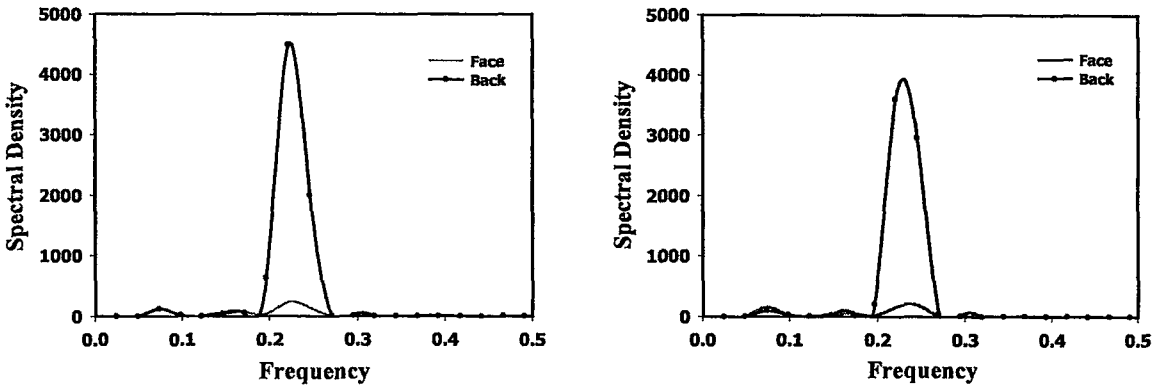

Figure A.9. Power Spectrum from Fabric D (Horizontal and Vertical)

T.C. YÜKSEKÖĞRETİM KURULU
DOKÜMANTASYON MERKEZİ

CURRICULUM VITAE

Ömer Berk Berkalp was born in İzmir in 1973. He graduated from "Yeşilbahar İlkokulu" in 1983, from "Özel Doğuş Lisesi" in 1990 and from Istanbul Technical University, Textile Engineering Department in 1994. After his graduation, he continued his education and got his M.Sc. degree from I.T.U. by his study on "Performance of Carpets" in 1997. He had also started his academic career in 1995 as a research assistant in I.T.U. After he got his masters degree, he attended to the Navy to complete his military service as a protocol officer in Ankara. After completing his military service in 1998, he started his doctorate. He worked in North Carolina State University for 1.5 years as a visiting scholar for his Ph.D. study. He is still a research assistant in I.T.U. He can speak and write English.